

# Multiparticle Entanglement and Interference in Cavity Quantum Electrodynamics

A THESIS SUBMITTED TO

GUJARAT UNIVERSITY

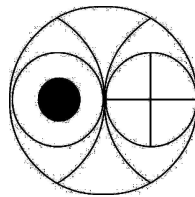
for

the degree of

**Doctor of Philosophy in Physics**

BY

**Pradyumna Kumar Pathak**



Quantum Optics & Quantum Information Division

**PHYSICAL RESEARCH LABORATORY**

AHMEDABAD -380 009

INDIA

May 2006

## CERTIFICATE

I hereby declare that the work presented in this thesis is original and has not formed the basis for the award of any degree or diploma by any University or institution.

**Pradyumna Kumar Pathak**  
(Author)

Certified by:

**Prof. G.S. Agarwal**

(Thesis Supervisor)

Quantum Optics & Quantum Information Division

Physical Research Laboratory

Navrangpura, Ahmedabad-380 009.

*dedicated to*

*my father*

*for his love, care and inspiration*

---

## Contents

---

<b>Acknowledgement</b>	<b>vi</b>
<b>Abstract</b>	<b>vii</b>
<b>1 Introduction</b>	<b>1</b>
1.1 Quantization of Electromagnetic Field in a Cavity . . . . .	1
1.2 Interaction of Radiation with Matter . . . . .	4
1.3 Jaynes Cummings Interaction . . . . .	7
1.4 Quantum Entanglement in Cavity QED . . . . .	8
1.5 Quasi-Probability Distributions and Phase Space Description . . . . .	10
1.5.1 Wigner distribution . . . . .	11
1.5.2 P-distribution . . . . .	13
1.5.3 Q-distribution . . . . .	14
<b>2 Generation of Superposition of multiple Mesoscopic States</b>	<b>16</b>
2.1 Compass State of the Electromagnetic Field . . . . .	17
2.2 Generation of the Superposition of multiple Mesoscopic States using Dispersive Interaction between Atoms and Cavity . . . . .	20
2.3 Generation of the Superposition of multiple Mesoscopic States using Resonant Interaction Between Atoms and Cavity . . . . .	23
2.4 Detection of the Generated Superposition of Mesoscopic States . . . . .	31
2.4.1 Homodyne detection of the generated superposition state . . . . .	31
2.5 Effects of non-unity Detection Efficiency . . . . .	33
2.6 Decoherence of the Generated Superposition State . . . . .	34
2.7 Summary . . . . .	36

<b>3 Ramsey Interferometry with Quantized Field</b>	<b>37</b>
3.1 Ramsey Interferometry . . . . .	38
3.2 Ramsey Interferometry with Quantized Fields . . . . .	41
3.3 Dependence of the fringes on quantum statistics of the fields . . . . .	44
3.3.1 Ramsey fringes with fields at single photon level . . . . .	46
3.3.2 Photon-photon interaction mediated by a single atom and quantum entanglement of two cavities . . . . .	47
3.4 Two Atom Interferometry . . . . .	48
3.4.1 Preparation of the entangled state $\alpha 2, 0\rangle + \beta 0, 2\rangle$ . . . . .	50
3.4.2 Entanglement Transfer from Fields to Atoms . . . . .	52
3.5 Summary . . . . .	53
<b>4 Multi-photon Processes in Cavities</b>	<b>54</b>
4.1 Two Photon Processes . . . . .	55
4.2 Two Photon Emission in two Identical Atoms in a two Mode Cavity . . . . .	57
4.3 Two Photon Emission in two Nonidentical Atoms in a Single Mode Cavity . . . . .	61
4.4 Effects of Cavity Damping . . . . .	63
4.5 Summary . . . . .	65
<b>5 Manipulation of Atomic Lifetime in Cavities Using dc-Fields</b>	<b>66</b>
5.1 Spontaneous Decay of an Atom inside the Cavity . . . . .	67
5.2 Manipulation of Atomic Lifetime Using dc-Fields . . . . .	69
5.3 Summary . . . . .	73
<b>6 Quantum Random Walk of Photons in High Quality Cavity</b>	<b>75</b>
6.1 Cavity-QED Model for Quantum Random Walk . . . . .	76
6.2 Quantum Random Walk of Photons . . . . .	78
6.3 Measurement of the State of the Random Walker . . . . .	83
6.4 Decoherence in Quantum Random Walk . . . . .	85
6.5 Summary . . . . .	87
<b>Conclusions and Future Outlook</b>	<b>88</b>
<b>Appendix</b>	<b>91</b>
<b>References</b>	<b>95</b>
<b>List of Publications</b>	<b>105</b>

---

## Acknowledgement

---

I feel a great pleasure to express my gratitude to Prof. G. S. Agarwal for his excellent guidance throughout my research work. His deep insight and an elegant approach to the subject as well as exceptional capacity to work have been a great source of inspiration for me. I am also grateful to Prof. V. B. Sheorey, Dr. R. Rangarajan, Dr. S. Mohanti, and Dr. J. Bhatt for their encouragement to enter in this field during my graduate course work. I thank Dr. R. P. Singh, Dr. P. K. Panigrahi, Dr. Bimalendu Deb, and Dr. J. Banerji for their fruitful discussions and suggestions during my research work. I thank all staff members of PRL for their kind cooperation and friendly behavior, without their help this work was not possible.

Though, I have passed most of my life in hostels but life at PRL hostel was wonderful and unforgettable, specially teatime, lunchtime, and Kaka's chay discussions. All students were always very nice and friendly to me. I thank all my friends with whom I shared most beautiful moments of my life as well as my tough times too. I am specially thankful to my table tennis playmates.

This work was partially done in Oklahoma State University, USA. I am thankful to Dr. Paul Westhaus and Dr. James Wicksted for their kind cooperation and providing all facilities to me at OSU.

Finally, I must remember my family members for their love and affection.

**Pradyumna Kumar Pathak**

---

## Abstract

---

The work presented in this thesis concerns cavity quantum electrodynamics techniques for generating quantum entanglement and interference effects in various atom-cavity systems for application in quantum computation and quantum optics.

In chapter 1, we present a brief introduction to field quantization and interaction of a quantized field with matter. We discuss phase space description of quantum states in terms of quasiprobability distributions.

In chapter 2, we propose cavity quantum electrodynamics schemes to generate superposition of four coherent states

$$|\psi\rangle \sim |\alpha\rangle + |i\alpha\rangle + |-\alpha\rangle + |-i\alpha\rangle. \quad (0.1)$$

We use resonant as well as dispersive interaction between atoms and the field inside the cavity. We discuss the nonclassical character of these states in terms of quasi-probability distributions [M. Hillery, et al, Phys. Rep. **106**, 121(1984)]. We also show that these superposition states can exhibit regions in phase space with sub-Planck structures [W. H. Zurek, Nature (London) **412**, 712 (2001)], i.e. the area of the variations of the two quadratures can be much smaller than the Planck's constant  $\hbar$ . These structures are direct signatures of quantum coherence and are formed as a result of interference between two superposed cat states. We discuss decoherence of such superposition due to the leakage of photons from the cavity. We discuss methods for monitoring these superposition states.

In chapter 3, we study Ramsey interferometer [N. F. Ramsey, Phys. Rev. **78**, 695, (1950)] with quantized fields and discuss the effects of field statistics on the visibility of interference fringes. In our scheme, we replace two Ramsey zones with two identical high quality

cavities and field is treated quantum mechanically. We find that interferences do not occur if the fields in two Ramsey zones have precise number of photons i.e. in Fock states. However, by passing two atoms one by one it is shown how an analog of Hanbury-Brown Twiss photon-photon correlation interferometry can be used to restore interferences as the two independent Ramsey zones get entangled by the passage of first atom. We also discuss interferences at a single photon level. Though interferences are absent with precise number of photons in Ramsey zones but for states like  $1/\sqrt{2}(|0\rangle + |1\rangle)$  interferences are restored. This occurs because of lack of information about the cavity in which atom makes transition. We also discuss generation of various maximally entangled states as well as the transfer of entanglement from atoms to photons and vice versa using Ramsey interferometer.

In chapter 4, we report an unusual cooperative effect in two photon processes in two atoms. Earlier studies of two-photon processes in two atoms deal with cooperative effect in the presence of strong dipole-dipole interaction between the atoms. Such interaction is significant only when the inter-atomic separation is less than the wavelength of the radiation [G. V. Varada, and G. S. Agarwal, *Phys. Rev. A* **45**, 6721 (1992); C. Hettich et al., *Science* **298**, 385 (2002)]. We show that it is advantageous to use a cavity for the study of such two photon processes as one would not be constrained by the requirement of small inter-atomic separation. In high quality cavities inter-atomic interactions can arise when different atoms interact with a common quantized field and thus these interactions do not depend on the inter-atomic separation. We demonstrate that the two-atom two-photon resonant effect could be very large thus opening up the possibility of a variety of multi-photon cooperative phenomena in non-resonant cavities. The two photon transition occurs as a result of simultaneous excitation or de-excitation of both atoms with two photon resonance condition  $\omega_1 + \omega_2 \approx \omega_a + \omega_b$ , where  $\omega_1, \omega_2$  are the atomic transition frequencies and  $\omega_a, \omega_b$  are the frequencies of the emitted photons. We study such two-photon resonant processes in two different systems (1) two identical atoms interacting with field in a two mode cavity, (2) two nonidentical atoms in a single mode cavity.

In chapter 5, we show how a possible control of spontaneous emission can be obtained in a cavity by using dc-fields. We find that in the presence of dc-fields in the cavities the spontaneous emission of atoms can be modified significantly as a result of dc-field induced stark shifts. Further, the change in spontaneous emission depends on the square of

applied dc-field. We find that in the case of cavities resonant to atomic transition spontaneous emission can be inhibited significantly using dc-fields. In the case of cavities having negligible mode density around atomic frequency the presence of dc field shows significant inhibition or enhancement of spontaneous emission depending on whether the cavity is tuned below the atomic transition frequency or above the transition frequency.

In chapter 6, we show how quantum random walk can be realized in cavities. Using resonant interaction between atoms and the field in a high quality cavity, we present a scheme for realizing quantum random walk. The atoms are driven strongly by a classical field. Under conditions of strong driving field we could realize an effective interaction of the form  $iS^x(a - a^\dagger)$  in terms of the spin operator  $S^x$  associated with the two level atom and the field operators  $a$  and  $a^\dagger$  [E. Solano et al., Phys. Rev. Lett. **90**, 027903 (2003)]. This effective interaction generates displacement in wavefunction of the field depending on the state of the atom. Measurements of the state of the atom would then generate effective state of the field. Thus in our scheme, measurement of atomic states is corresponding to the flipping of the coin while the field inside the cavity acts as a walker. Using the homodyne technique, state of the quantum random walker can be monitored. We also discuss the decoherence effects and the time scales at which quantum nature of random walks persists.

Finally, we present conclusions and future outlook.

# CHAPTER 1

---

## Introduction

---

Cavity quantum electrodynamics (cavity-QED) [1] deals with the interaction of few atoms with few photons inside a high quality cavity. Thus the effects of quantization of electromagnetic field become significant. In this chapter, quantization of electromagnetic field is discussed and the interaction of a single atom with quantized field inside the cavity is described. The phase space description for quantum states is presented.

### 1.1 Quantization of Electromagnetic Field in a Cavity

The classical description of electromagnetic field [2] is given by Maxwell's equations

$$\vec{\nabla} \cdot \vec{E} = 0 \quad (1.1)$$

$$\vec{\nabla} \cdot \vec{B} = 0 \quad (1.2)$$

$$\vec{\nabla} \times \vec{E} = -\frac{\partial \vec{B}}{\partial t} \quad (1.3)$$

$$\vec{\nabla} \times \vec{B} = \mu_0 \epsilon_0 \frac{\partial \vec{E}}{\partial t} \quad (1.4)$$

where  $\vec{E}(\vec{r}, t)$  and  $\vec{B}(\vec{r}, t)$  are electric and magnetic field vectors and  $\epsilon_0$  and  $\mu_0$  are the free space permittivity and permeability, respectively. Now taking the curl of Eq. (1.3) and using Eqs. (1.1) and (1.4), it follows that the electric field vector  $\vec{E}(\vec{r}, t)$  satisfies the wave equation

$$\nabla^2 \vec{E} - \mu_0 \epsilon_0 \frac{\partial^2 \vec{E}}{\partial t^2} = 0. \quad (1.5)$$

Solution to the Eq.(1.5) can be written as

$$\vec{E}(\vec{r}, t) = \vec{E}^+(\vec{r})e^{-i\omega t} + \vec{E}^-(\vec{r})e^{i\omega t} \quad (1.6)$$

where  $\omega$  is frequency of the field and  $(\vec{E}^+(\vec{r}))^* = \vec{E}^-(\vec{r})$  is spatial part of the electric field. A similar description can be found for magnetic field  $\vec{B}(\vec{r}, t)$ .

For quantization of electromagnetic field [3], consider the field inside a cavity of length  $L$  along  $z$ -axis and transverse area  $A$ . We assume that the field is linearly polarized in  $x$ -direction. The field inside the cavity can be expanded in terms of the modes of cavity as

$$E_x(z, t) = \sum_n C_n q_n(t) \sin(k_n z), \quad (1.7)$$

where  $q_n(t)$  is amplitude of the  $n$ -th cavity mode,  $k_n = n\pi/L$  is corresponding propagation vector, and the expansion coefficients are given by

$$C_n = \sqrt{\frac{2\omega_n^2}{AL\epsilon_0}}, \quad \text{with } \omega_n = k_n c, \quad (1.8)$$

where  $c = (\mu_0\epsilon_0)^{-1/2}$  is velocity of light in vacuum. Using Eqs. (1.7) and (1.4), the nonvanishing component of magnetic field  $B_y$  inside the cavity is given by

$$B_y(z, t) = \sum_n \mu_0\epsilon_0 C_n \frac{\dot{q}_n}{k_n} \cos(k_n z). \quad (1.9)$$

The Hamiltonian  $H$  for the field is given by

$$H = \frac{1}{2} \int_V d\tau \left( \epsilon_0 E_x^2 + \frac{B_y^2}{\mu_0} \right), \quad (1.10)$$

where the integration is over the volume of the cavity. Now substituting values of  $E_x$  and  $B_y$  from Eqs. (1.7) and (1.9) in Eq. (1.10),

$$H = \frac{1}{2} \sum_n (\omega_n^2 q_n^2 + \dot{q}_n^2) \quad (1.11)$$

$$= \frac{1}{2} \sum_n (\omega_n^2 q_n^2 + p_n^2), \quad (1.12)$$

where  $p_n = \dot{q}_n$  is the canonical momentum of the  $n$ th mode. From Eq. (1.12), it is clear that each mode of electromagnetic field inside the cavity is equivalent to a harmonic oscillator of unit mass. Thus the electromagnetic field inside the cavity can be quantized by identifying two quadratures  $q_n$  and  $p_n$  as operators which satisfy the commutation relations,

$$[q_n, p_m] = i\hbar\delta_{mn}, \quad [q_n, q_m] = [p_n, p_m] = 0. \quad (1.13)$$

From the analogy to the harmonic oscillator it is convenient to choose the operators  $q_n$  and  $p_n$  in the form

$$a_n e^{-i\omega_n t} = \frac{1}{\sqrt{2\hbar\omega_n}} (\omega_n q_n + ip_n) \quad (1.14)$$

$$a_n^\dagger e^{i\omega_n t} = \frac{1}{\sqrt{2\hbar\omega_n}} (\omega_n q_n - ip_n), \quad (1.15)$$

where  $a_n$  and  $a_n^\dagger$  are annihilation and creation operator for field in  $n$ th mode and satisfy the commutation relations

$$[a_n, a_m^\dagger] = i\hbar\delta_{mn}, \quad [a_n, a_m] = [a_n^\dagger, a_m^\dagger] = 0. \quad (1.16)$$

In terms of  $a$  and  $a^\dagger$ , the Hamiltonian (1.12) becomes

$$H = \hbar \sum_n \omega_n \left( a_n^\dagger a_n + \frac{1}{2} \right). \quad (1.17)$$

Now the electric field (1.7) and the magnetic field (1.9) inside the cavity can be expanded in terms of  $a_n$  and  $a_n^\dagger$  as

$$E_x(z, t) = \sum_n \mathcal{E}_n (a_n e^{-i\omega_n t} + a_n^\dagger e^{i\omega_n t}) \sin(k_n z), \quad (1.18)$$

$$B_y(z, t) = -i\mu_0 \epsilon_0 c \sum_n \mathcal{E}_n (a_n e^{-i\omega_n t} - a_n^\dagger e^{i\omega_n t}) \cos(k_n z), \quad (1.19)$$

where  $\mathcal{E}_n = \sqrt{\hbar\omega_n/\epsilon_0 V}$  has the dimension of electric field.

For quantization of electromagnetic field in free space, the classical electric and magnetic field are expanded in terms of the plane waves as follow

$$\vec{E}(\vec{r}, t) = \sum_k \hat{n}_k \mathcal{E}_k \alpha_k e^{-i\omega_k t + i\vec{k} \cdot \vec{r}} + c.c., \quad (1.20)$$

$$\vec{B}(\vec{r}, t) = \sum_k \frac{\vec{k} \times \hat{n}_k}{\omega_k} \mathcal{E}_k \alpha_k e^{-i\omega_k t + i\vec{k} \cdot \vec{r}} + c.c., \quad (1.21)$$

where the summation is over the discrete values of wave vector  $\vec{k} = \{k_x, k_y, k_z\}$ ,  $\alpha_k$  is a dimensionless amplitude and  $\hat{n}_k$  is unit vector along the direction of polarization and

$$\mathcal{E}_k = \sqrt{\frac{\hbar\omega_k}{2\epsilon_0 V}}. \quad (1.22)$$

The value of different components of wave vector  $\vec{k}$  are given by periodic boundary conditions over the length  $L$  as follow

$$k_x = \frac{2\pi n_x}{L}, \quad k_y = \frac{2\pi n_y}{L}, \quad k_z = \frac{2\pi n_z}{L}, \quad (1.23)$$

where  $k_x, k_y$  and  $k_z$  are integers ( $0, \pm 1, \pm 2, \dots$ ). The particular set of values of  $n_x, n_y,$  and  $n_z$  defines a mode of the field.

Now, similarly to the quantization in the cavity, the amplitudes  $\alpha_k$  can be transformed to the annihilation operator  $a_k$  for quantization. The electric and magnetic field components takes the form

$$\vec{E}(\vec{r}, t) = \sum_k \hat{n}_k \mathcal{E}_k a_k e^{-i\omega_k t + i\vec{k} \cdot \vec{r}} + H.c., \quad (1.24)$$

$$\vec{B}(\vec{r}, t) = \sum_k \frac{\vec{k} \times \hat{n}_k}{\omega_k} \mathcal{E}_k a_k e^{-i\omega_k t + i\vec{k} \cdot \vec{r}} + H.c., \quad (1.25)$$

where H.c. stands for Hermitian conjugate.

## 1.2 Interaction of Radiation with Matter

Classically, the electromagnetic field is treated by Maxwell's equations while the atom is considered to have quantized energy levels and the dynamics is given by the Schrödinger equation. For simplicity, let us assume the atom has a single electron of charge  $e$  and mass  $m$  interacting with an external electromagnetic field. The interaction between atom and field is described by the following Hamiltonian [4]

$$H = \frac{[\vec{P} - e\vec{A}(\vec{r}, t)]^2}{2m} + e\Phi(\vec{r}, t) + V(r), \quad (1.26)$$

where  $\vec{P}$  is the momentum of the electron,  $\vec{A}(\vec{r}, t)$  and  $\Phi(\vec{r}, t)$  are the vector and scalar potentials of the external field respectively. Here  $V(r)$  is a central potential experienced by the bound electron due to the presence of motionless nucleus. Quantization of the electron motion can be done by replacing the classical variable with operators, *e.g.*,

$$\vec{P} \longrightarrow -i\hbar\vec{\nabla}, \quad H \longrightarrow i\hbar\partial/\partial t. \quad (1.27)$$

Here  $\hbar = h/2\pi$ , where  $h$  is the Planck's constant. Therefore, the motion of electron is described by the Schrödinger equation

$$\begin{aligned} i\hbar \frac{\partial |\Psi(\vec{r}, t)\rangle}{\partial t} &= \left\{ \frac{[-i\hbar\vec{\nabla} - \frac{e}{c}\vec{A}(\vec{r}, t)]^2}{2m} + V(r) + e\Phi(\vec{r}, t) \right\} |\Psi(\vec{r}, t)\rangle \\ &= (H_0 + H_I)|\Psi(\vec{r}, t)\rangle, \end{aligned} \quad (1.28)$$

where the unperturbed Hamiltonian is given by

$$H_0 = -\frac{\hbar^2}{2m}\vec{\nabla}^2 + V(r) + e\Phi \quad (1.29)$$

and the interaction Hamiltonian involves only the vector potential  $\vec{A}$ :

$$H_I = \frac{e}{2mc} \left[ 2i\hbar\vec{A}(\vec{r}, t) \cdot \vec{\nabla} + i\hbar\vec{\nabla} \cdot \vec{A}(\vec{r}, t) \right] + \frac{e^2}{2mc^2} \vec{A}(\vec{r}, t) \cdot \vec{A}(\vec{r}, t) \quad (1.30)$$

In passing we note that, the transformations  $\vec{A} \longrightarrow \vec{A}' = \vec{A} + \frac{\hbar}{e}\vec{\nabla}\chi$  and  $\Phi \longrightarrow \Phi' = \Phi - \frac{\hbar}{e}\frac{\partial\chi}{\partial t}$ , leave the  $\vec{E}$  and  $\vec{B}$  as invariant quantities which are thus gauge independent [2]. Here,  $\chi$  is any arbitrary scalar function. This allows one to choose a suitable gauge to simplify the problem. Here we are working in the radiation gauge in which  $\Phi(\vec{r}, t) = 0$  and  $\vec{\nabla} \cdot \vec{A} = 0$ . Under the radiation gauge condition, the interaction Hamiltonian becomes

$$H_I = \frac{ie\hbar}{mc} \vec{A}(\vec{r}, t) \cdot \vec{\nabla} + \frac{e^2}{2mc^2} \vec{A}(\vec{r}, t) \cdot \vec{A}(\vec{r}, t) \quad (1.31)$$

The dipole moment approximation is often used in quantum optics [2], which simplifies the interaction Hamiltonian term. This approximation assumes that the whole atom is submerged in a plane electromagnetic wave described by a vector potential,  $\vec{A}(\vec{r} + \vec{r}_0, t)$ , which is assumed to have no spatial variation in the vicinity of the atom whose nucleus is located at  $\vec{r}_0$ . For such a case,

$$\begin{aligned} \vec{A}(\vec{r} + \vec{r}_0, t) &= \vec{A}(t) \exp \left[ i\vec{k} \cdot (\vec{r} + \vec{r}_0) \right] \\ &= \vec{A}(t) \exp(i\vec{k} \cdot \vec{r}_0) (1 + i\vec{k} \cdot \vec{r} + \dots) \end{aligned} \quad (1.32)$$

Taking  $\vec{k} \cdot \vec{r} \ll 1$ , we obtain

$$\vec{A}(\vec{r} + \vec{r}_0, t) \approx \vec{A}(t) \exp(i\vec{k} \cdot \vec{r}_0). \quad (1.33)$$

Using the unitary transformation  $|\Psi(\vec{r}, t)\rangle = e^{\frac{ie}{\hbar}\vec{r} \cdot \vec{A}_0} |\psi(\vec{r}, t)\rangle$  in Eq. (1.28), we get

$$\begin{aligned} i\hbar \frac{\partial |\psi(\vec{r}, t)\rangle}{\partial t} &= \left\{ \frac{\hbar^2}{2m} \vec{\nabla}^2 + V(r) - e\vec{r} \cdot \vec{E}(t) \right\} |\psi(\vec{r}, t)\rangle \\ &= (H_0 + H_I) |\psi(\vec{r}, t)\rangle \end{aligned} \quad (1.34)$$

The atom-field interaction Hamiltonian in the semiclassical picture is given by

$$H_I = -e\vec{r} \cdot \vec{E} = -\vec{d} \cdot \vec{E} \quad (1.35)$$

where the dipole moment operator  $\vec{d}$  is  $e\vec{r}$ . A significant contribution towards understanding radiation-matter interaction was given by Einstein [5, 6]. He employed the basic ideas of quantum mechanics to lay the foundation for the quantitative analysis of the absorption and emission of light by atoms. Later this simple theory has been extensively verified by rigorous quantum mechanical calculations.

From the above discussion, the complete Hamiltonian for the interaction of radiation with a single electron atom under the dipole approximation can be written as

$$H = H_A + H_F - e\vec{r} \cdot \vec{E}, \quad (1.36)$$

where  $H_A$  and  $H_F$  are the energies of the atom and radiation field respectively, and  $-e\vec{r} \cdot \vec{E}$  is interaction between the atom and the radiation.

For atomic energy, let us assume that  $\{|i\rangle\}$  represents the complete set of energy eigenstates of the atom such that

$$\sum_i |i\rangle\langle i| = 1, \quad (1.37)$$

$$H_A|i\rangle = E_i|i\rangle, \quad (1.38)$$

where  $E_i$  is the energy eigenvalue of  $i$ th atomic state. It follows that

$$H_A = \sum_i E_i |i\rangle\langle i| \quad (1.39)$$

The Hamiltonian for electromagnetic field in terms of operators is given by

$$H_F = \sum_n \hbar\omega \left( a_n^\dagger a_n + \frac{1}{2} \right). \quad (1.40)$$

Now the interaction part can also be rewritten in the form

$$H_I = - \left( \sum_{i,j} e|i\rangle\langle i|\vec{r}|j\rangle\langle j| \right) \vec{E} \quad (1.41)$$

$$= - \left( \sum_{i,j} \mathcal{P}_{ij}|i\rangle\langle j| \right) \vec{E}. \quad (1.42)$$

Here  $e\langle i|\vec{r}|j\rangle = \mathcal{P}_{ij}$  is transition dipole matrix element. For simplicity, if we assume that initially ( $t = 0$ ) atom is placed at origin, the electric field  $\vec{E}$  from Eq.(1.24) takes the form

$$\vec{E} = \sum_k \hat{n}_k \mathcal{E}_k (a_k + a_k^\dagger). \quad (1.43)$$

Using Eqs. (1.39), (1.40), (1.42), and (1.43), the Hamiltonian (1.36) takes the form

$$H = \sum_i E_i |i\rangle\langle i| + \sum_k \hbar\omega \left( a_k^\dagger a_k + \frac{1}{2} \right) + \hbar \sum_{i,j,k} g_k^{ij} |i\rangle\langle j| (a_k + a_k^\dagger), \quad (1.44)$$

$$\text{with } g_k^{ij} = -\frac{\mathcal{P}_{ij} \cdot \hat{n}_k \mathcal{E}_k}{\hbar}. \quad (1.45)$$

The coupling  $g_{ij}^k$  between field and atom depends on the field amplitude  $\mathcal{E}_k$  and the transition dipole matrix. In the case of superconducting cavities strong coupling has been achieved by using Rydberg atoms [7] which have large values of transition dipole moment.

### 1.3 Jaynes Cummings Interaction

The simplest model, for radiation-matter interaction, is the interaction of a two level atom with single mode radiation field, which has been solved exactly by Jaynes and Cummings [8]. Consider a two level atom with upper energy level  $|e\rangle$  and lower energy level  $|g\rangle$  interacts with a single mode electromagnetic field of frequency  $\omega$ . In this case the Hamiltonian (1.44) takes the form

$$H = \hbar(\omega_e |e\rangle\langle e| + \omega_g |g\rangle\langle g|) + \hbar\omega \left( a^\dagger a + \frac{1}{2} \right) + \hbar g (|e\rangle\langle g| + |g\rangle\langle e|) (a + a^\dagger), \quad (1.46)$$

where  $\hbar\omega_e$  and  $\hbar\omega_g$  are the energies of the upper and the lower atomic levels and  $a$  and  $a^\dagger$  are annihilation and creation operators for the single mode field. We have assumed coupling constant to be real,  $g_{eg} = g_{ge} = g$ . The first term in (1.46) can be simplified as

$$\hbar(\omega_e |e\rangle\langle e| + \omega_g |g\rangle\langle g|) = \hbar \frac{(\omega_e - \omega_g)}{2} (|e\rangle\langle e| - |g\rangle\langle g|) + \hbar \frac{(\omega_e + \omega_g)}{2} \quad (1.47)$$

$$= \frac{\hbar\omega_0}{2} (|e\rangle\langle e| - |g\rangle\langle g|), \quad (1.48)$$

where we use  $\omega_e - \omega_g = \omega_0$  and the completeness condition  $|e\rangle\langle e| + |g\rangle\langle g| = 1$ . The constant energy term  $\hbar(\omega_e + \omega_g)/2$  has been ignored. In the Hamiltonian (1.46) the interaction part has four terms. The terms  $|e\rangle\langle g|a^\dagger$  and  $|g\rangle\langle e|a$  are corresponding to the atomic transition from lower energy level to higher energy level followed by the emission of one photon and the transition from higher level to lower level followed by the absorption of one photon, respectively. These processes are energy nonconserving and thus can be dropped. Other two terms are energy conserving and photon is emitted when atom makes transition from upper level to lower level and photon is absorbed when transition occurs from lower level to

higher level. Following the above conventions and simplifications the Hamiltonian (1.46) takes the form

$$H = \frac{\hbar\omega_0}{2}(|e\rangle\langle e| - |g\rangle\langle g|) + \hbar\omega \left( a^\dagger a + \frac{1}{2} \right) + \hbar g(a|e\rangle\langle g| + a^\dagger|g\rangle\langle e|), \quad (1.49)$$

The Hamiltonian (1.49) can be diagonalized in the basis of atom-field states  $|e, n\rangle$  and  $|g, n+1\rangle$ , where  $n$  represents the photon numbers in the field. The eigenstates of the Hamiltonian  $H$  are given by

$$|+, n\rangle = \cos \theta_n |e, n\rangle + \sin \theta_n |g, n+1\rangle, \quad (1.50)$$

$$|-, n\rangle = \cos \theta_n |g, n+1\rangle - \sin \theta_n |e, n\rangle, \quad (1.51)$$

where  $\tan 2\theta_n = 2g\sqrt{n+1}/\Delta$  and  $\Delta = \omega_0 - \omega$  is detuning of the cavity field to the atomic transition. The corresponding eigenvalues are

$$E_{\pm, n} = \hbar\omega(n+1) \pm \hbar\Omega_n/2; \quad \Omega_n = \sqrt{\Delta^2 + 4g^2(n+1)}. \quad (1.52)$$

Clearly the atom and the photons inside the cavity behave as a composite system after they have interacted and are generally entangled. As a remark, we note that the advances of the Jaynes Cummings interaction are extensively reviewed in the literature [1, 9, 10].

## 1.4 Quantum Entanglement in Cavity QED

Entanglement can be defined as a quantum correlation between two subsystems of a composite system. For example, in the case of atom-field system the state of the atom and the field after interaction remains no more separable as a tensor product of atomic states and the field states. The measurement of atomic states can project the information about the field and viceversa. Historically, the concept of entanglement came after Einstein, Podolsky, and Rosen (EPR) paradox [11], in which they discussed the state of a composite system of two spin half particles,

$$|\psi_{EPR}\rangle = \frac{1}{\sqrt{2}}(|+1, -2\rangle - |-1, +2\rangle), \quad (1.53)$$

where  $|\pm_i\rangle$ ,  $i = 1, 2$ , represents the spin eigen states of particle 1 and 2, respectively. The state (1.53) is superposition of the states of composite system of two particles which is not separable as a tensor product of eigen states of the particles. Clearly the measurement of the spin of one particle provides complete information about the spin of the other.

Entanglement is at the heart of quantum information and has applications in quantum cryptography, teleportation of quantum states, and realization of various quantum logics. In quantum information a two state quantum system is used as quantum bit (qubit). The entanglement generated between two qubits, after they have interacted, can be used for realizing various quantum logic conditions [7] or cryptographic key distribution [12]. Further entanglement is nonlocal correlation and can exist between two widely separated quantum systems. These nonlocal features have been used for teleporting quantum states between two distant places [13].

In cavity-QED experiments, atoms are passed from one side of the cavity and detected on the other side after they have interacted with the field stored inside the cavity. The interaction between the atoms and the field is given by the Hamiltonian (1.44). For simplicity, we consider the case of two level atoms passing through a single mode cavity one by one and the cavity mode is resonant with the atomic transition ( $\omega_0 = \omega$ ). The hamiltonian in this case becomes

$$H = \hbar\omega(|e\rangle\langle e| - |g\rangle\langle g|) + \hbar\omega a^\dagger a + \hbar g(a|e\rangle\langle g| + a^\dagger|g\rangle\langle e|), \quad (1.54)$$

where we have neglected the constant energy term  $\hbar\omega/2$ . The evolution of atom-cavity system is given by

$$|g, n\rangle \rightarrow \cos(gt\sqrt{n})|g, n\rangle - i \sin(gt\sqrt{n})|e, n-1\rangle \quad (1.55)$$

$$|e, n-1\rangle \rightarrow \cos(gt\sqrt{n})|e, n-1\rangle - i \sin(gt\sqrt{n})|g, n\rangle \quad (1.56)$$

where  $|g, n\rangle$  [ $|e, n-1\rangle$ ] represents that atom is in its lower [higher] energy state and cavity has  $n$  [ $(n-1)$ ] photons.

Let us consider first an atom comes in its higher energy state  $|e_1\rangle$  and there is no photon inside the cavity. The initial state of the atom-cavity system will be  $|e_1, 0\rangle$ . If the atom interacts with the field for time  $t_1$  inside the cavity. The final state of the system after passage of the atom is given by

$$|\psi_1\rangle = \cos(gt_1)|e_1, 0\rangle - i \sin(gt_1)|g_1, 1\rangle. \quad (1.57)$$

By selecting velocity of the atom properly, the value of interaction time  $t_1$  can be fixed arbitrarily. For example, if we choose interaction time such that  $gt_1 = \pi/4$  then the state (1.57) becomes

$$|\psi_1\rangle = \frac{1}{\sqrt{2}}(|e, 0\rangle - i|g, 1\rangle) \quad (1.58)$$

The state (1.58) is an entangled state of the atom and the field. If the atom is detected in state  $|e_1\rangle$  that reflects that the field has no photon, on the other hand, if the measured state of atom is  $|g_1\rangle$  the field has one photon. Now, if we pass second atom coming in its ground state  $|g_2\rangle$  and select the interaction time  $t_2$  such that  $gt_2 = \pi/2$ . The atom undergoes transition from its lower state  $|g_2\rangle$  to higher state  $|e_2\rangle$  with 100% probability if photon is present in the cavity and will leave in the same state  $|g_2\rangle$  if there is no photon. Finally, the cavity will have no photon after passage of the second atom and the state of the atoms is given by

$$|\psi_2\rangle = \frac{1}{\sqrt{2}}(|e_1, g_2\rangle - |g_1, e_2\rangle). \quad (1.59)$$

Clearly both atoms are in entangled state similar to the EPR state (1.53). Thus cavity works as an entangling machine for atoms and photons [7].

## 1.5 Quasi-Probability Distributions and Phase Space Description

In classical physics, the state of a system is characterized by the position  $x$  and the momentum  $p$ , which is represented by a point in the phase space. In the case of ensemble of large number of systems,  $x$  and  $p$  follow a well defined probability distribution  $P(x, p)$  statistically. The average of any function  $f(x, p)$  is expressed as

$$\langle f \rangle_{classical} = \int dx \int dp f(x, p) P(x, p). \quad (1.60)$$

In quantum physics, because of introduced uncertainty, the two quadratures  $x$  and  $p$  can not be measured simultaneously, *i.e.*, one can not define a true phase space probability distribution. A quantum system is described by a density matrix  $\hat{\rho}$  and the average of a function of the position and momentum operators,  $\hat{f}(\hat{x}, \hat{p})$  is defined by

$$\langle \hat{f} \rangle_{quantum} = Trace(\hat{f}\hat{\rho}). \quad (1.61)$$

The quasiprobability distributions provide the way to express Eq.(1.61) in the form of Eq.(1.60). The average value of any quantum mechanical operator, in terms of quasiprobability distributions  $P_Q(x, p)$ , is defined in a way similar to classical physics

$$\langle \hat{f} \rangle_{quantum} = \int dx \int dp f(x, p) P_Q(x, p), \quad (1.62)$$

where the function  $f(x, p)$  can be derived from the operator  $\hat{f}(\hat{x}, \hat{p})$  by well defined correspondence rules and  $P_Q(x, p)$  is derived from the density matrix  $\hat{\rho}$ . Thus quasiprobability

distributions provide correspondence between quantum physics and classical physics and have proven to be a useful tool for studying many quantum systems.

### 1.5.1 Wigner distribution

Historically, Wigner function was defined in terms of position  $\hat{x}$  and momentum  $\hat{p}$  [14] in the form

$$W(x, p) = \frac{1}{\pi\hbar} \int dy \langle x - y | \rho | x + y \rangle e^{-2ipy/\hbar}. \quad (1.63)$$

Here  $|x\rangle$  is eigenstate of the quadrature operator  $\hat{x}$ . In coherent state representation the definition (1.63) can be expressed as [3]

$$W(\alpha) = \frac{2e^{2|\alpha|^2}}{\pi^2} \int \langle -\beta | \hat{\rho} | \beta \rangle e^{2(\alpha\beta^* - \alpha^*\beta)} d^2\beta. \quad (1.64)$$

Wigner function is widely used in quantum optics for visualizing coherence character of the states. It is well behaved function for all quantum mechanical states. In Fig. 1.1, we show wigner distribution for Schrödinger cat state  $N(|\beta\rangle + |-\beta\rangle)$ , where  $N$  is normalization constant. In the central region there are interference fringes which show the coherence in the superposition. The Wigner function have negative values in this region which indicates that this state has nonclassical nature. Here it should be noted that in coherent state representation, real part of  $\alpha$  and imaginary part of  $\alpha$  correspond to two independent quadratures.

There is lot of progress for measuring Wigner function in quantum optics. Vogel and Risken [15] first showed, that for propagating fields Wigner function can be reconstructed by using quantum tomography methods. In quantum tomography, quadrature amplitude distributions are measured by using homodyne techniques [16] in which field is superimposed on a strong coherent field. By changing amplitude and phase of the coherent field, quadrature distribution is measured in the different location in phase space. If the two quadratures are

$$\hat{x} = \frac{1}{\sqrt{2}}(a + a^\dagger) \quad (1.65)$$

$$\hat{p} = \frac{1}{i\sqrt{2}}(a - a^\dagger). \quad (1.66)$$

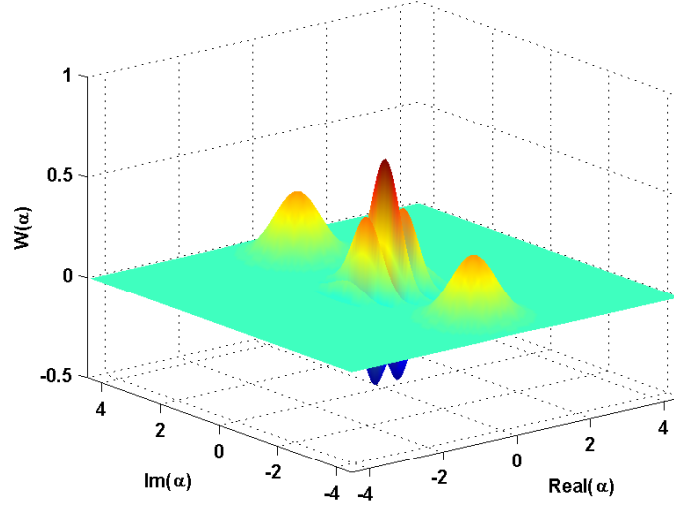


**Figure 1.1:** The Wigner distribution for the state  $N(|\beta\rangle + |-\beta\rangle)$  for  $\beta = 3$ .

The measured values of quadratures at phase angle  $\phi$  are given by

$$\begin{aligned}\hat{x}_\phi &= \hat{x} \cos \phi + \hat{p} \sin \phi \\ \hat{p}_\phi &= \hat{p} \cos \phi - \hat{x} \sin \phi.\end{aligned}\tag{1.67}$$

The Wigner function  $W(x, p)$  is the joint probability distribution of measuring both quadratures thus the probability of measuring quadrature amplitude  $x_\phi$  is

$$P(x, \phi) = \int_{-\infty}^{\infty} W(\hat{x}_\phi \cos \phi - \hat{p}_\phi \sin \phi, \hat{p}_\phi \cos \phi + \hat{x}_\phi \sin \phi) dp_\phi.\tag{1.68}$$

The Wigner function is then reconstructed from the measured values of  $P(x, \phi)$  by inverting Eq.(1.68) using numerical algorithms of Radon transform. Raymer and coworkers [16] have reconstructed Wigner function for vacuum and a squeezed state of single mode field using quantum tomography methods. Further, a direct measurement of Wigner function for vacuum and weak coherent states has been done by Wodkiewicz group [17] using photon counting. Since the early work of Vogel and Risken, the mapping of the full quantum state has become a subject by itself [18]. In the case of field states in cavities, Lutterbach and Davidovich [19] have proposed a simple scheme for measuring Wigner function of the field in a cavity which has been implemented by Bertet *et al.* [20] for single photon Fock state. Their method is based on an operational definition of Wigner function [21], which is

written as, for the state having density matrix  $\rho$

$$W(\alpha) = \frac{2}{\pi} \text{Tr}[D(-\alpha)\rho D(\alpha)(-1)^{a^\dagger a}], \quad (1.69)$$

where  $D(\alpha) \equiv e^{\alpha a^\dagger - \alpha^* a}$  is displacement operator. The Eq.(1.69) is nothing but the expectation value of the parity operator after displacing the cavity field by  $-\alpha$ . The parity of displaced field state has been measured by passing an atom through the cavity in the dispersive regime. For the final remark, the work on radiation fields has been extended to determine the quantum state of an ion trapped in a potential [22].

### 1.5.2 P-distribution

For establishing equivalence between classical and quantum statistics of electromagnetic fields, Sudarshan [23] introduced a diagonal representation of density matrix in the basis of coherent states [24],

$$\hat{\rho} = \int d^2\alpha P(\alpha) |\alpha\rangle \langle \alpha|. \quad (1.70)$$

Here  $P(\alpha)$  is P-distribution in coherent state representation and  $|\alpha\rangle$  is coherent state. This description of density matrix is particularly interesting in the case of operators  $\hat{O}(a, a^\dagger)$  expanded in the normal order,

$$\hat{O} = \sum_{n,m} c_{n,m} (a^\dagger)^n a^m. \quad (1.71)$$

Here  $c_{n,m}$  are expansion coefficients and  $a$  and  $a^\dagger$  are annihilation and creation operators for electromagnetic field. Let us calculate the average value of operator  $\hat{O}$ , it follows that

$$\text{Trace}(\hat{O}\hat{\rho}) = \frac{1}{\pi} \int d^2\beta \int d^2\alpha P(\alpha) \langle \beta | \hat{O} | \alpha \rangle \langle \alpha | \beta \rangle \quad (1.72)$$

$$= \int d^2\alpha P(\alpha) O(\alpha, \alpha^*) \quad (1.73)$$

where

$$\frac{1}{\pi} \int d^2\beta |\beta\rangle \langle \beta| = 1 \quad (1.74)$$

$$O(\alpha, \alpha^*) = \sum_{n,m} c_{n,m} (\alpha^*)^n \alpha^m. \quad (1.75)$$

The Eq.(1.73) is similar to the classical description of average value, and the operator  $\hat{O}(a, a^\dagger)$  is associated with  $O(\alpha, \alpha^*)$  in this representation.

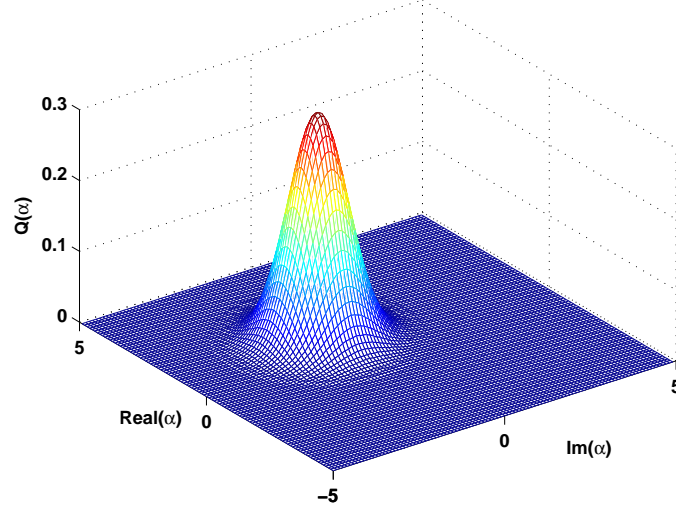


**Figure 1.2:** The Q-distribution for the state  $|\beta\rangle$  for  $\beta = 1 - i$ .

Now, we derive the expression for  $P(\alpha)$  from density matrix  $\hat{\rho}$  in the following. Let  $|\beta\rangle$  and  $|\beta\rangle$  are the coherent states with eigenvalues  $\beta$  and  $-\beta$  of the operator  $a$ , respectively. Then calculate the value

$$\langle -\beta|\hat{\rho}|\beta\rangle = \int d^2\alpha P(\alpha)\langle -\beta|\rho|\beta\rangle, \quad (1.76)$$

$$= e^{-|\beta|^2} \int d^2\alpha \{P(\alpha)e^{-|\alpha|^2}\} e^{\beta\alpha^* - \beta^*\alpha}. \quad (1.77)$$

From Eq.(1.77), it is clear that  $\langle -\beta|\rho|\beta\rangle$  is two dimensional Fourier transform of  $P(\alpha)e^{-|\alpha|^2}$ . Thus inverse Fourier transform of Eq.(1.77) gives expression for  $P(\alpha)$

$$P(\alpha) = \frac{e^{|\alpha|^2}}{\pi^2} \int d^2\beta \langle -\beta|\hat{\rho}|\beta\rangle e^{|\beta|^2} e^{\alpha\beta^* - \beta\alpha^*}. \quad (1.78)$$

The Eq.(1.78) is the required expression of P-distribution.

### 1.5.3 Q-distribution

The Q-distribution is defined for antinormally ordered operators  $\hat{O}_a(a, a^\dagger)$ ,

$$\hat{O}_a = \sum_{n,m} d_{n,m} a^n (a^\dagger)^m. \quad (1.79)$$

The function corresponding to the operator  $\hat{O}_n$  can be calculated similar to Eq.(1.75),

$$O_a(\alpha, \alpha^*) = \sum_{n,m} d_{n,m} \alpha^n (\alpha^*)^m. \quad (1.80)$$

Let us calculate the average value of operator  $\hat{O}_a$  in a state characterized by density matrix  $\hat{\rho}$ ,

$$\begin{aligned} \langle \hat{O} \rangle &= \text{Trace} \left[ \sum_{n,m} d_{n,m} (a^n a^\dagger)^m \hat{\rho} \right], \\ &= \sum_{n,m} d_{m,n} \text{Trace} \left[ \frac{1}{\pi} \int a^n |\alpha\rangle \langle \alpha| (a^\dagger)^m \hat{\rho} d^2\alpha \right], \\ &= \sum_{n,m} d_{n,m} \frac{1}{\pi} \int \alpha^n (\alpha^*)^m \langle \alpha | \hat{\rho} | \alpha \rangle d^2\alpha, \\ &= \int O_a(\alpha, \alpha^*) Q(\alpha) d^2\alpha, \end{aligned} \quad (1.81)$$

where we get the expression for Q-distribution as

$$Q(\alpha) = \frac{1}{\pi} \int \langle \alpha | \hat{\rho} | \alpha \rangle. \quad (1.82)$$

In Fig. 1.2, we show Q-distribution for a coherent state  $|\beta\rangle$ . We note that in Ref.[25], it is shown that the experiments performed for phase measurement of the radiation field are equivalent to the measurement of  $Q$  function. The measured probability distribution for the joint measurement of the two quadratures  $x$  and  $p$ , is directly proportional to the  $Q$  function.

---

### Generation of Superposition of multiple Mesoscopic States

---

In quantum mechanics, a system can exist in a superposition of its eigenstates while in the classical world no such superposition of states exists and the system always stays in one of its states precisely. This has been pointed out as "cat paradox" by Schrödinger in his famous paper [26]. Mesoscopic states are the states of a system, which is larger than the microscopic systems and smaller than the macroscopic systems, thus are interface between the classical and the quantum world i.e. macroscopic and microscopic world. In recent times superposition of mesoscopic states has attracted a great deal of attention as these superpositions exhibit very important interference effects [27, 28, 29] many of which have now been realized experimentally [30, 31, 32, 33, 34]. It has been proposed earlier that these superposition states can be produced by passing a single mode field through a Kerr medium [35, 36, 37]. However, an efficient production of such states would require large Kerr nonlinearity which is not available though some proposals for the enhancement of the Kerr nonlinearity exist [38]. The existence of such superpositions is closely connected to the occurrence of fractional revivals in the nonlinear dynamics of quantum systems [34, 39, 40, 41].

We note that many authors [31, 32, 29, 42] have shown how cavities, which are far detuned from the atomic transitions, can be used to produce a superposition of two mesoscopic states. It turns out that one can have fairly large dispersive interaction in high quality cavities. This high dispersion has been utilized in many other experiments [43, 20].

Eiselt and Risken [44] had discovered that if a cavity contains a coherent field with

large photon numbers, say of the order of 10, then the state of the field for certain times splits into two parts. Each part can be characterized approximately by a coherent state. Several authors have studied many aspects of such splittings [45, 30]. Auffeves et al. [30] made a successful observation of this splitting and realized Schrödinger cat state in a high quality cavity.

The simplest superposition would consist of two coherent states one centered at  $\alpha$  and the other at  $-\alpha$ , which is known as Schrödinger cat state. Further, the studies of the superpositions of more than two coherent states have found many novel features. For example, Zurek [46] noticed that such superpositions lead to structures in phase space which are smaller than Planck's constant. In this chapter, we show how to prepare superpositions of four coherent states by using dispersive as well as resonant interaction in a high quality cavity. We discuss the nonclassical character of these states in terms of negativity of the Wigner function [21] as well as zeros of Q-distribution [21]. We discuss methods for monitoring these superposition states. Using homodyne techniques, one can detect the phase space position of the coherent states in the generated superposition. We discuss decoherence of such superposition due to the leakage of photons from the cavity.

## 2.1 Compass State of the Electromagnetic Field

Let  $|\alpha\rangle$  be a coherent state for the field with amplitude  $\alpha$ . The most commonly studied superpositions are of the form

$$|\psi\rangle \sim |\alpha\rangle + |e^{i\theta}\alpha\rangle. \quad (2.1)$$

Here  $\theta$  is an arbitrary phase. Extensive literature on this state exists. It is well known [27, 28] that the quantum character of this state is reflected in the regions of phase space where the Wigner function becomes negative. The area of the negative region is of the order of Planck constant. There are several methods of producing such a state [29, 33, 34, 35]. Zurek [46] has studied a superposition state of four Gaussian wave packets

$$\psi(x) \sim \exp\left\{-\frac{(x-x_0)^2}{\xi^2} + \frac{ip_0x}{\hbar}\right\}, \quad (2.2)$$

with one each placed in the east, west, north and south direction in the phase space and calculated the Wigner function for such a state, defined by

$$W(x, p) = \frac{1}{2\pi\hbar} \int e^{ipy/\hbar} \psi\left(x - \frac{y}{2}\right) \psi^*\left(x + \frac{y}{2}\right) dy. \quad (2.3)$$

He found that it exhibits negative regions in phase space as well as structures with areas which could be much smaller than Planck's constant. Since coherent states correspond to Gaussian wave packets, in the following we consider a superposition of four coherent states of the form

$$|\phi\rangle = N (|\alpha\rangle + |i\alpha\rangle + |-\alpha\rangle + | -i\alpha\rangle), \quad (2.4)$$

where  $N$  is the normalization constant and  $\alpha$  is complex. Because of the positions of the coherent states in the superposition (2.4) along four directions in the phase space, Zurek named the state (2.4) as "compass state". The Wigner function for any state  $|\phi\rangle$  can be obtained using coherent states as [21]

$$W(\gamma, \gamma^*) = \frac{2}{\pi^2} e^{2|\gamma|^2} \int \langle -\beta|\phi\rangle \langle \phi|\beta\rangle e^{-2(\beta\gamma^* - \beta^*\gamma)} d^2\beta. \quad (2.5)$$

For the state (2.4) the Wigner function is found to be

$$\begin{aligned} W(\gamma, \gamma^*) = & |N|^2 \frac{4e^{-2|\gamma|^2}}{\pi} \times \\ & \left[ 2e^{-2|\alpha|^2} \cosh\{(1+i)\alpha\gamma^* + (1-i)\alpha^*\gamma\} \cosh\{(1-i)\alpha\gamma^* + (1+i)\alpha^*\gamma\} \right. \\ & + 2 \cos\{(1+i)\alpha\gamma^* + (1-i)\alpha^*\gamma\} \cos\{(1-i)\alpha\gamma^* + (1+i)\alpha^*\gamma\} \\ & + e^{-(|\alpha|^2 - (1+i)\alpha\gamma^* - (1-i)\alpha^*\gamma)} \cos\{|\alpha|^2 - (1+i)\alpha\gamma^* - (1-i)\alpha^*\gamma\} \\ & + e^{-(|\alpha|^2 - (1-i)\alpha\gamma^* - (1+i)\alpha^*\gamma)} \cos\{|\alpha|^2 - (1-i)\alpha\gamma^* - (1+i)\alpha^*\gamma\} \\ & + e^{-(|\alpha|^2 + (1+i)\alpha\gamma^* + (1-i)\alpha^*\gamma)} \cos\{|\alpha|^2 + (1+i)\alpha\gamma^* + (1-i)\alpha^*\gamma\} \\ & \left. + e^{-(|\alpha|^2 + (1-i)\alpha\gamma^* + (1+i)\alpha^*\gamma)} \cos\{|\alpha|^2 + (1-i)\alpha\gamma^* + (1+i)\alpha^*\gamma\} \right]. \quad (2.6) \end{aligned}$$

Each cosine term in Eq. (2.6) arises from the interference of a pair of coherent states in the superposition state (2.4). The sub-Planck structures arise from further interference of two cosine terms which come from the diagonal pairs. The first two terms in Eq. (2.6) are such terms coming from the diagonal pairs  $|\alpha\rangle, |-\alpha\rangle$  and  $|i\alpha\rangle, |-i\alpha\rangle$ . The first term is significant for smaller values of  $|\alpha|$  and shows exponential decrease in the Wigner function away from the center and the second term which is significant for larger values of  $|\alpha|$  shows the interference pattern in the central region ( $\gamma \rightarrow 0$ ). In Figs. 2.1 and 2.2, we plot the Wigner function for some typical values of  $|\alpha|$ . We found that for smaller values of  $|\alpha|$  (Fig. 2.1), the central part has a continuum and no other structures appear but for larger values of  $|\alpha|$  (Fig. 2.2), a chess board pattern as noticed earlier by Zurek appears in the central region. The reason for the disappearance of the interference pattern in the central region

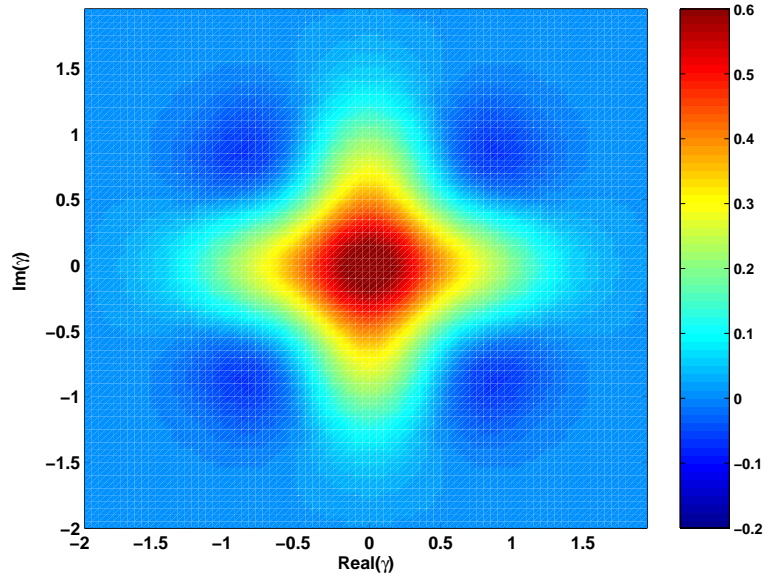


**Figure 2.1:** The Wigner function for mesoscopic superposition state  $N(|\alpha\rangle + |-\alpha\rangle + |i\alpha\rangle + |-i\alpha\rangle)$  for  $|\alpha| = 1$ .

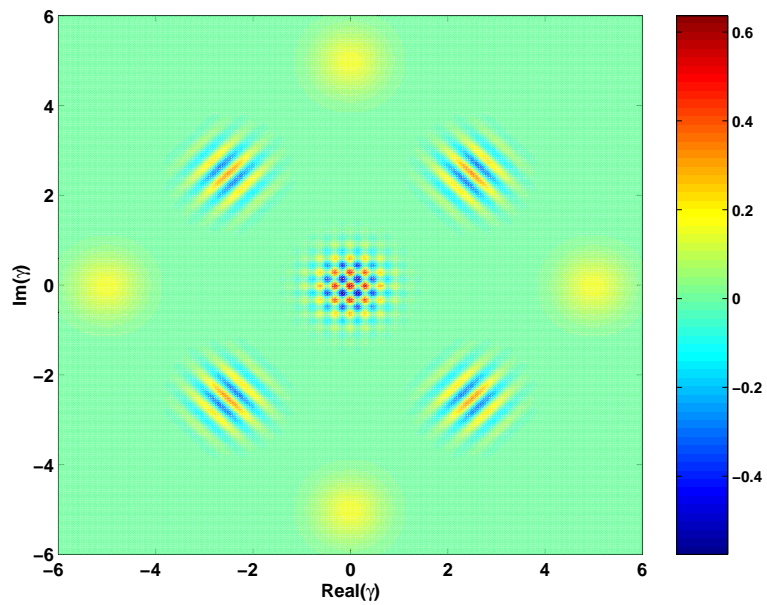


**Figure 2.2:** The Wigner function for mesoscopic superposition state  $N(|\alpha\rangle + |-\alpha\rangle + |i\alpha\rangle + |-i\alpha\rangle)$  for  $|\alpha| = 5$ .

for smaller values of  $|\alpha|$  is because in this case the coherent states overlap to a large extent so the interference effects are not visible.

## 2.2 Generation of the Superposition of multiple Mesoscopic States using Dispersive Interaction between Atoms and Cavity

Consider a single mode high quality cavity containing a small amount of a coherent field so that the initial state of the cavity field is  $|\alpha\rangle$ . Let  $\omega_c$  be the cavity frequency. Consider the passage of a two level atom with the excited and ground states  $|e\rangle$  and  $|g\rangle$  with transition frequency  $\omega$ . The atom is initially prepared in a superposition state

$$|\Phi\rangle = c_e|e\rangle + c_g|g\rangle. \quad (2.7)$$

The Hamiltonian of the atom-cavity system is given by

$$H = \hbar\omega_c a^\dagger a + \frac{\hbar\omega}{2}(|e\rangle\langle e| - |g\rangle\langle g|) + \hbar g(|e\rangle\langle g|a + |g\rangle\langle e|a^\dagger). \quad (2.8)$$

In a frame rotating with the atomic transition frequency  $\omega$ , the interaction Hamiltonian is given by

$$H = \hbar\delta a^\dagger a + \hbar g(|e\rangle\langle g|a + |g\rangle\langle e|a^\dagger), \quad \delta = (\omega_c - \omega). \quad (2.9)$$

We assume that the cavity is far detuned from the atomic transition frequency so that  $\delta \gg g$ . We can do a second order perturbation calculation and obtain an effective Hamiltonian

$$H \simeq \hbar\delta a^\dagger a + \phi_0 \hbar a^\dagger a |g\rangle\langle g| - \phi_0 \hbar a a^\dagger |e\rangle\langle e|, \quad (2.10)$$

where the parameter  $\phi_0$  is equal to  $g^2/\delta$ . Physically it gives the shift of the excited state in the absence of any cavity field. Under the effect of the Hamiltonian (2.10), the states evolve as

$$\begin{aligned} |g, n\rangle &\rightarrow e^{-in\phi_0\tau - in\delta\tau} |g, n\rangle \\ |e, n\rangle &\rightarrow e^{i(n+1)\phi_0\tau - in\delta\tau} |e, n\rangle, \end{aligned} \quad (2.11)$$

where  $\tau$  is the interaction time. Using (2.11), we easily obtain the evolution of a field in a coherent state  $|\alpha\rangle$

$$\begin{aligned} |g, \alpha\rangle &\rightarrow |g, \alpha e^{-i\phi - i\delta\tau}\rangle \\ |e, \alpha\rangle &\rightarrow e^{i\phi} |e, \alpha e^{i\phi - i\delta\tau}\rangle, \quad \phi = \phi_0\tau. \end{aligned} \quad (2.12)$$

Therefore the atom field system in the state  $|\Phi, \alpha\rangle$  will evolve into

$$|\Phi, \alpha\rangle \rightarrow c_e e^{i\phi} |e, \alpha e^{i\phi - i\delta\tau}\rangle + c_g |g, \alpha e^{-i\phi - i\delta\tau}\rangle. \quad (2.13)$$

The probability of detection of the atom in the state  $|\psi\rangle = \psi_e |e\rangle + \psi_g |g\rangle$  will be

$$P_\psi = ||c_e \psi_e^* e^{i\phi} |\alpha e^{i\phi - i\delta\tau}\rangle + c_g \psi_g^* |\alpha e^{-i\phi - i\delta\tau}\rangle||^2 \quad (2.14)$$

$$= |c_e \psi_e^*|^2 + |c_g \psi_g^*|^2 + 2 \text{Real} \left( c_g^* \psi_g c_e \psi_e^* e^{i\phi} \langle \alpha e^{-i(\phi + \delta\tau)} | \alpha e^{i(\phi - \delta\tau)} \rangle \right). \quad (2.15)$$

The last term in Eq. (2.15) yields the interference fringes. For the special case of the initial state and the detection state having equal superposition of the ground and the excited states  $|c_g^* \psi_g c_e \psi_e^*| = 1/4$ . The visibility depends on the scalar product of two coherent states that are shifted in phase by  $2\phi$ . The phase shift is a measure of the cavity interaction. Haroche and coworkers have used the above for the production and detection of mesoscopic superposition of the field states. In the present case the generated mesoscopic superposition is the state

$$c_e \psi_e^* e^{i\phi} |\alpha e^{i\phi - i\delta\tau}\rangle + c_g \psi_g^* |\alpha e^{-i\phi - i\delta\tau}\rangle. \quad (2.16)$$

We next demonstrate how the compass state can be produced by following similar ideas. Let us write the state (2.13) in the form

$$|\Phi, \alpha\rangle = f_e |e\rangle |\alpha_e\rangle + f_g |g\rangle |\alpha_g\rangle. \quad (2.17)$$

Let us consider the passage of two atoms labeled as A and B in succession through the cavity. After the passage of the atom A we get the state (2.17). Clearly the net state of the system consisting of two atoms A, B and the cavity field would have the structure

$$|\Psi\rangle = f_e h_e |e_A, e_B\rangle |\alpha_{ee'}\rangle + f_e h_g |e_A, g_B\rangle |\alpha_{eg'}\rangle + f_g h_e |g_A, e_B\rangle |\alpha_{ge'}\rangle + f_g h_g |g_A, g_B\rangle |\alpha_{gg'}\rangle. \quad (2.18)$$

The joint detection of the atoms in the state  $|\chi\rangle \equiv \chi_{ee'} |e_A, e_B\rangle + \chi_{eg'} |e_A, g_B\rangle + \chi_{ge'} |g_A, e_B\rangle + \chi_{gg'} |g_A, g_B\rangle$  will project state(2.18) to (unnormalized state)

$$\langle \chi | \Psi \rangle \equiv |C\rangle = f_e h_e \chi_{ee'}^* |\alpha_{ee'}\rangle + f_e h_g \chi_{eg'}^* |\alpha_{eg'}\rangle + f_g h_e \chi_{ge'}^* |\alpha_{ge'}\rangle + f_g h_g \chi_{gg'}^* |\alpha_{gg'}\rangle. \quad (2.19)$$

Clearly such a conditional detection reduces the state of the cavity field to a state which in general would be a mesoscopic superposition of four coherent sates  $|\alpha_{ij}\rangle$ . The value of  $\alpha_{ij}$

can be read from Eq. (2.13),

$$\alpha_{ee'} = \alpha_0 e^{i\phi+i\phi'}, \alpha_{eg'} = \alpha_0 e^{i\phi-i\phi'}, \alpha_{ge'} = \alpha_0 e^{-i\phi+i\phi'}, \alpha_{gg'} = \alpha_0 e^{-i\phi-i\phi'}; \quad (2.20)$$

$$\phi = \frac{g_A^2 \tau_A}{\delta}, \phi' = \frac{g_B^2 \tau_B}{\delta}; \alpha_0 = \alpha e^{-i\delta\tau - i\delta\tau'}. \quad (2.21)$$

Clearly by varying  $\phi$  and  $\phi'$  we can produce a variety of superpositions. Consider, for example,  $\phi = \pi/4$  and  $\phi' = \pi/2$ , then

$$\alpha_{ee'} = \alpha_0 e^{3i\pi/4}, \alpha_{eg'} = \alpha_0 e^{-i\pi/4}, \alpha_{ge'} = \alpha_0 e^{i\pi/4}, \alpha_{gg'} = \alpha_0 e^{-3i\pi/4}, \quad (2.22)$$

so the state (2.19) is a compass state. The expansion coefficients in (2.19) depend on the initial preparation of the atoms  $A$  and  $B$  and the detection of these atoms. This is usually done by using two Ramsey zones before and after the cavity. Let us for simplicity assume that

$$\begin{aligned} |\Phi_j\rangle &= \frac{1}{\sqrt{2}} \left( e^{i\eta_j} |e\rangle + e^{i\theta_j} |g\rangle \right); j = A, B, \\ |\chi\rangle &= |\Phi'_A\rangle |\Phi'_B\rangle, \end{aligned} \quad (2.23)$$

where  $|\Phi'_j\rangle$  is obtained from  $|\Phi_j\rangle$  by using  $\eta_j \rightarrow \eta'_j$  and  $\theta_j \rightarrow \theta'_j$ . Substituting values of  $\alpha_{ij}$  from (2.22) we rewrite (2.19) as

$$\begin{aligned} |C\rangle &= \frac{1}{4} \left( e^{i(\eta_1+\eta_2+3\pi/4)} |-\alpha\rangle + e^{i(\eta_1+\theta_2+\pi/4)} |\alpha\rangle + e^{i(\theta_1+\eta_2+\pi/2)} |i\alpha\rangle \right. \\ &\quad \left. + e^{i(\theta_1+\theta_2)} |-i\alpha\rangle \right), \end{aligned} \quad (2.24)$$

$$\eta_1 = \eta_A - \eta'_A, \eta_2 = \eta_B - \eta'_B, \theta_1 = \theta_A - \theta'_A, \theta_2 = \theta_B - \theta'_B,$$

we have also set  $\alpha_0 = \alpha e^{i\pi/4}$ . For  $\theta_1 = \eta_1 + \pi/4$  and  $\theta_2 = \eta_2 + \pi/2$  the state (2.24) becomes the compass state (2.4)

$$|C\rangle = \frac{1}{4} e^{i(\eta_1+\eta_2+3\pi/4)} (|-\alpha\rangle + |\alpha\rangle + |i\alpha\rangle + |-i\alpha\rangle). \quad (2.25)$$

It is clear that the probability of joint measurements on the atoms  $A$  and  $B$  would be

$$P = Tr_c \langle \chi | \psi \rangle \langle \psi | \chi \rangle, \quad (2.26)$$

where  $Tr_c$  stands for tracing over the cavity field. Using Eq(2.19) and Eq(2.23), we find the result

$$\begin{aligned} P &= \frac{1}{4} + \frac{1}{8} \text{Real} \left( e^{i(\theta_2-\eta_2-\pi/2)} \langle -\alpha | \alpha \rangle + e^{i(\theta_1-\eta_1-\pi/4)} \langle -\alpha | i\alpha \rangle \right. \\ &\quad \left. + e^{i(\theta_1+\theta_2-\eta_1-\eta_2-3\pi/4)} \langle -\alpha | -i\alpha \rangle + e^{i(\theta_1-\eta_1-\pi/4)} \langle \alpha | -i\alpha \rangle \right. \\ &\quad \left. + e^{i(\theta_1+\eta_2-\eta_1-\theta_2+\pi/4)} \langle \alpha | i\alpha \rangle + e^{i(\theta_2-\eta_2-\pi/2)} \langle i\alpha | -i\alpha \rangle \right) \equiv \langle C | C \rangle. \end{aligned} \quad (2.27)$$

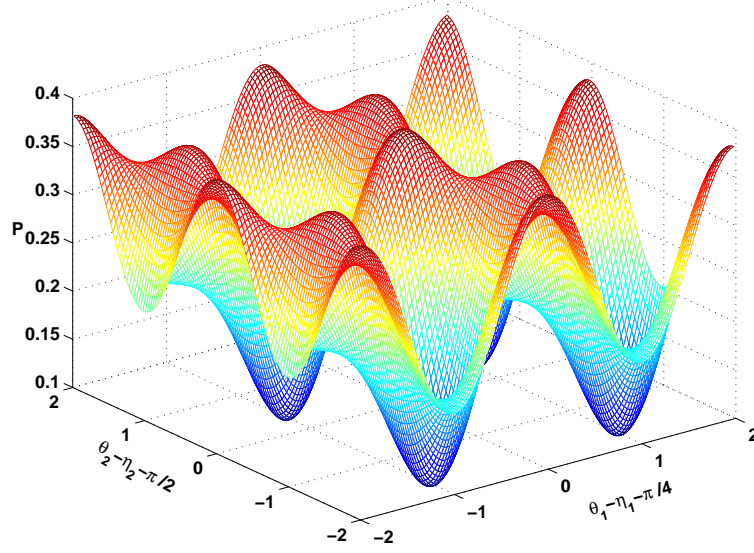


**Figure 2.3:** The probability  $P$  for  $|\alpha|^2 = 1$  is plotted with phases of the initial atomic state and the detected state. The scale along  $x$  axis and  $y$  axis is in units of  $\pi$ .

In Fig. 2.3, we show  $P$  as a function of phases of initial atomic state and the detected atomic state for  $|\alpha| = 1$ . These interferences become less prominent for larger values of  $|\alpha|$ . The exact nature of interferences depends on the choice of the phase factors  $\eta_j$  and  $\theta_j$ .

### 2.3 Generation of the Superposition of multiple Mesoscopic States using Resonant Interaction Between Atoms and Cavity

In a recent experiment, Auffeves *et al.* [30] have observed a superposition of two distinguishable states of the field in a high quality cavity using resonant interaction between an atom and the field inside the cavity. This observation is in agreement with the theoretical prediction of Eiselt and Risken [44]. When a two level Rydberg atom interacts with a microwave field, it splits the field into two parts whose phases move in opposite directions. If the interaction time is chosen such that the phase difference between the split parts becomes  $\pi$ , then the cavity field can be projected into a superposition similar to a cat state,  $|\alpha\rangle + |-\alpha\rangle$ .

In this section, we show that the above method can be used for the preparation of a superposition of four mesoscopic states of the field. We consider a two level Rydberg atom

having its higher-energy state  $|e\rangle$  and lower-energy state  $|g\rangle$  and the cavity has a strong coherent field  $|\alpha\rangle$ . The atom passes through the cavity and interacts resonantly with the field. The Hamiltonian for the system in the interaction picture is written as

$$H = \hbar g \left( |e\rangle\langle g|a + a^\dagger|g\rangle\langle e| \right), \quad (2.28)$$

where  $g$  is the coupling constant for the atom with the cavity field, and  $a$  ( $a^\dagger$ ) is the annihilation (creation) operator. The state of the atom-cavity system is written as

$$|\psi(t)\rangle = \sum_n (c_{en}(t)|e, n\rangle + c_{gn}(t)|g, n\rangle). \quad (2.29)$$

Using Hamiltonian (2.28), the Schrödinger equation in terms of  $c_{en}$  and  $c_{gn}$  is

$$\dot{c}_{en-1} = -ig\sqrt{n}c_{gn}, \quad (2.30)$$

$$\dot{c}_{gn} = -ig\sqrt{n}c_{en-1}. \quad (2.31)$$

We assume that the atom enters the cavity in its lower state  $|g\rangle$  and after interacting with the field for time  $t_1$ , it is detected in the same state  $|g\rangle$ . Thus, effectively, the atom absorbs no photon but it projects the cavity field into the state

$$|\psi_c\rangle = \sum_n c_n \cos(g\sqrt{n}t_1)|n\rangle, \quad (2.32)$$

$$= \frac{1}{2} \sum_n c_n e^{ig\sqrt{n}t_1}|n\rangle + c_n e^{-ig\sqrt{n}t_1}|n\rangle, \quad (2.33)$$

$$c_n = \frac{\alpha^n}{\sqrt{n!}} e^{-|\alpha|^2/2}.$$

As a result, the cavity field splits into two parts whose phases move in directions opposite to each other. Now we consider the passage of a second identical atom through the cavity. The second atom enters the cavity in its lower state  $|g\rangle$  and, after interacting with the field for time  $t_2$ , is detected in the same state  $|g\rangle$ . The state of the field inside the cavity after passing the second atom is

$$|\psi_c'\rangle = \sum_n c_n \cos(g\sqrt{n}t_1) \cos(g\sqrt{n}t_2)|n\rangle, \quad (2.34)$$

$$= \frac{1}{4} \sum_n c_n \left[ e^{ig\sqrt{n}(t_1+t_2)}|n\rangle + e^{-ig\sqrt{n}(t_1+t_2)}|n\rangle + e^{ig\sqrt{n}(t_1-t_2)}|n\rangle + e^{-ig\sqrt{n}(t_1-t_2)}|n\rangle \right]. \quad (2.35)$$

Thus after passing second atom, the state of the field inside the cavity splits into four parts.

In the coherent state  $|\alpha\rangle$ , the photon distribution follows Poisson statistics, so in Eq. (2.35), most of the contribution to the summation comes from the terms  $n \approx |\alpha|^2$ . Thus we can expand  $\sqrt{n}$  in phase terms around the average number of photons  $\bar{n} = |\alpha|^2$  in Eq. (2.35). In fact for  $\bar{n} \sim 10$ , only the terms up to second order in  $(n - \bar{n})$  are significant and other terms are negligible,

$$\sqrt{n} = \sqrt{\bar{n}} + \frac{n - \bar{n}}{2\sqrt{\bar{n}}} - \frac{(n - \bar{n})^2}{8\bar{n}^{3/2}}. \quad (2.36)$$

If we substitute the value of  $\sqrt{n}$  from Eq. (2.36) in Eq. (2.35), the term proportional to  $n$  will change the phase of the coherent field while the second- and higher-order terms in  $(n - \bar{n})$  will distort the shape of the coherent state in phase space. For simplification, in order to understand the nature of the generated superposition state, we do not consider the distortion in the coherent state. Then Eq. (2.35) can be approximated by

$$|\psi'_c\rangle = \frac{1}{4} \left[ e^{i(\eta_1 + \eta_2)} |\alpha e^{i(\theta_1 + \theta_2)}\rangle + e^{-i(\eta_1 + \eta_2)} |\alpha e^{-i(\theta_1 + \theta_2)}\rangle + e^{i(\eta_1 - \eta_2)} |\alpha e^{i(\theta_1 - \theta_2)}\rangle + e^{-i(\eta_1 - \eta_2)} |\alpha e^{-i(\theta_1 - \theta_2)}\rangle \right]; \quad (2.37)$$

$$\eta_i = \frac{gt_i \sqrt{\bar{n}}}{2}, \quad \theta_i = \frac{gt_i}{2\sqrt{\bar{n}}}, \quad i = 1, 2 \quad (2.38)$$

If we choose interaction times  $t_1$  and  $t_2$  such that  $\theta_1 = \pi/2$  and  $\theta_2 = \pi/4$ , we get the superposition of four mesoscopic coherent states placed in the east, west, north and south directions in phase space,

$$|\psi'_c\rangle = \frac{1}{4} \left[ e^{-i(\eta_1 - \eta_2)} |\alpha'\rangle + e^{i(\eta_1 + \eta_2)} |-\alpha'\rangle + e^{i(\eta_1 - \eta_2)} |i\alpha'\rangle + e^{-i(\eta_1 + \eta_2)} |-i\alpha'\rangle \right]; \quad (2.39)$$

where we set  $\alpha = \alpha' e^{i\pi/4}$ .

Now we calculate the Wigner distribution for the state (2.34). The density matrix  $\rho_c$  for state (2.34) in terms of number states is

$$\rho_c = \sum_{n,m} \frac{\alpha^n \alpha^{*m}}{\sqrt{n!m!}} e^{-|\alpha|^2} \cos(gt_1 \sqrt{n}) \cos(gt_2 \sqrt{n}) \cos(gt_1 \sqrt{m}) \cos(gt_2 \sqrt{m}) |n\rangle \langle m|. \quad (2.40)$$

Using equations (2.5) and (2.40), the Wigner distribution for the state (2.34) is

$$W(\gamma) = \frac{2e^{2|\gamma|^2}}{\pi^2} \sum_{n,m} \frac{\alpha^n \alpha^{*m}}{n!m!} e^{-|\alpha|^2} \cos(gt_1 \sqrt{n}) \cos(gt_2 \sqrt{n}) \cos(gt_1 \sqrt{m}) \times \cos(gt_2 \sqrt{m}) \int (-\beta^*)^n \beta^m e^{-|\beta|^2} \exp[-2(\beta\gamma^* - \beta^*\gamma)] d^2\beta. \quad (2.41)$$

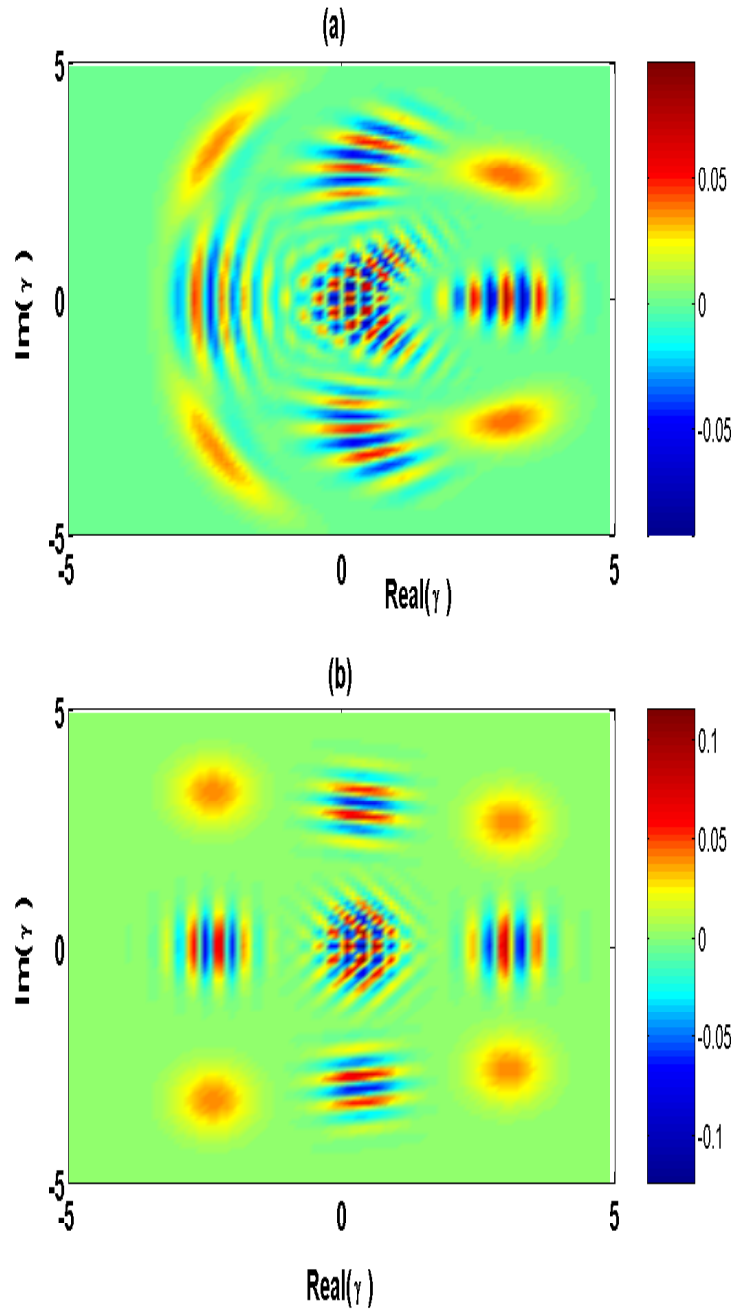


**Figure 2.4:** The Wigner distribution  $W(\gamma)$  for (a) the generated state (2.35) and (b) the approximated state (2.37), using parameters  $\alpha = 4$ ,  $gt_1 = 3.7\pi$ ,  $gt_2 = 1.9\pi$ .

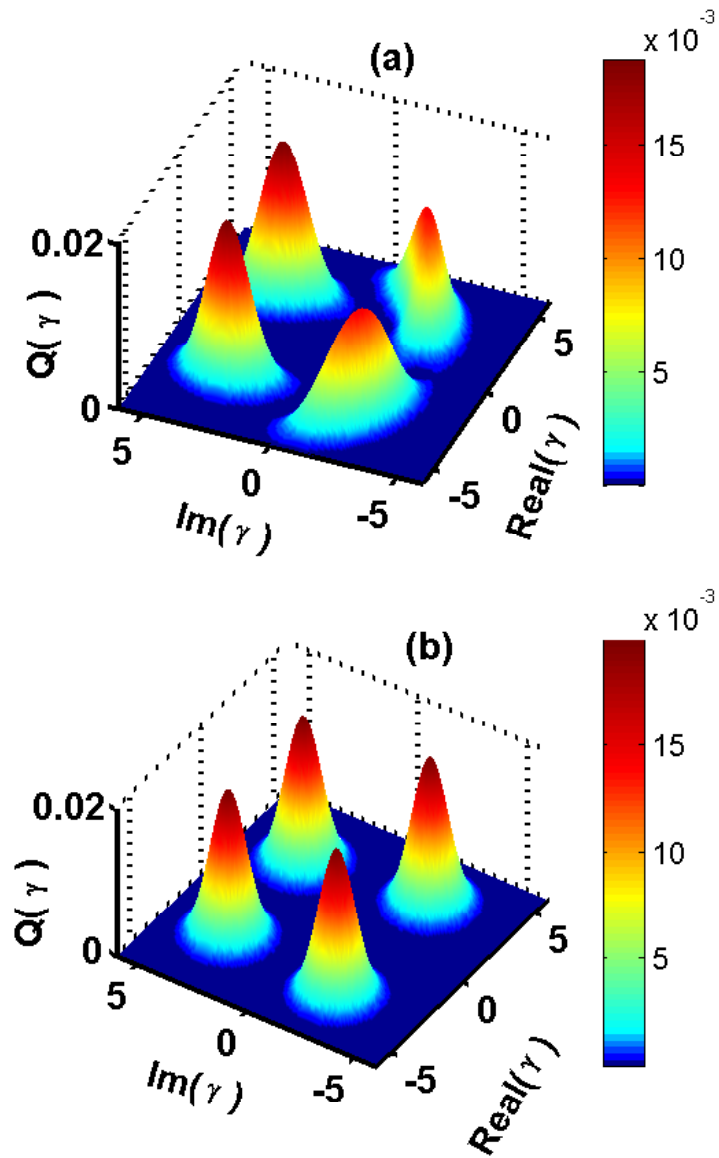


**Figure 2.5:** The Q-distribution function  $Q(\gamma)$  for (a) the generated state (2.35) and (b) the approximated state (2.37), using same parameters as in Fig. 1.

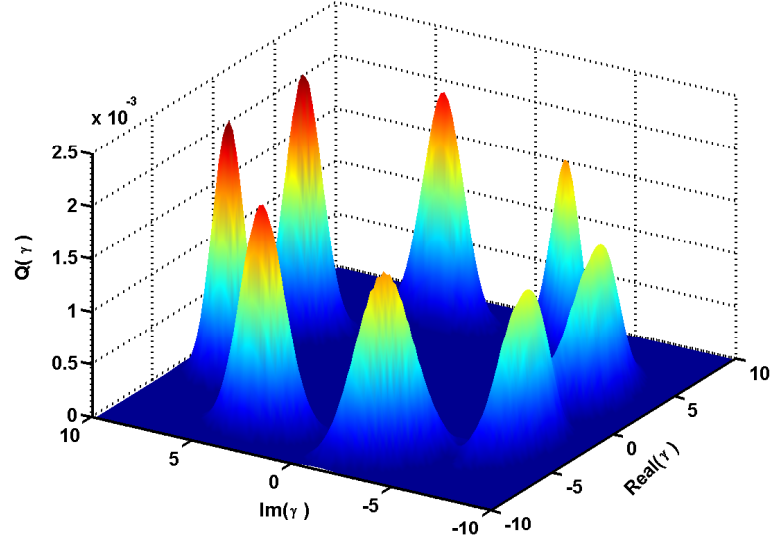


**Figure 2.6:** The  $Q$ -distribution function  $Q(\gamma)$  for the generated state after passing three atoms through the cavity, for  $\alpha = 8$ . The interaction times for the first atom, second atom and the third atom are chosen such that  $gt_1 = 8\pi$ ,  $gt_2 = 4\pi$ ,  $gt_3 = 2\pi$ .

After evaluating the integral, Eq. (2.41) is simplified to the form

$$W(\gamma) = \frac{2e^{2|\gamma|^2}}{\pi} \sum_{n,m} \frac{(-1)^{n+m} \alpha^n \alpha^{*m}}{2^{n+m} n! m!} e^{-|\alpha|^2} \cos(gt_1 \sqrt{n}) \times \cos(gt_2 \sqrt{n}) \cos(gt_1 \sqrt{m}) \cos(gt_2 \sqrt{m}) \frac{\partial^{n+m}}{\partial \gamma^n \partial \gamma^{*m}} e^{-4|\gamma|^2}. \quad (2.42)$$

In the Fig. 2.4, we show the Wigner distributions for the generated superposition state (2.35) as well as for the approximated state (2.37) using some typical values of parameters. There are four patches at the corners corresponding to four mesoscopic states of the field and between each pair of states of the field there are interference fringes indicating the coherence between the states. In the central part, there are subplanck structures as noticed by Zurek [46] which form as a result of quantum interference between the two diagonal pairs. The comparison of Figs. 2.4 (a) and (b) shows that a significant squeezing perpendicular to the arc of the circle  $|z| = |\alpha|$  occurs due to the effects of the higher order terms in  $(n - \bar{n})$  (see Eq. (2.36)). Squeezing in the resonant Jaynes-Cummings model [47] has been studied very well earlier. As a result of small differences in the field statistics, there are differences in the interference patterns. In Fig. 2.5, the  $Q$ -distributions for the states (2.35) and (2.37) are shown with the same parameters used in Fig. 2.4. We select the interaction times such

that there is no overlapping between two states of the field. A comparison of Figs. 2.5 (a) and (b) shows that the states of the field corresponding to the phases  $\pm g\sqrt{n}(t_1 + t_2)$  [see (2.35)] in the generated mesoscopic state have more spread along the circle  $|z| = |\alpha|$  and squeezing perpendicular to it in phase space because of larger distortion terms. Thus the split states of the field in the generated superposition state are situated at the same position as in the approximated state but with changed shape.

We further mention that after passing  $N$  atoms through the cavity and properly selecting the interaction times, we can generate the superposition of  $2^N$  mesoscopic states of the field placed along the arc of a circle of radius  $|\alpha|$  in phase space. In Fig. 2.6, we show the Q-distribution for the generated state of the field after passing three atoms through the cavity. It is clear that the generated state is a coherent superposition of eight mesoscopic states.

In this method of preparing superposition of mesoscopic field states, most of the time atoms are in their ground states, thus decoherence effects due to atomic damping are negligible. Only the decoherence of the generated superposition states after passage of first atom may lead to the generation of undesirable statistical mixture of states [29, 31, 32]. The mesoscopic states in the generated superposition after passage of first atom lie on the circle of radii  $|\alpha|$  in the phase space. Thus they decohere as  $\exp(-2|\alpha|^2\kappa t)$  [c.f. Eq. (2.61)]. The required interaction time for first atom is given by  $gt_1 \approx \pi|\alpha|$ . The required interaction time for the next atom is half the interaction time for the previous atom. We assume that all atoms come in a proper sequence so that total time in the generation of the state is equal to the total interaction time of the cavity field with the atoms. Then the time required after passage of the first atom in the preparation of  $2^N$  mesoscopic states, for large  $N$ , is given by

$$\frac{t_1}{2} + \frac{t_1}{4} + \frac{t_1}{8} + \dots (N-1)\text{term} \dots \approx t_1. \quad (2.43)$$

Thus the probability of generating the desired state, for large  $N$ , is reduced by the factor  $\exp(-2|\alpha|^2 t_1/t_{cav})$ , where  $t_{cav} = 1/\kappa$  is the life time of the field in the cavity. In the case of good cavities,  $gt_{cav} \approx 400$  is feasible. The probability of generating state (2.34) in these cavities, for  $|\alpha|^2 \sim 10$ , will be more than 80%.

The relation between the Q-distribution and the P-distribution for a state, [21], is given by

$$Q(\gamma) = \int P(\alpha) e^{-|\alpha-\gamma|^2} d^2\alpha. \quad (2.44)$$

From Eq. (2.44), it is clear that for  $Q = 0$  the P-distribution will oscillate between  $+ve$  and  $-ve$  values. The negative value of  $P$  is a signature of the nonclassical nature of the state. Thus the exact zeros of the Q-distribution are also signatures of nonclassical nature. Here it will be interesting to analyze the exact zeros of the Q-distribution of the approximated state (2.39). The Q-distribution for state (2.39) is

$$Q(\gamma) = \frac{1}{\pi} \left| \langle \gamma | \alpha' \rangle e^{-i(\eta_1 - \eta_2)} + \langle \gamma | -\alpha' \rangle e^{i(\eta_1 + \eta_2)} + \langle \gamma | i\alpha' \rangle e^{i(\eta_1 - \eta_2)} + \langle \gamma | -i\alpha' \rangle e^{-i(\eta_1 + \eta_2)} \right|^2. \quad (2.45)$$

The exact zeros of  $Q(\gamma)$  will be given by

$$\left| \langle \gamma | \alpha' \rangle e^{-i(\eta_1 - \eta_2)} + \langle \gamma | -\alpha' \rangle e^{i(\eta_1 + \eta_2)} + \langle \gamma | i\alpha' \rangle e^{i(\eta_1 - \eta_2)} + \langle \gamma | -i\alpha' \rangle e^{-i(\eta_1 + \eta_2)} \right| = 0. \quad (2.46)$$

Thus the Q-distribution shows nonclassical behavior at all phase points  $\gamma$  satisfying the condition (2.46). For example, if we take  $\alpha'$  to be real and observe the Q-distribution along the line  $\gamma = |\gamma|e^{i\pi/4}$  in phase space, the condition for nonclassicality (2.46) simplifies to

$$e^{-\frac{|\gamma|\alpha'}{\sqrt{2}}} \cos \left[ \eta_1 + \eta_2 + \frac{|\gamma|\alpha'}{\sqrt{2}} \right] + e^{\frac{|\gamma|\alpha'}{\sqrt{2}}} \cos \left[ \eta_1 - \eta_2 + \frac{|\gamma|\alpha'}{\sqrt{2}} \right] = 0. \quad (2.47)$$

For  $|\gamma| = 0$  the condition (2.47) becomes  $\cos \eta_1 \cos \eta_2 = 0$ . For  $|\gamma| \neq 0$ , using the values of  $\eta_1 = \pi|\alpha'|^2/2$ ,  $\eta_2 = \pi|\alpha'|^2/4$  (see Eq. (2.38)), the condition (2.47) can be rewritten as the simultaneous equations

$$\begin{aligned} \frac{|\gamma|}{\sqrt{2}\alpha'} + \frac{3\pi}{4} &= (2n_1 + 1) \frac{\pi}{2\alpha'^2}, \\ \frac{|\gamma|}{\sqrt{2}\alpha'} + \frac{\pi}{4} &= (2n_2 + 1) \frac{\pi}{2\alpha'^2}; \quad n_i = 1, 2, \dots \end{aligned} \quad (2.48)$$

The solution of the equations (2.48) gives  $\alpha'^2 = 2(n_1 - n_2)$ , thus  $\alpha'^2$  must be an even integer and the values of  $|\gamma|$  are given by

$$|\gamma| = \frac{\pi}{2\sqrt{(n_1 - n_2)}} (3n_2 - n_1 + 1); \quad n_1 > n_2. \quad (2.49)$$

In the above paragraph, we have outlined an analytical approach for getting information about the non classical behavior of a state by finding exact zeros of  $Q$  function. It is quite clear from the above that a simple analysis of the  $Q$  function can provide information of the nonclassical behavior of the state. Thus this is an alternate analytical approach for checking nonclassical behavior of the state. In general, analyzing zeros of  $Q$  function is easier than looking for  $-ve$  value of Wigner function. In Ref.[25], it is shown that the experiments performed for phase measurement of the radiation field are equivalent to the measurement of  $Q$  function.

## 2.4 Detection of the Generated Superposition of Mesoscopic States

In the previous sections, we have shown how the cavity field can be projected into a superposition of four mesoscopic states of the field after passing two atoms through the cavity. In order to explore the characteristics of the state (2.4), we have to bring a third atom  $C$  and examine the probability of its detection in a given state. This would be similar to what was done in the experiment of Brune *et al.* [31] to study the cat state. In fact, the compass state can be detected using the methods sensitive to its field statistics. For the compass state photon distribution is very special, it has number states having photon number in the integral multiple of four. The state (2.4) can be expressed in terms of number states as follow

$$|\phi\rangle = N \sum_p \frac{\alpha^{4p}}{\sqrt{(4p)!}} e^{-|\alpha|^2/2} |4p\rangle, \quad (2.50)$$

where  $p$  is an integer. We propose a simple method for detecting the compass state using a two level atom interacting resonantly with the cavity field as a probe. The Hamiltonian for resonant interaction is given by (2.28). We can calculate the probabilities of detection for the atom in its different states after passing through the cavity. The probabilities of detection if atom enters the cavity in its lower state  $|g\rangle$  and detected in its state  $|g\rangle$  and  $|e\rangle$ ,  $P_g^g$  and  $P_g^e$  respectively are

$$P_g^g = \sum_p \left| N \frac{\alpha^{4p}}{\sqrt{(4p)!}} e^{-|\alpha|^2/2} \cos(2gt\sqrt{p}) \right|^2, \quad (2.51)$$

$$P_g^e = \sum_p \left| N \frac{\alpha^{4p}}{\sqrt{(4p)!}} e^{-|\alpha|^2/2} \sin(2gt\sqrt{p}) \right|^2. \quad (2.52)$$

In the Fig. 2.7, we show the comparison of detection probabilities for cavity field in compass state, Schrödinger cat state  $N_0(|\alpha\rangle + |-\alpha\rangle)$ , and coherent state  $|\alpha\rangle$ . We observe that the revival time is larger for cat state than the revival time for compass state and revival time is larger for coherent state than the revival time for cat states. The reduction in revival times is because of increasing granular nature of photon distribution from coherent state to compass state.

### 2.4.1 Homodyne detection of the generated superposition state

An elegant method for detecting the generated superposition can also be homodyne detection [30], which can be implemented in the same experimental set up. After preparing the

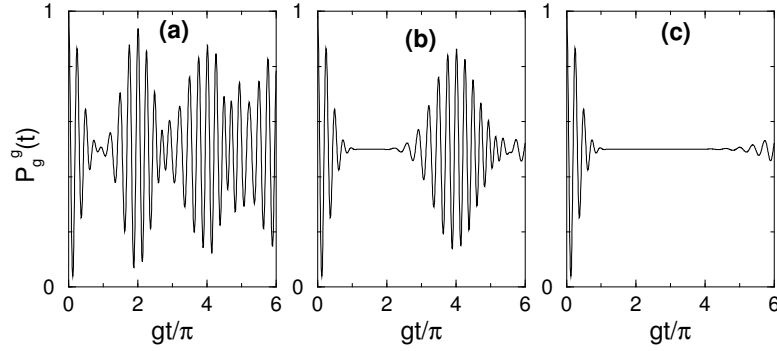


**Figure 2.7:** The probability of detection of the atom in its ground state  $|g\rangle$  for cavity field in (a) compass state, (b) Schrödinger cat state  $N_0(|\alpha\rangle + |-\alpha\rangle)$ , and (c) coherent state  $|\alpha\rangle$ , for  $|\alpha|^2 = 16$ .

cavity in the desired superposition state, a resonant external coherent field  $|\beta\rangle$  is injected into the cavity. After adding the external field, the state of the resultant field in the cavity is

$$\begin{aligned}
 |C_h\rangle &= ND(\beta) [|\alpha\rangle + |i\alpha\rangle + |-\alpha\rangle + |-i\alpha\rangle] \\
 &= N \sum_m \langle m|D(\beta) [|\alpha\rangle + |i\alpha\rangle + |-\alpha\rangle + |-i\alpha\rangle] |m\rangle, \\
 &= \sum_m F_m |m\rangle
 \end{aligned} \tag{2.53}$$

$$F_m = N \langle m|D(\beta) [|\alpha\rangle + |i\alpha\rangle + |-\alpha\rangle + |-i\alpha\rangle], \tag{2.54}$$

where  $D(\beta) \equiv e^{\beta a^\dagger - \beta^* a}$  is displacement operator. Now we bring the third atom in its lower energy state  $|g\rangle$  to probe the cavity field. The probability of detecting the probe atom in its lower state  $|g\rangle$  after crossing the cavity in time  $t_p$  is

$$P_g = \sum_m |F_m|^2 \cos^2(gt_p \sqrt{m}). \tag{2.55}$$

The interaction time  $t_p$  for the probe atom is selected such that if there are photons in the cavity it leaves the cavity, in its higher energy state  $|e\rangle$  with larger probability. We have shown in the earlier section that all the states of the field in the superposition lie on a circle of radius  $|\alpha|$ , so if we choose the external field  $|\beta\rangle$  having amplitude  $|\alpha|$  and phase  $\phi$ , the probe atom will leave the cavity in its ground state with larger probability when the value of  $\pi + \phi$  will match to the phases of the states of the field in the generated superposition. Thus the probability of the probe atom leaving the cavity in its lower state  $|g\rangle$  would, as a function of  $\phi$ , have peaks corresponding to the positions of the centers of the superposed

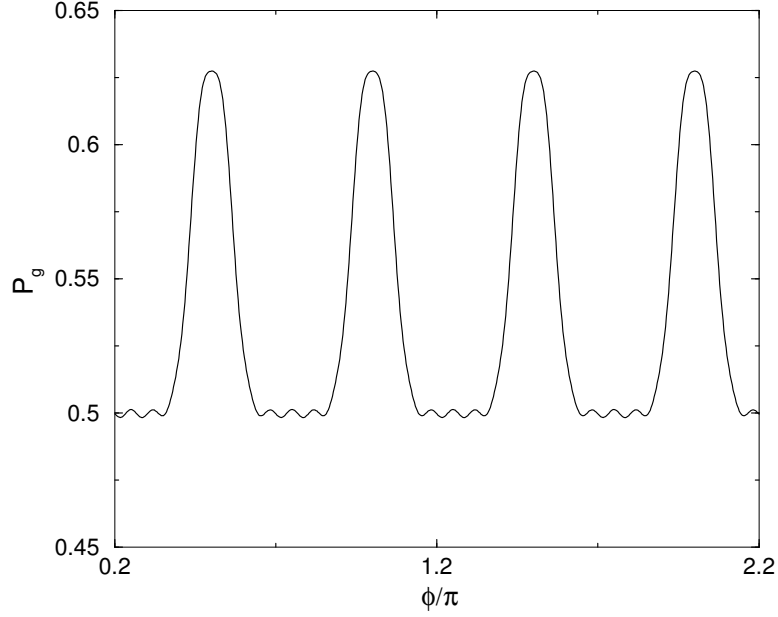


**Figure 2.8:** The probability of detecting probe atom in its ground state as a function of  $\phi$  for the generated superposition (2.4). The interaction time for the probe atom is selected such that  $gt_p = \pi$ .

mesoscopic states. In Fig. 2.8, we plot the probability of detecting the probe atom in its lower state with  $\phi$ . It shows four peaks at the positions of the four states of the field in the generated superposition state.

## 2.5 Effects of non-unity Detection Efficiency

In this section, we follow the argument of Davidovich *et. al.* [29] to show that the detection efficiency is not a serious issue in the generation of state (2.4). After passing the first atom  $A$  through the cavity, the field state is projected

$$|C_A\rangle = N \left( e^{i\eta_1 + \pi/4} |\alpha e^{i\pi/4}\rangle + e^{i\theta_1} |\alpha e^{-i\pi/4}\rangle \right), \quad (2.56)$$

where the velocity of atom  $A$  is selected such that the phase change in the cavity field  $\phi = \pi/4$ . If one atom similar to atom  $A$  passes through the cavity undetected, the combined state will be

$$\begin{aligned} |\psi'\rangle &= N e^{i(\eta_1 + \pi/4)} \left( e^{i\eta_1 + \pi/4} |\alpha' e^{i\pi/2}\rangle + e^{i\theta_1} |\alpha'\rangle \right) |e\rangle \\ &+ N e^{i\theta_1} \left( e^{i\eta_1 + \pi/4} |\alpha'\rangle + e^{i\theta_1} |\alpha' e^{-i\pi/2}\rangle \right) |g\rangle, \end{aligned} \quad (2.57)$$

where  $\alpha' = \alpha e^{-i\delta t_1}$ . We trace out the atomic state as the atom passes undetected, the cavity field will be in the state

$$|C'_A\rangle = N' \left[ e^{i\eta_1 + \pi/4} (|\alpha'\rangle + |i\alpha'\rangle) + e^{i\theta_1} (|\alpha'\rangle + |-i\alpha'\rangle) \right]. \quad (2.58)$$

Now if the second atom  $B$  enters the cavity and detected after passing the cavity in earlier defined states. The velocity of second atom is chosen such that it changes phase of cavity field by  $\pi/2$ . The detection of second atom will project the cavity field in the state

$$\begin{aligned} |C_B\rangle = & \frac{N'}{2} \left[ e^{i\eta_1 + \eta_2 + 3\pi/4} (|\alpha'' e^{i\pi/2}\rangle + |i\alpha'' e^{i\pi/2}\rangle) \right. \\ & + e^{i(\theta_1 + \eta_2 + \pi/2)} (|\alpha'' e^{i\pi/2}\rangle + |-i\alpha'' e^{i\pi/2}\rangle) \\ & + e^{i\eta_1 + \theta_2 + \pi/4} (|\alpha'' e^{-i\pi/2}\rangle + |i\alpha'' e^{-i\pi/2}\rangle) \\ & \left. + e^{i(\theta_1 + \theta_2)} (|\alpha'' e^{-i\pi/2}\rangle + |-i\alpha'' e^{-i\pi/2}\rangle) \right], \quad (2.59) \end{aligned}$$

where  $\alpha'' = \alpha' e^{-i\delta t_2}$ . For earlier defined conditions on phases in the method for preparing the compass state (2.4),  $\theta_1 = \eta_1 + \pi/4$  and  $\theta_2 = \eta_2 + \pi/2$  the state (2.59) becomes same as state (2.25). In a similar way one can see that the prepared state will be a compass state if one atom similar to atom  $B$  passes undetected between the atoms  $A$  and  $B$ .

## 2.6 Decoherence of the Generated Superposition State

Next we study the decoherence of the generated superposition state (2.4). This can be done using the master equation

$$\dot{\rho} = -\frac{\kappa}{2} (a^\dagger a \rho - 2a \rho a^\dagger + \rho a^\dagger a), \quad (2.60)$$

where  $\kappa$  is cavity field decay parameter and we carry analysis in the absence of thermal photons. For initial state (2.4), we find the density matrix after time  $t$

$$\begin{aligned} \rho(t) = & \frac{1}{16} [ (|\alpha_t\rangle\langle\alpha_t| + |-\alpha_t\rangle\langle-\alpha_t| + |i\alpha_t\rangle\langle i\alpha_t| + |-i\alpha_t\rangle\langle -i\alpha_t|) \\ & + e^{-2|\alpha|^2(1-e^{-\kappa t})} (|\alpha_t\rangle\langle-\alpha_t| + |-\alpha_t\rangle\langle\alpha_t| + |i\alpha_t\rangle\langle -i\alpha_t| + |-i\alpha_t\rangle\langle i\alpha_t|) \\ & + e^{-|\alpha|^2(1-i)(1-e^{-\kappa t})} (|\alpha_t\rangle\langle i\alpha_t| + |-i\alpha_t\rangle\langle\alpha_t| + |-\alpha_t\rangle\langle -i\alpha_t| + |i\alpha_t\rangle\langle -\alpha_t|) \\ & + e^{-|\alpha|^2(1+i)(1-e^{-\kappa t})} (|i\alpha_t\rangle\langle\alpha_t| + |\alpha_t\rangle\langle -i\alpha_t| + |-i\alpha_t\rangle\langle -\alpha_t| + |-\alpha_t\rangle\langle i\alpha_t|) ]; \quad (2.61) \\ & \alpha_t = \alpha e^{-\kappa t/2}. \end{aligned}$$

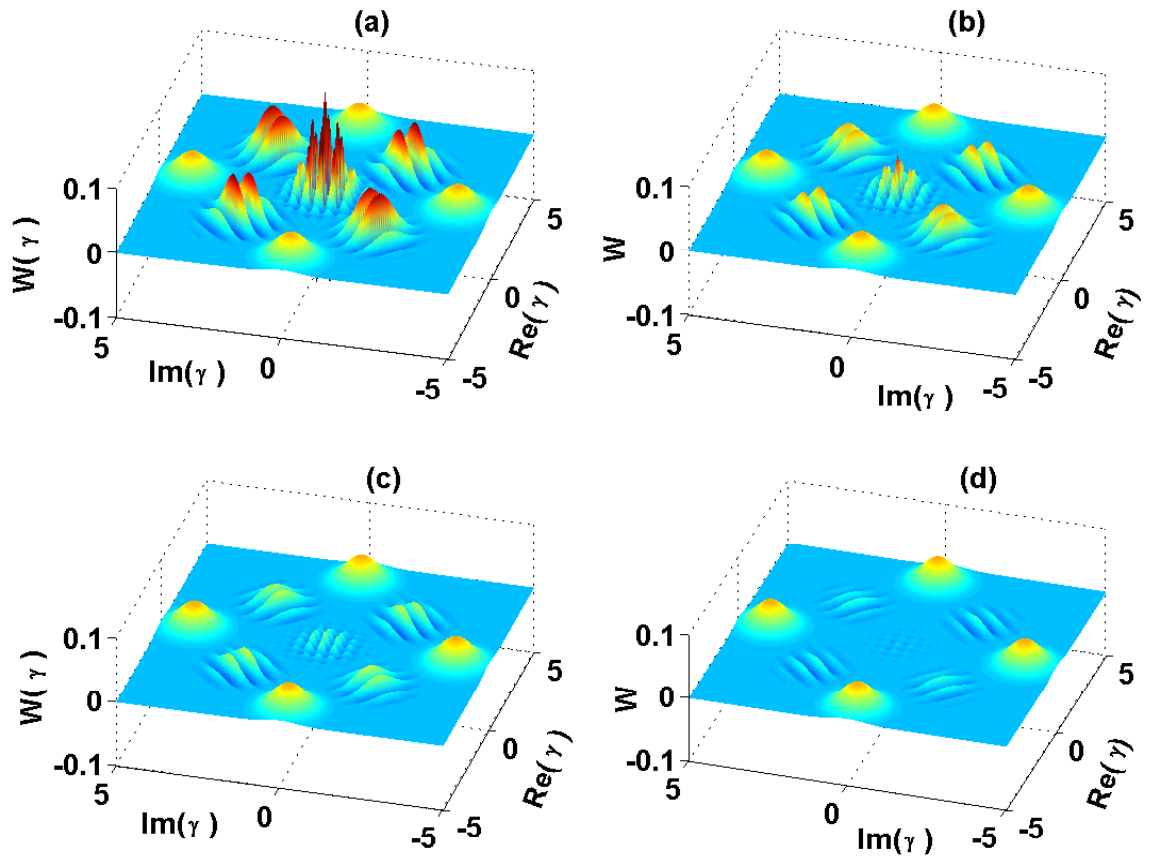


**Figure 2.9:** The decoherence of the state (2.4) in terms of Wigner function at different times, (a) for  $\kappa t = 0$ , (b) for  $\kappa t = 1/2|\alpha|^2$ , (c) for  $\kappa t = 1/|\alpha|^2$ , (d) for  $\kappa t = 2/|\alpha|^2$ , for  $|\alpha| = 4$ .

In Eq. (2.61), the second, third, and the fourth terms reflect the coherent character of the superposition. These are the terms which decohere due to interaction with the environment. The contribution to the Wigner function from the second term in Eq. (2.61) is

$$\frac{e^{-2|\gamma|^2-2|\alpha|^2(1-e^{-\kappa t})}}{4\pi} \{\cos[i(\alpha\gamma^* - \alpha^*\gamma)] + \cos[(\alpha\gamma^* + \alpha^*\gamma)]\}, \quad (2.62)$$

which decays as  $e^{-2|\alpha|^2(1-e^{-\kappa t})} \approx e^{-2|\alpha|^2\kappa t}$  for  $\kappa t \ll 1$ . This term arises from the coherence between the pair  $|\alpha\rangle, |-\alpha\rangle$  and the pair  $|i\alpha\rangle, |-i\alpha\rangle$ , and is responsible for the central sub-Planck structures. The term in curly bracket can be written as  $\{\cos[2\alpha|\gamma|\sin\theta] + \cos[2\alpha|\gamma|\cos\theta]\}$ . Thus in any direction  $\theta \neq n\pi/2$  one has an interference pattern which arises from two cosine terms with different periodicity. Thus the sub-Planck structures decohere as  $e^{-2|\alpha|^2\kappa t}$ . The third and the fourth terms in Eq. (2.61) show the coherence between other pairs of coherent states, and decay as  $e^{-|\alpha|^2\kappa t}$ . In Fig. 2.9, we plot the decoherence of the state (2.4) in terms of the Wigner function at different times. As time progresses in Fig. 2.9 from (a) to (d), the central interference patterns decay faster and disappear earlier than the interference fringes between the coherent states, say  $|\alpha\rangle$  and  $|i\alpha\rangle$ , disappear. This is clear from the equation (2.61) that the central interference patterns decohere two times faster than the interference fringes between the coherent states like  $|\alpha\rangle$  and  $|i\alpha\rangle$ .

## 2.7 Summary

We have discussed the properties of the compass state for radiation field and the methods of generating a compass state using the dispersive as well as resonant interaction between atoms and field inside the cavity. The conditional measurements enable one to study some aspects of the mesoscopic superposition of coherent states. We have shown that the nonunity detection efficiency in the preparation of the compass state is not a serious issue. We have discussed the properties of the quasi-probability distributions of the generated state. We have discussed the time scale over which the state decoheres and discussed the methods for monitoring the generated state. Another way to detect such superposition is by doing tomography [48] of such states.

---

### Ramsey Interferometry with Quantized Field

---

Entanglement is one of the most interesting phenomena in quantum mechanics. A large number of methods exist for generating various types of entangled states [7, 11, 49, 50]. Many of these states have been implemented in quantum information processing [12, 13, 51, 52]. In chapter 1, we have discussed nonlocal characteristics [53] of entanglement and shown how cavities can be used to generate atom-atom and atom-field entangled states. In this chapter, we discuss how one can generate entangled state of two spatially separated cavities. We note that entanglement between two modes in a single cavity has been reported by Rauschenbeutel et al [54]. Further, in a recent experiment, the entangled spin-state of two macroscopic atomic samples has been realized by passing a polarized light pulse [55].

We consider two spatially separated high quality cavities aligned along their axis and atoms are passed one by one through the cavities. Thus, our arrangement is equivalent to the Ramsey interferometer [56]. We discuss the role of quantum statistics of the fields in Ramsey interferometry and examine the conditions on the fields so that interference fringes are obtained. In the case of fixed number of photons in the cavities, interference does not occur in the excitation probability of a single atom [57]. We show how the interference can be restored by passing successively two atoms through the cavities and measuring atom-atom correlations [58]. We generate various entangled states by passing a single or two atoms through cavities and show entanglement can be transferred from fields to atoms and viceversa.

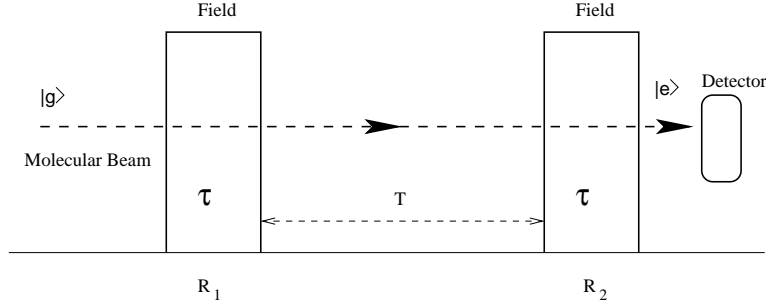


**Figure 3.1:** Ramsey interferometry with two spatially separated fields.

### 3.1 Ramsey Interferometry

Ramsey proposed a new technique of doing molecular beam resonance experiments [56]. He used two spatially separated fields instead of using uniform single field as shown in Fig. 3.1. Ramsey technique has advantage of higher precision measurement over an experiment with continuous single field. The higher precision in Ramsey technique is due to the occurrence of sharper resonance curves with two spatially separated fields. It was originally proposed as a technique in the microwave domain [56] which was then extended to studies in optical domain [59]. Achieving higher resolution by using two separated fields in molecular or atomic beam experiments can be understood as follows.

Consider a two level atom having upper level  $|e\rangle$  and lower level  $|g\rangle$ . The state of the atom at anytime  $t$  is given by

$$|\psi_a(t)\rangle = c_e(t)|e\rangle + c_g(t)|g\rangle. \quad (3.1)$$

The field in each Ramsey zones is  $E(t) = \mathcal{E} \cos \omega t$ . When an atom enters in the field, the atom-field interaction is given by

$$\begin{aligned} H_I &= -(\mathcal{P}_{eg}|e\rangle\langle g| + \mathcal{P}_{ge}|g\rangle\langle e|)\mathcal{E} \cos(\omega t), \\ &= -\hbar(\Omega_R|e\rangle\langle g| + \Omega_R^*|g\rangle\langle e|) \cos(\omega t), \end{aligned} \quad (3.2)$$

where  $\mathcal{P}_{eg} = \mathcal{P}_{ge}^*$ , are transition dipole matrix elements and  $|\Omega_R| = |\mathcal{P}_{eg}\mathcal{E}/\hbar|$  is Rabi frequency. Thus the Hamiltonian of the atom-field system is given by

$$H = \hbar\omega_e|e\rangle\langle e| + \hbar\omega_g|g\rangle\langle g| - \hbar(\Omega_R|e\rangle\langle g| + \Omega_R^*|g\rangle\langle e|)(e^{i\omega t} + e^{-i\omega t}), \quad (3.3)$$

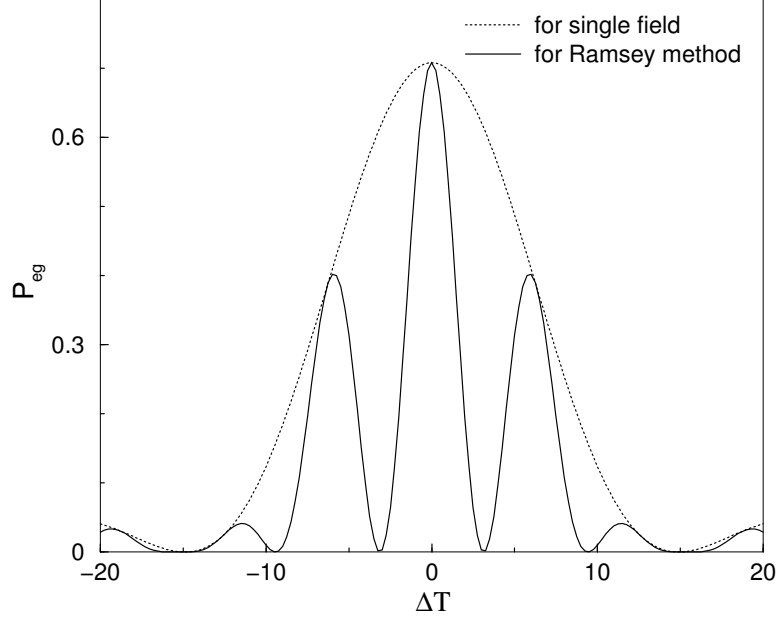


**Figure 3.2:** Comparison between resonance curves using single field and Ramsey method of two spatially separated fields.

where  $\omega_e$  and  $\omega_g$  are frequencies corresponding to the higher and the lower energy levels, respectively. Using interaction picture and rotating wave approximation, the Hamiltonian  $H$  reduces to

$$H = -\frac{\hbar}{2}(\Omega_R e^{i\Delta t}|e\rangle\langle g| + \Omega_R^* e^{-i\Delta t}|g\rangle\langle e|), \quad \text{where } \Delta = (\omega_e - \omega_g) - \omega. \quad (3.4)$$

Therefore, the Hamiltonian for Ramsey method is given by

$$H = -\frac{\hbar}{2}(\Omega_R e^{i\Delta t}|e\rangle\langle g| + \Omega_R^* e^{-i\Delta t}|g\rangle\langle e|), \quad \text{for } 0 < t \leq \tau, T + \tau < t \leq T + 2\tau \quad (3.5)$$

$$H = 0, \quad \text{for } \tau < t \leq T + \tau.$$

Using atomic state (3.1) and Hamiltonian (3.5), Schrödinger equation takes the form

$$\dot{c}_e(t) = \frac{i\Omega_R}{2} e^{i\Delta t} c_g(t), \quad \dot{c}_g(t) = \frac{i\Omega_R^*}{2} e^{-i\Delta t} c_e(t), \quad \text{in Ramsey zones,} \quad (3.6)$$

$$\dot{c}_e(t) = \dot{c}_g(t) = 0 \quad \text{every where else.}$$

Using differential equation (3.6), the evolution of the atomic state can be calculated. The probability of detecting the atom in a particular state  $|\psi_f\rangle$  after total time  $T + 2\tau$  is defined

as

$$P_{fa} = \langle \psi_f | \psi_a(T + 2\tau) \rangle \langle \psi_a(T + 2\tau) | \psi_f \rangle. \quad (3.7)$$

If an atom is coming in lower state  $|g\rangle$ , the probability of detecting the atom in the upper state  $|e\rangle$  is found to be, for spatially separated fields

$$P_{eg} = \frac{|\Omega_R|^2}{\Omega^2} \sin^2\left(\frac{\Omega\tau}{2}\right) \left\{ \cos^2\left(\frac{\Omega\tau}{2}\right) \cos^2\left(\frac{\Delta T}{2}\right) + \frac{\Delta^2}{\Omega^2} \sin^2\left(\frac{\Omega\tau}{2}\right) \sin^2\left(\frac{\Delta T}{2}\right) \right\}, \quad (3.8)$$

and for single field

$$P_{eg} = \frac{|\Omega_R|^2}{\Omega^2} \sin^2\left(\frac{\Omega\tau}{2}\right). \quad (3.9)$$

Here  $\Omega = \sqrt{\Delta^2 + \Omega_R^2}$ . Generally  $\Omega\tau$  is a small number, so we can drop the terms having  $\sin^4(\Omega\tau/2)$  and the expression (3.8) simplifies to

$$P_{eg} \approx \frac{|\Omega_R|^2}{\Omega^2} \sin^2\left(\frac{\Omega\tau}{2}\right) \cos^2\left(\frac{\Delta T}{2}\right). \quad (3.10)$$

In Fig. 3.2, we show the transition probabilities  $P_{eg}$ , for the two separated fields and for the single field, defined by equations (3.9) and (3.10). Clearly, the presence of cosine term in (3.10) modulates the transition probability and the resolution in the resonance curves becomes proportional to  $1/\Delta T$ .

In an interferometer interference occurs when two monochromatic coherent waves travel to the detector through two different ways. In Ramsey method of two separated fields, a particular transition in atomic states occurs through two different ways and interference fringes appear in the transition probability similar to wave interferometer. For the transition of an atom from its lower state  $|g\rangle$  to higher state  $|e\rangle$  in Ramsey interferometer, the atom follows two different paths

$$|g\rangle \xrightarrow{\text{first zone}} |g\rangle \xrightarrow{\text{second zone}} |e\rangle, \quad (3.11)$$

$$|g\rangle \xrightarrow{\text{first zone}} |e\rangle \xrightarrow{\text{second zone}} |e\rangle. \quad (3.12)$$

The existence of fringes in the transition probability has been interpreted as due to quantum interference between the transition amplitudes [56], therefore Ramsey method is a way of doing atomic interferometry.

More recently, Ramsey interferometry has been used very successfully in the studies of quantum entanglement resulting from the interaction of atoms with radiation in a high quality cavity. Haroche and coworkers [7, 60, 61] have detected a variety of cavity-QED

effects [62] using Ramsey interferometry. Other potential applications of Ramsey interferometry are in the context of quantum nondemolition measurements [43], complementarity test [61], quantum gates [51], EPR states [7] etc. Ramsey technique has also been suggested for the measurement of phase diffusion in a micromaser [63]. Most of these studies consider the field in each Ramsey zone as a coherent field which does not evolve even though it is interacting with the atom.

### 3.2 Ramsey Interferometry with Quantized Fields

These days interference effects at a single photon or few photon levels are becoming quite common [64, 65, 66, 67], it is natural to enquire how the results of Ramsey interferometry would be modified if the coherent field in each Ramsey zone is replaced by a quantized field [68].

We consider a high quality cavity [62] as the Ramsey zone of quantized field. If the number of photons in the cavity is large and the field has a well-defined phase, then it would approach to the classical Ramsey interferometry. We thus consider the situation shown in the Fig. 3.3. An atom with two levels  $|e\rangle$  and  $|g\rangle$ , with frequency separation  $\omega_0$ , interacts with two single-mode cavities with identical frequencies  $\omega$ . Let the annihilation and creation operators in the  $i$ -th cavity be denoted by  $a_i$  and  $a_i^\dagger$ , respectively. For the situation shown in the Fig. 3.3, the Hamiltonian in the interaction picture is

$$\begin{aligned}
 H_1 &= \hbar g_1 (|e\rangle\langle g| a_1 e^{i\Delta t} + a_1^\dagger |g\rangle\langle e| e^{-i\Delta t}) & 0 < t \leq \tau_1, \\
 H_1 &= 0 & \tau_1 < t \leq T + \tau_1, \\
 H_1 &= \hbar g_2 (|e\rangle\langle g| a_2 e^{i\Delta t} + a_2^\dagger |g\rangle\langle e| e^{-i\Delta t}) & T + \tau_1 < t \leq T + \tau_1 + \tau_2.
 \end{aligned} \tag{3.13}$$

Here  $\Delta = \omega_0 - \omega$  and  $g_i$  is the coupling constant of the atom with the vacuum in the  $i$ -th cavity. Let us consider an initial state with atom in the lower state  $|g\rangle$  and the fields characterized by the state  $\sum_{n,\mu} F_{n,\mu} |n, \mu\rangle$ . Here  $|n\rangle(|\mu\rangle)$  represents the Fock state in first (second) cavity and  $F_{n,\mu}$  is photon distribution function. Let  $\phi_e, \phi_g$  be the phase shifts in  $|e\rangle$  and  $|g\rangle$ , which we might introduce using some external perturbation between the cavities. Using the interaction Hamiltonian (3.13), the time evolution of the state can be calculated.

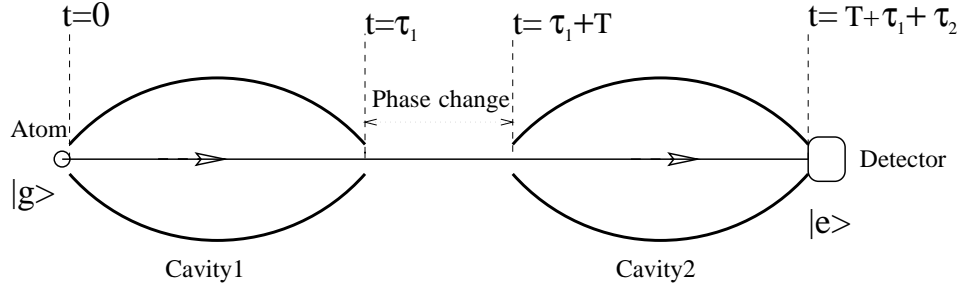


**Figure 3.3:** A schematic arrangement for Ramsey interferometry with quantized fields. Each classical Ramsey zone is replaced by a cavity. There is a phase change between two cavities as  $|e\rangle \rightarrow e^{-i\phi_e}|e\rangle$  and  $|g\rangle \rightarrow e^{-i\phi_g}|g\rangle$ .

The state of the atom and cavity fields is found to be

$$\begin{aligned}
 |\psi(\tau_1 + T + \tau_2)\rangle &= \sum_{n,\mu} [F_{n,\mu} C_{n-1}(\tau_1) C_{\mu-1}(\tau_2) \exp(-i\Delta(\tau_1 + \tau_2)/2 - i\phi_g) \\
 &+ F_{n+1,\mu-1} S_n(\tau_1) S_{\mu-1}(\tau_2) \exp(-i\Delta(\tau_1 + \tau_2 + 2T)/2 - i\phi_e)] |g, n, \mu\rangle \\
 &+ \sum_{n,\mu} [F_{n+1,\mu} S_n^*(\tau_1) C_\mu^*(\tau_2) \exp(i\Delta(\tau_1 + \tau_2)/2 - i\phi_e) \\
 &+ F_{n,\mu+1} C_{n-1}(\tau_1) S_\mu^*(\tau_2) \exp(i\Delta(\tau_1 + \tau_2 + 2T)/2 - i\phi_g)] |e, n, \mu\rangle \quad (3.14)
 \end{aligned}$$

where

$$\begin{aligned}
 C_\alpha(\tau) &= \cos(\Omega_\alpha \tau/2) + \frac{i\Delta}{\Omega_\alpha} \sin(\Omega_\alpha \tau/2) \\
 S_\alpha(\tau) &= \frac{2ig_\alpha \sqrt{\alpha+1}}{\Omega_\alpha} \sin(\Omega_\alpha \tau/2), \\
 \Omega_\alpha &\equiv \sqrt{(\Delta^2 + 4g_\alpha^2(\alpha+1))}, \quad (3.15)
 \end{aligned}$$

$$\alpha = n, \mu \text{ and } g_n = g_1, g_\mu = g_2.$$

The functions  $C_\alpha$  and  $S_\alpha$  describe the dynamics of the atom interacting with a single mode cavity with initial state as a Fock state. Note that  $C_\alpha(S_\alpha)$  gives the probability amplitude of finding the atom in the excited (ground) state given that it was in the excited state at time  $t = 0$ .

The structure of the state clearly suggests that a given final state is reached in two different ways. Consider a measurement in which the outgoing atom is found in the excited state. The probability of excitation  $P_{eg}$  defined by

$$P_{eg} = \text{Tr}_{field} \langle e | \psi(T + \tau_1 + \tau_2) \rangle \langle \psi(T + \tau_1 + \tau_2) | e \rangle \quad (3.16)$$

can be calculated using Eq. (3.14). We find the result

$$P_{eg} = \sum_{n,\mu} |F_{n+1,\mu} X_{n+1,\mu} + e^{i\Delta T + i\phi} F_{n,\mu+1} Y_{n,\mu+1}|^2, \quad (3.17)$$

where

$$\begin{aligned} \phi &= \phi_e - \phi_g \\ X_{n+1,\mu} &= S_n^*(\tau_1) C_\mu^*(\tau_2) \\ Y_{n,\mu+1} &= C_{n-1}(\tau_1) S_\mu^*(\tau_2). \end{aligned} \quad (3.18)$$

A similar result is obtained for  $P_{ge}$ , i.e., the probability of finding the atom in the ground state if initially the atom is in the excited state,

$$P_{ge} = \sum_{n,\mu} |F_{n-1,\mu} X_{n,\mu-1}^* + e^{-i\Delta T + i\phi} F_{n,\mu-1} Y_{n+1,\mu}^*|^2. \quad (3.19)$$

Results (3.17) and (3.19) are important for understanding Ramsey interferometry with quantized fields. These give rise to a number of important consequences as far as the fundamentals of atom-field interaction are concerned. For classical fields, result (3.19) can be modified, since probability amplitude functions  $F_{n,\mu}$  is peaked around average number of photons  $\bar{n}$  and  $\bar{\mu}$ . So in the summation, we can replace

$$\begin{aligned} X_{n,\mu-1} &\rightarrow X_{\bar{n},\bar{\mu}}, \\ Y_{n+1,\mu} &\rightarrow Y_{\bar{n},\bar{\mu}}. \end{aligned} \quad (3.20)$$

Further for large  $n$  and  $\mu$ , make the following replacements:

$$\begin{aligned} F_{n-1,\mu+1} &\rightarrow F_{n,\mu} \\ F_{n,\mu-1} &\rightarrow F_{n,\mu}. \end{aligned} \quad (3.21)$$

For normalized photon probability amplitude functions  $F_{n,\mu}$ , Eq. (3.19) reduces to

$$P_{ge} = |X_{\bar{n},\bar{\mu}}^* + e^{-i\Delta T + i\phi} Y_{\bar{n},\bar{\mu}}^*|^2. \quad (3.22)$$

Equation (3.22) is the result for classical fields.

### 3.3 Dependence of the fringes on quantum statistics of the fields

We now examine the consequences of the quantized nature of the field and, in particular, investigate when the interferences are most pronounced. From result(3.17), we see there are two paths which contribute to the amplitude for detecting the atom in excited state:

$$\begin{aligned} |g, n, \mu\rangle &\rightarrow |e, n-1, \mu\rangle \rightarrow |e, n-1, \mu\rangle, \\ |g, n, \mu\rangle &\rightarrow |g, n, \mu\rangle \rightarrow |e, n, \mu-1\rangle. \end{aligned} \quad (3.23)$$

The interference between these two paths depends on the nature of the photon statistics, i.e., on the functions  $F_{n,\mu}$ . Clearly, if the field in each cavity is in a Fock state  $|n_0, \mu_0\rangle$ , then the interference terms in (3.17) drop out and the two paths (3.23) become independent. This happens even for Fock states with large number of photons. Interferences are obtained as long as the photon statistics is such that the cross terms in (3.17) are nonzero. Consider a situation where detuning  $\Delta$  can be ignored while considering evolution in Ramsey zone, i.e., in each cavity. It can be shown that the cross terms in (3.17) are nonzero if the field statistics is such that,

$$\langle a_1^\dagger \frac{1}{\sqrt{a_1 a_1^\dagger}} \sin(g_1 \tau_1 \sqrt{a_1 a_1^\dagger}) \cos(g_1 \tau_1 \sqrt{a_1^\dagger a_1}) \cos(g_2 \tau_2 \sqrt{a_2 a_2^\dagger}) \frac{1}{\sqrt{a_2 a_2^\dagger}} \sin(g_2 \tau_2 \sqrt{a_2 a_2^\dagger}) a_2 \rangle \neq 0, \quad (3.24)$$

which for small interaction times reduces to

$$\langle a_1^\dagger a_2 \rangle \neq 0. \quad (3.25)$$

Thus, the nature of interference depends on the quantum statistics of the fields in the two Ramsey zones. The conditions (3.24) and (3.25) imply that if the cavities are independent, then the field in each cavity must have a well defined phase for interference to occur. The interference would also not occur if one cavity has a definite number of photons and the other has a field in coherent state. However, interference is obtained if fields in the two cavities are entangled even though the field in each cavity does not have a well-defined phase. In Fig. 3.4, results for classical as well as quantized fields are plotted when each Ramsey zone has a coherent field with average number of photons ( $|\alpha|^2 = 5$ ). Interference fringes for classical fields show higher visibility than in the case of quantized fields.

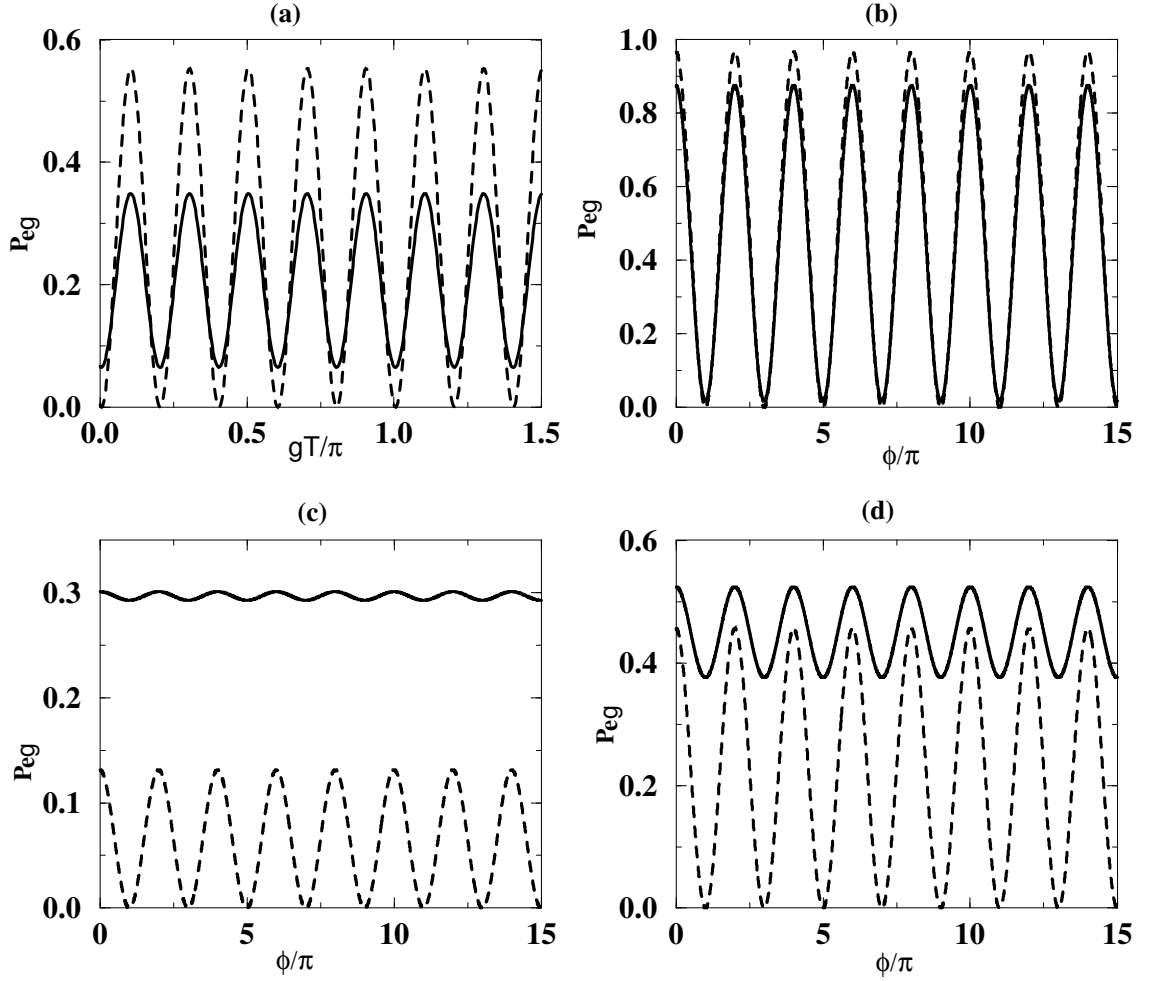


**Figure 3.4:** Interference fringes in the probability of detecting a single atom in the excited state when the atom is initially in the ground state for quantized (solidlines) and classical (dashedlines) fields. The parameters are (a)  $g\tau = \pi$ ,  $\Delta/g = 10$ ,  $\phi = 0$ ,  $V_q = 0.68$  (b)  $\Delta = 0$ ,  $g\tau = \pi/8$ ,  $V_q = 0.96$  (c)  $\Delta = 0$ ,  $g\tau = \pi/4$ ,  $V_q = 0.14E - 01$  and (d)  $\Delta = 0$ ,  $g\tau = \pi/2$ ,  $V_q = 0.16$ . The common parameters for above graphs are  $|\alpha|^2 = 5$ ,  $\tau_1 = \tau_2 = \tau$ ,  $g_1 = g_2 = g$ ,  $V_c = 1.00$ .  $V_c, V_q$  are the visibilities for classical fields and quantized fields.

### 3.3.1 Ramsey fringes with fields at single photon level

Having shown that Ramsey fringes vanish if each cavity contains one photon, the next question is what happens if the field in each cavity is at single photon level [65]? For this purpose, we consider a case where each cavity is pumped by a weak coherent state so that the initial state of the cavities is

$$|\psi_{cavities}\rangle \cong \frac{1}{(1 + |\alpha|^2)} (|0\rangle + \alpha|1\rangle)(|0\rangle + \alpha e^{i\theta}|1\rangle). \quad (3.26)$$

In this case, the result (3.17) leads to

$$\begin{aligned} P_{eg} &= \frac{4|\alpha|^2}{(1 + |\alpha|^2)^2} \left| \frac{g_1}{\Omega_0} \sin(\Omega_0\tau_1/2) \left( \cos(\Omega_0\tau_2/2) - \frac{i\Delta}{\Omega_0} \sin(\Omega_0\tau_2/2) \right) \right. \\ &\quad \left. + \frac{g_2}{\Omega_0} \sin(\Omega_0\tau_2/2) \exp[i\{\Delta(T + \tau_1/2) + \theta + \phi\}] \right|^2 + O(|\alpha|^4), \end{aligned} \quad (3.27)$$

which for  $\Delta = 0$  and  $g_1\tau_1 = \sqrt{2}g_2\tau_2 = \pi/2$  reduces to

$$P_{eg} = \frac{|\alpha|^2}{(1 + |\alpha|^2)^2} \left( 1 + \sin(\pi/\sqrt{2}) \cos(\theta + \phi) \right). \quad (3.28)$$

This leads to high visibility for the fringes (about 80%) though the absolute value of the signal is small. It is clear that the interference in Eq. (3.27) arises from the cross terms in Eq. (3.26), as such cross terms lead to the same final state via two different pathways:

$$\begin{aligned} |g, 1, 0\rangle &\rightarrow |e, 0, 0\rangle \rightarrow |e, 0, 0\rangle, \\ |g, 0, 1\rangle &\rightarrow |g, 0, 1\rangle \rightarrow |e, 0, 0\rangle. \end{aligned} \quad (3.29)$$

The other terms in Eq. (3.26) do not result in interference, since  $|1, 1\rangle$  leads to different final states and  $|0, 0\rangle$  can not produce excitation. It should be noted that Eq. (3.27) is different from the result obtained for classical fields, i.e., when one ignores the back-action of atoms on the field. Recently, an arbitrary superposition of  $|0\rangle$  and  $|1\rangle$  states  $|\psi_n\rangle = \frac{1}{\sqrt{1+|\alpha|^2}}(|0\rangle + \alpha|1\rangle)$  has been realized [66, 67]; here the parameter  $\alpha$  need not be small. Such a state is highly nonclassical and is quite distinct from a coherent state with very small excitation. This nonclassical state also has the important characteristics that the average value of the field is nonzero and thus the off-diagonal elements of the density matrix are nonzero. For such a nonclassical state and for  $\Delta = 0$ , the Ramsey fringes are given by

$$\begin{aligned} P_{eg} &= \frac{|\alpha|^2}{(1 + |\alpha|^2)^2} |\sin(g_1\tau_1) \cos(g_2\tau_2) + \sin(g_2\tau_2) \exp\{i\phi\}|^2 \\ &\quad + \frac{|\alpha|^4}{(1 + |\alpha|^2)^2} \left\{ \sin^2(g_1\tau_1) \cos^2(g_2\sqrt{2}\tau_2) + \cos^2(g_1\tau_1) \sin^2(g_2\tau_2) \right\} \end{aligned} \quad (3.30)$$

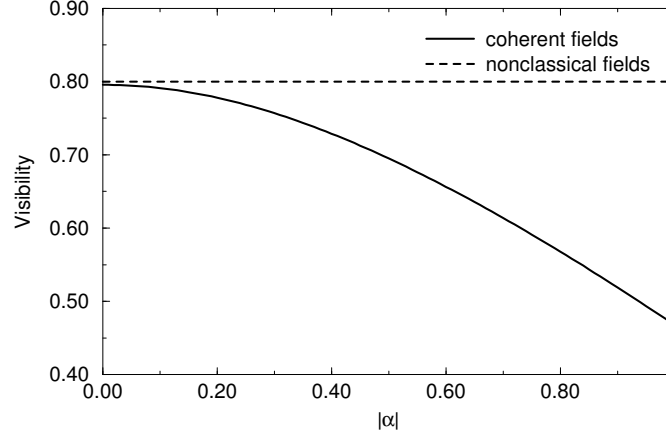


**Figure 3.5:** The visibility of interference fringes vs.  $|\alpha|$  for weak coherent fields (solidline) and for a nonclassical state (dashedline)  $\frac{1}{\sqrt{1+|\alpha|^2}}(|0\rangle + \alpha|1\rangle)$ , with parameters  $g\tau_1 = g\sqrt{2}\tau_2 = \pi/2$  and  $\Delta = 0$ .

For  $g_1\tau_1 = g_2\sqrt{2}\tau_2 = \pi/2$ , it reduces to the previously derived result (3.28). Remarkably, the visibility from result(3.30) does not depend on  $\alpha$ . We show in the Fig. (3.5) a comparison of the visibility in the case of coherent field and a nonclassical field. It may be noted that for the state  $|0\rangle + \alpha|1\rangle$ , the P-distribution is highly singular. We note that in the context of cavity quantum electrodynamics the state  $|\psi_n\rangle$  can be produced by following scheme [69]. We could consider a resonant cavity in vacuum state. If a two level atom in the superposition state  $\frac{1}{\sqrt{1+|\alpha|^2}}(|g\rangle + \alpha|e\rangle)$  is sent through the cavity with the interaction time adjusted so that the atom can emit one photon in the cavity, then the state of the cavity would be  $|\psi_n\rangle$ .

### 3.3.2 Photon-photon interaction mediated by a single atom and quantum entanglement of two cavities

It is well known in nonlinear optics in a macroscopic system that the fields effectively interact and one knows many examples of three wave and four wave interactions in a medium. Such interactions are significant at macroscopic densities of atoms. In this section, we demonstrate a rather remarkable result that a single atom in a high quality cavity can produce photon-photon interaction. For this purpose, consider an atom in the ground state passing through the two cavity system. We calculate the state of the two cavity system

subject to the condition that the atom at the output is detected in the ground state. Such a conditional field state is found to be

$$\begin{aligned}
 |\psi_{c,g}\rangle &= \langle g|\psi(T + \tau_1 + \tau_2)\rangle, \\
 &= C_{n-1}(\tau_1)C_{\mu-1}(\tau_2) \exp(-i\Delta(\tau_1 + \tau_2)/2 - i\phi_g) |n, \mu\rangle \\
 &+ S_{n-1}(\tau_1)S_{\mu}(\tau_2) \exp(-i\Delta(\tau_1 + \tau_2 + 2T)/2 - i\phi_e) |n-1, \mu+1\rangle. \quad (3.31)
 \end{aligned}$$

This involves a linear combination of states  $|n, \mu\rangle$  and  $|n-1, \mu+1\rangle$  leading to the entanglement of two cavities. We note that the entanglement of two macroscopically separated cavities was proposed by Meystre [70]. In addition, the passage of one atom transfers one photon from the first cavity to the second cavity. The transfer from one cavity to the other will be complete if  $C_{n-1}(\tau_1) = C_{\mu-1}(\tau_2) = 0$ . Other entangled states are also possible; for example, if the atom was initially in the ground state and if it is detected in the excited state, then the conditional state of the cavities is,

$$\begin{aligned}
 |\psi_{c,e}\rangle &= \langle e|\psi(T + \tau_1 + \tau_2)\rangle, \\
 &= S_{n-1}^*(\tau_1)C_{\mu}^*(\tau_2) \exp(i\Delta(\tau_1 + \tau_2)/2 - i\phi_e) |n-1, \mu\rangle \\
 &+ C_{n-1}(\tau_1)S_{\mu-1}^*(\tau_2) \exp(i\Delta(\tau_1 + \tau_2 + 2T)/2 - i\phi_g) |n, \mu-1\rangle. \quad (3.32)
 \end{aligned}$$

We may also note that the entanglement of two modes in the same cavity has been achieved by Rauschenbeutel et al [54].

### 3.4 Two Atom Interferometry

In previous section, we considered the possibility of producing entanglement between the two cavities by conditional detection of the atomic state [50]. We next examine how such entanglement (3.32) can be detected. From our previous discussion leading to Eq. (3.17) and Eq. (3.24) it is clear that if we send a second atom and measure its excitation probability, then such a probability would exhibit interference fringes.

For a second atom coming in the ground state  $|g\rangle$  and detected in the excited state,

following are the possible pathways:

$$\begin{aligned}
 |n-1, \mu\rangle|g\rangle &\rightarrow |n-1, \mu\rangle|g\rangle \rightarrow |n-1, \mu-1\rangle|e\rangle, \\
 |n, \mu-1\rangle|g\rangle &\rightarrow |n-1, \mu-1\rangle|e\rangle \rightarrow |n-1, \mu-1\rangle|e\rangle, \\
 |n-1, \mu\rangle|g\rangle &\rightarrow |n-2, \mu\rangle|e\rangle \rightarrow |n-2, \mu\rangle|e\rangle, \\
 |n, \mu-1\rangle|g\rangle &\rightarrow |n, \mu-1\rangle|g\rangle \rightarrow |n, \mu-2\rangle|e\rangle.
 \end{aligned} \tag{3.33}$$

In summary, the system as a whole starting with an initial state  $|n, \mu, g_1, g_2\rangle$  has two different pathways leading to the detection of the atom-cavity system in state  $|n-1, \mu-1, e_1, e_2\rangle$ .

$$\begin{aligned}
 |n, \mu, g_1, g_2\rangle &\rightarrow |n-1, \mu, e_1, g_2\rangle \rightarrow |n-1, \mu-1, e_1, e_2\rangle, \\
 |n, \mu, g_1, g_2\rangle &\rightarrow |n, \mu-1, e_1, g_2\rangle \rightarrow |n-1, \mu-1, e_1, e_2\rangle.
 \end{aligned} \tag{3.34}$$

The joint probability of detecting both atoms in the excited state  $P_{g_1 g_2}^{e_1 e_2}$  can be used for doing atomic interferometry even if each cavity is in Fock state. This is reminiscent of photon-photon correlation measurements with light produced in the process of down conversion. Mandel and coworkers [71] carried out a series of measurements with photons from a down converted source where they reported no interferences in the measurement of mean intensities, whereas photon-photon correlation exhibited a variety of interference phenomena. In the context of Ramsey interferometry with quantized fields, we suggest a measurement of the atom-atom correlation. An explicit form of the joint detection probability can be obtained following Jaynes-Cummings dynamics. A long calculation leads to the following expression for the joint probability if the initial state of the cavities is  $|n, \mu\rangle$ :

$$\begin{aligned}
 P_{g_1 g_2}^{e_1 e_2} = & \left| S_{n-1}(\tau_1) S_{n-2}(\tau_1') C_\mu^*(\tau_2) C_\mu^*(\tau_2') \right|^2 + \left| C_{n-1}(\tau_1) C_{n-1}(\tau_1') S_{\mu-1}(\tau_2) S_{\mu-2}(\tau_2') \right|^2 \\
 & + \left| S_{n-1}(\tau_1') C_{n-1}(\tau_1) S_{\mu-1}(\tau_2) C_{\mu-1}^*(\tau_2') + S_{n-1}(\tau_1) C_{n-2}(\tau_1') S_{\mu-1}(\tau_2) C_\mu^*(\tau_2) \right. \\
 & \left. \exp[i(\Delta(T' - T) + \phi' - \phi)] \right|^2. \tag{3.35}
 \end{aligned}$$

Here, we allow the possibility of different interaction times and phases (denoted by a dash) for the second atom. In the special case where  $\Delta = 0, g_1 = g_2, \tau_1 = \tau_2 = \tau_1' = \tau_2'$  and  $g\tau = \pi/4$  and when initially cavities are in state  $|1, 1\rangle$ , the joint detection probability has

the form

$$\begin{aligned} P_{g_1 g_2}^{e_1 e_2} &= \frac{1}{16} + \frac{1}{4} \cos^2(\pi/2\sqrt{2}) + \frac{1}{4} \cos(\pi/2\sqrt{2}) \cos(\phi' - \phi) \\ &= 0.1118 + 0.1110 \cos(\phi' - \phi). \end{aligned} \quad (3.36)$$

Interference fringes with almost 100% visibility are obtained. Thus, two atom interferometry could produce perfect visibility in the situations where single atom interferometry exhibits no interferences. Other joint detection probabilities like finding one atom in the excited state and the other in the ground state also display interference fringes. An interesting situation also corresponds to sending both atoms in the excited state and measuring the final states of the two atoms. In the case when initially cavities are in the state  $|0, 0\rangle$  and  $\Delta = 0$ , the expression for the probability of detecting both the atoms in their ground states has the form

$$\begin{aligned} P_{e_1 e_2}^{g_1 g_2} &= \sin^2(g_1 \tau_1) \sin^2(g_1 \sqrt{2} \tau_1') + \sin^2(g_2 \tau_2) \sin^2(g_2 \sqrt{2} \tau_2') \cos^2(g_1 \tau_1) \cos^2(g_1 \tau_1') + \\ &\quad \left| \cos(g_1 \tau_1) \sin(g_1 \tau_1') \sin(g_2 \tau_2) \cos(g_2 \tau_2') + \sin(g_1 \tau_1) \cos(g_1 \sqrt{2} \tau_1') \sin(g_2 \tau_2') e^{i(\phi - \phi')} \right|^2. \end{aligned} \quad (3.37)$$

Consider the case when  $g_1 \sqrt{2} \tau_1' = g_2 \sqrt{2} \tau_2' = \pi$  and  $g_1 \tau_1 = g_2 \tau_2 = \pi/4$ . The probability of detecting both atoms in the ground states is given by

$$\begin{aligned} P_{e_1 e_2}^{g_1 g_2} &= \frac{1}{2} \left| \frac{1}{\sqrt{2}} \sin \frac{\pi}{\sqrt{2}} \cos \frac{\pi}{\sqrt{2}} - \sin \frac{\pi}{\sqrt{2}} \exp[i(\phi - \phi')] \right|^2, \\ &= 0.4327 + 0.3835 \cos(\phi - \phi'). \end{aligned} \quad (3.38)$$

The visibility of fringes in two atom interferometry is quite significant. We next show how two atom interferometry can be used to produce a variety of entangled states.

### 3.4.1 Preparation of the entangled state $\alpha|2, 0\rangle + \beta|0, 2\rangle$

Consider the situation when two identical atoms are coming in their excited states and each cavity is in vacuum state. The mode of each cavity is in resonance with the atomic transition frequency. If after passing through the cavities both atoms are detected in their

ground states, the state of the field inside the cavities is given by

$$\begin{aligned}
 |\Phi(\tau_1 + T + \tau_2)\rangle &= \sin(g_1\tau_1) \sin(g_1\sqrt{2}\tau'_1) \exp\{-i(\phi_g + \phi'_g)\}|2, 0\rangle \\
 &+ \cos(g_1\tau_1) \cos(g_1\tau'_1) \sin(g_2\tau_2) \sin(g_2\sqrt{2}\tau'_2) \exp\{-i(\phi_e + \phi'_e)\}|0, 2\rangle \\
 &+ \left[ \cos(g_1\tau_1) \sin(g_1\tau'_1) \sin(g_2\tau_2) \cos(g_2\tau'_2) \exp\{-i(\phi_e + \phi'_g)\} \right. \\
 &\left. + \sin(g_1\tau_1) \cos(g_1\sqrt{2}\tau'_1) \sin(g_2\tau'_2) \exp\{-i(\phi_g + \phi'_e)\} \right] |1, 1\rangle. \quad (3.39)
 \end{aligned}$$

The  $|1, 1\rangle$  component drops out for  $g_1\tau'_1 = g_2\tau'_2 = \pi$  and the cavities will be in the entangled state

$$\begin{aligned}
 |\Phi(\tau_1 + T + \tau_2)\rangle &= \sin(g_1\tau_1) \sin(\pi\sqrt{2}) \exp[-i(\phi_g + \phi'_g)]|2, 0\rangle \\
 &- \cos(g_1\tau_1) \sin(g_2\tau_2) \sin(\pi\sqrt{2}) \exp[-i(\phi_e + \phi'_e)]|0, 2\rangle. \quad (3.40)
 \end{aligned}$$

This entangled state is very interesting; we can change the degree of entanglement by changing the value of  $g_1\tau_1$  and  $g_2\tau_2$ . The state will be maximally entangled for  $g_1\tau_1 = \pi/4$  and  $g_2\tau_2 = \pi/2$ . This can be seen as first atom comes in excited state  $|e\rangle$ , interacts with the first cavity for a time such that  $g_1\tau_1 = \pi/4$ . The interaction is like an interaction with a  $\pi/2$  pulse; the state of the system evolves into

$$|e, 0, 0\rangle \rightarrow \frac{1}{\sqrt{2}}(|e, 0, 0\rangle - i|g, 1, 0\rangle). \quad (3.41)$$

In the second cavity, the interaction is a  $\pi$  pulse interaction and then the state of the total system becomes,

$$\frac{1}{\sqrt{2}}(|e, 0, 0\rangle - i|g, 1, 0\rangle) \rightarrow -\frac{i}{\sqrt{2}}(|g, 1, 0\rangle + |g, 0, 1\rangle). \quad (3.42)$$

Thus, after passing the first atom, the state of the fields in the cavities is

$$|\psi_1\rangle = -\frac{i}{\sqrt{2}}(|1, 0\rangle + |0, 1\rangle). \quad (3.43)$$

The second atom comes in the excited state  $|e\rangle$ , interacts with the fields inside the cavities for times  $\tau'_1$  and  $\tau'_2$  such that  $g_1\tau'_1 = g_2\tau'_2 = \pi$ , and after passing through the cavities the atom is detected in the ground state  $|g\rangle$ , so the atom can follow the two paths. The first path is

$$|e\rangle|1, 0\rangle \rightarrow \cos(\pi\sqrt{2})|e, 1, 0\rangle - i\sin(\pi\sqrt{2})|g, 2, 0\rangle \rightarrow -i\sin(\pi\sqrt{2})|g, 2, 0\rangle - \cos(\pi\sqrt{2})|e, 1, 0\rangle, \quad (3.44)$$

The second path is

$$|e\rangle|0, 1\rangle \rightarrow -|e, 0, 1\rangle \rightarrow i \sin(\pi\sqrt{2})|g, 0, 2\rangle - \cos(\pi\sqrt{2})|e, 0, 1\rangle. \quad (3.45)$$

Thus, passing both the atoms initially in the excited states and subsequently detecting them in their ground states, we obtain a maximally entangled state

$$|\psi_2\rangle = \frac{1}{\sqrt{2}} \sin(\pi\sqrt{2}) \left( \exp[-i(\phi_g + \phi'_g)]|2, 0\rangle - \exp[-i(\phi_e + \phi'_e)]|0, 2\rangle \right), \quad (3.46)$$

of the fields inside the cavities. The phase terms in Eq. (3.46) come from the phase change in the region between the cavities. Now, if we pass another atom initially in the excited state  $|e\rangle$  through the cavities having field in state (3.46) and the atom is detected in its ground state  $|g\rangle$  after passing through the cavities, an entangled state of three photons is generated. The degree of entanglement is controlled by the selection of interaction times in the cavities. For a special case, a three photons maximally entangled state,

$$|\psi_3\rangle = -\frac{i}{\sqrt{2}} \sin(\pi\sqrt{2}) \sin(\pi\sqrt{3}) \left[ e^{-i(\phi_g + \phi'_g + \phi''_g)}|3, 0\rangle + e^{-i(\phi_e + \phi'_e + \phi''_e)}|0, 3\rangle \right], \quad (3.47)$$

is generated if we choose interaction times  $\tau_1''$  and  $\tau_2''$  for third atom such that  $g_1\tau_1'' = g_2\tau_2'' = \pi$ .

### 3.4.2 Entanglement Transfer from Fields to Atoms

Here we show how entanglement of fields [50, 55] is transferred to the atoms. For this purpose, consider the fields inside the cavities are in an entangled state:

$$|\psi_{cf}\rangle = \alpha|0, 1\rangle + \beta|1, 0\rangle. \quad (3.48)$$

An atom initially in the ground state  $|g\rangle$  is passed through the cavities and the fields inside the cavities are in resonance with atomic transition frequency; then the state of the cavity-atom system is

$$\begin{aligned} |\psi_4\rangle &= \left\{ \alpha \cos(g_2\tau_2)e^{-i\phi_g} - \beta \sin(g_1\tau_1) \sin(g_2\tau_2)e^{-i\phi_e} \right\} |g, 0, 1\rangle + \beta \cos(g_1\tau_1)e^{-i\phi_e} |g, 1, 0\rangle \\ &\quad - i \left( \alpha \sin(g_2\tau_2)e^{-i\phi_g} + \beta \sin(g_1\tau_1) \cos(g_2\tau_2)e^{-i\phi_e} \right) |e, 0, 0\rangle. \end{aligned} \quad (3.49)$$

If another atom coming in the ground state  $|g\rangle$ , interacts with the fields in both the cavities for the times  $\tau_1'$  and  $\tau_2'$  such that  $g_1\tau_1' = g_2\tau_2' = \pi/2$ , then the state of the cavity-atom system

is

$$\begin{aligned}
 |\psi_5\rangle &= -i \left( \alpha \sin(g_2\tau_2) e^{-i(\phi_g + \phi'_g)} + \beta \sin(g_1\tau_1) \cos(g_2\tau_2) e^{-i(\phi_e + \phi'_g)} \right) |e, g\rangle |0, 0\rangle \\
 &- i \left( \alpha \cos(g_2\tau_2) e^{-i(\phi_g + \phi'_g)} + \beta \sin(g_1\tau_1) \sin(g_2\tau_2) e^{-i(\phi_e + \phi'_g)} \right) |g, e\rangle |0, 0\rangle \\
 &- \beta \cos(g_1\tau_1) e^{-i(\phi_e + \phi'_g)} |g, g\rangle |1, 0\rangle.
 \end{aligned} \tag{3.50}$$

If we choose the interaction time for first atom in first cavity such that  $g_1\tau_1 = \pi/2$ , the state (3.50) becomes

$$\begin{aligned}
 |\psi_6\rangle &= -i \left( \alpha \sin(g_2\tau_2) e^{-i(\phi_g + \phi'_g)} + \beta \cos(g_2\tau_2) e^{-i(\phi_e + \phi'_g)} \right) |e, g\rangle |0, 0\rangle \\
 &- i \left( \alpha \cos(g_2\tau_2) e^{-i(\phi_g + \phi'_g)} + \beta \sin(g_2\tau_2) e^{-i(\phi_e + \phi'_g)} \right) |g, e\rangle |0, 0\rangle.
 \end{aligned} \tag{3.51}$$

State (3.51) shows that the atoms are now in entangled state and fields are in independent states, so the entanglement of fields has been transferred to the atoms.

### 3.5 Summary

We have discussed in detail the theory of Ramsey interferometry with quantized fields. The interference is very sensitive to the quantum statistics of the fields in the two Ramsey zones. We have derived general conditions for interference to occur. We have shown how an analog of Hanbury-Brown Twiss photon-photon correlation interferometry can be used to discern a variety of interference effects even in situations where the single atom detection probabilities do not exhibit interferences. We have demonstrated atoms acting as a mediator for photon-photon interaction between two cavities and entanglement can be transferred from fields to atoms. We have generated entangled state of two and three photons by passing two and three atoms through the cavities.

---

## Multi-photon Processes in Cavities

---

In high quality cavities most of the studies deal with the interaction of single atom with field [72, 73]. On the other hand, the investigations of cooperative effects such as optical bistability [74] involve a large number of atoms. In this chapter, we discuss cooperative two-photon processes in two atoms in a cavity. Earlier studies of two-photon processes in two atoms deal with cooperative effect in the presence of strong dipole-dipole interaction between the atoms [75, 76]. Such interaction is significant only when the inter-atomic separation is less than the wavelength of the radiation. These dipole-dipole induced two photon processes involving two atoms in free space are widely studied theoretically [75] as well as experimentally [76]. We show that it is advantageous to use a cavity for the study of such two photon processes as one would not be constrained by the requirement of small inter-atomic separation [77, 78]. In high quality cavities inter-atomic interactions can arise when different atoms interact with a common quantized field and therefore, these interactions do not depend on the inter-atomic separation. We demonstrate that the two-atom two-photon resonant effect could be very large, thus opening up the possibility of a variety of multi-photon cooperative phenomena in non-resonant cavities. The two photon transition occurs as a result of simultaneous excitation or de-excitation of both atoms with two photon resonance condition  $\omega_1 + \omega_2 \approx \omega_a + \omega_b$ , where  $\omega_1, \omega_2$  are the atomic transition frequencies and  $\omega_a, \omega_b$  are the frequencies of the emitted photons. The actual resonance condition depends on the vacuum Rabi couplings. We study such two-photon resonant processes in two different systems: (i) two identical atoms interacting with field in a two

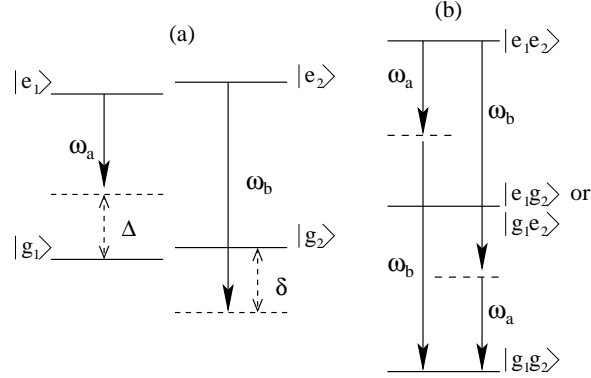


**Figure 4.1:** (a) The system of two identical atoms interacting with two modes of the vacuum. (b) Two pathways for two atom two photon emission.

mode cavity (see Fig. 4.1), (ii) two nonidentical atoms in a single mode cavity (see Fig. 4.2).

## 4.1 Two Photon Processes

In a single two level atom, two-photon transitions between the excited state  $|e\rangle$  and the ground state  $|g\rangle$  occur at a frequency given by  $\omega_{eg} = 2\omega$ , where  $\omega_{eg}$  is the atomic transition frequency and  $\omega$  is the frequency of the photons. The process proceeds via intermediate states  $|i\rangle$ , which are away from a single photon resonance and thus no population is transferred to the intermediate states in the process. We note that the two photon micromaser in a single mode cavity has been realized [79].

Now consider a cooperative two photon emission process involving two two-level atoms with distinct transition frequencies  $\omega_1$  and  $\omega_2$  such that  $\omega_1 - \omega$  and  $\omega_2 - \omega$  are large, so that single photon transitions in individual atoms are negligible. However, a two photon resonant process such that  $\omega_1 + \omega_2 = 2\omega$ , as shown in Fig. 4.2(a), can dominate in such systems. The composite system of two two-level atoms is equivalent to a four level atomic system as shown in Fig. 4.2(b). The two photon emission from state  $|e_1, e_2\rangle$  to  $|g_1, g_2\rangle$  occurs through two possible pathways via intermediate states  $|e_1, g_2\rangle$  and  $|g_1, e_2\rangle$ . The interaction Hamiltonian for the system can be written as

$$H_I = H_+ e^{-i\omega t} + H_- e^{i\omega t}, \quad (4.1)$$

where  $H_+$  ( $H_-$ ) is the interaction corresponding to the absorption (emission) of a photon.

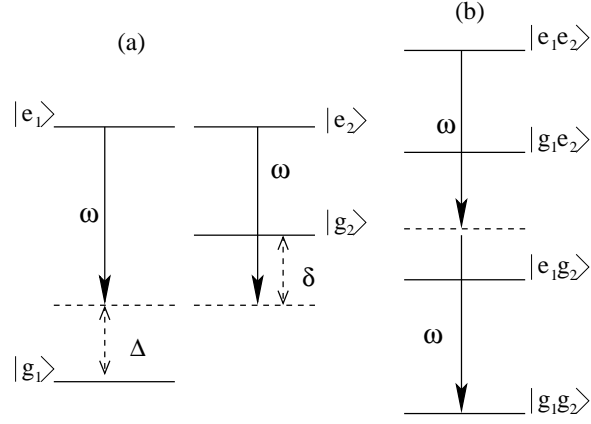


**Figure 4.2:** (a) Two nonidentical atoms interacting with a single mode vacuum. (b) Two pathways for two atom two photon emission corresponding to two possible intermediate states  $|e_1, g_2\rangle$  and  $|g_1, e_2\rangle$ .

The second order perturbation theory leads to the following expression for the rate of two photon emission

$$R_c = \frac{2\pi}{\hbar^2} \left| \frac{\langle g_1, g_2 | H_- | g_1, e_2 \rangle \langle g_1, e_2 | H_- | e_1, e_2 \rangle}{\hbar(\omega_1 - \omega)} + \frac{\langle g_1, g_2 | H_- | e_1, g_2 \rangle \langle e_1, g_2 | H_- | e_1, e_2 \rangle}{\hbar(\omega_2 - \omega)} \right|^2 \times \delta(\omega_1 + \omega_2 - 2\omega). \quad (4.2)$$

Surprisingly  $R_c = 0$ , as the two terms in the expression cancel each other when  $\omega_1 + \omega_2 = 2\omega$ . This can be explained as the two paths for two photon emission interfere destructively. Therefore, it is necessary to include inter-atomic interactions [75, 76] for nonzero two photon emission. However, these interactions are significant only if the inter-atomic separation is less than a wavelength. Thus, it imposes a nontrivial constrain to study two atom two photon processes in free space, as it is not easy to resolve the spectrum of such closely placed atoms. Though a beautiful demonstration of such two photon cooperative effects in solids is given in a recent work [76], using very sophisticated techniques. Similar results apply to the case of two photon emission by two identical atoms if the photons of frequencies  $\omega_a$  and  $\omega_b$  are emitted (see Fig. 4.1), such that

$$\omega_a + \omega_b = 2\omega_0. \quad (4.3)$$

We examine such two photon emission processes in a cavity. We demonstrate that in high quality cavities such processes lead to a large two photon Rabi oscillation [80, 81, 82, 83] involving two atoms.

## 4.2 Two Photon Emission in two Identical Atoms in a two Mode Cavity

Let us consider two identical two level atoms, with transition frequency  $\omega_0$ , interacting with two modes of the vacuum having frequencies  $\omega_a$  and  $\omega_b$  in a cavity as shown in Fig. 4.1. The Hamiltonian for the system is

$$H = \hbar\omega_a a^\dagger a + \hbar\omega_b b^\dagger b + \sum_{i=1,2} \hbar \left[ \frac{\omega_0}{2} (|e_i\rangle\langle e_i| - |g_i\rangle\langle g_i|) + |e_i\rangle\langle g_i|(g_1 a + g_2 b) + |g_i\rangle\langle e_i|(g_1 a^\dagger + g_2 b^\dagger) \right], \quad (4.4)$$

where  $a$  and  $a^\dagger$  ( $b$  and  $b^\dagger$ ) are annihilation and creation operators for the first (second) mode of the cavity,  $g_1$  and  $g_2$  are the coupling constants. In a frame rotating with frequency  $\omega_0$ , the Hamiltonian (4.4) becomes

$$H = -\hbar\Delta a^\dagger a - \hbar\delta b^\dagger b + \sum_{i=1,2} \hbar \left[ |e_i\rangle\langle g_i|(g_1 a + g_2 b) + |g_i\rangle\langle e_i|(g_1 a^\dagger + g_2 b^\dagger) \right], \quad (4.5)$$

$$\Delta = \omega_0 - \omega_a, \quad \delta = \omega_0 - \omega_b.$$

We consider the special case of two photon emission when both atoms are in their excited states and there is vacuum inside the cavity. Thus the initial state of the atom-cavity system is

$$|\psi(0)\rangle = |e_1, e_2, 0, 0\rangle. \quad (4.6)$$

Considering all possible states of the system in evolution, the state of the system at time  $t$  can be written as

$$|\psi(t)\rangle = c_1(t)|e_1, e_2, 0, 0\rangle + \frac{1}{\sqrt{2}} (|e_1, g_2\rangle + |g_1, e_2\rangle) \{c_2(t)|1, 0\rangle + c_3(t)|0, 1\rangle\} + |g_1, g_2\rangle \{c_4(t)|1, 1\rangle + c_5(t)|2, 0\rangle + c_6(t)|0, 2\rangle\}. \quad (4.7)$$

Different terms in the wave function (4.7) correspond to no photon emission, one photon emission, and two photon emission. The photon emission can take place in either mode. Here we are interested in a resonant two photon emission *i.e.*, when one photon is emitted in each mode. A very interesting aspect of the state (4.7) is its entangled nature. This provides a method of producing entangled states, say, entanglement of two cavity modes [54]. Now using Schrodinger equation and Hamiltonian (4.5), the time dependent amplitudes

$c_i(t)$  are determined by

$$\begin{aligned}
\dot{c}_1 &= -ig_1\sqrt{2}c_2 - ig_2\sqrt{2}c_3 \\
\dot{c}_2 &= i\Delta c_2 - ig_1\sqrt{2}c_1 - ig_2\sqrt{2}c_4 - 2ig_1c_5 \\
\dot{c}_3 &= i\delta c_3 - ig_2\sqrt{2}c_1 - ig_1\sqrt{2}c_4 - 2ig_2c_6 \\
\dot{c}_4 &= i(\Delta + \delta)c_4 - ig_2\sqrt{2}c_2 - ig_1\sqrt{2}c_3 \\
\dot{c}_5 &= 2i\Delta c_5 - 2ig_1c_2 \\
\dot{c}_6 &= 2i\delta c_6 - 2ig_2c_3.
\end{aligned} \tag{4.8}$$

In order to understand the nature of the two atom two photon resonance we present numerical as well as approximate analysis which can capture the physics of the cooperative process. We consider the case when detunings to the cavity field are much larger than the couplings, *i.e.*,  $|\Delta|, |\delta| \gg g_1, g_2$  but  $|\Delta + \delta|$  is small, keeping in mind that the condition for two photon resonance is  $\Delta + \delta = 0$ . In such a case cooperative two photon process should dominate and single photon processes would be insignificant. The results of numerical integration of Eq. (4.8) are plotted in Fig. 4.3. In the case when  $g_1 \neq g_2$  a novel resonance is achieved. The probability of two photon emission at resonance is quite high. The resonance is shifted from the position  $\Delta + \delta = 0$ . This shift is due to the strong coupling to the vacuum field in the cavity. For  $g_2/g_1 = 1.5$  and  $\Delta = -5g_1$  maximum two photon emission probability is approximately 0.9 and the interaction time required for achieving maximum probability is given by  $g_1 t \approx 6\pi$ .

Having established numerically that the two photon resonance can be large in cavities, we present approximate analysis to demonstrate it. Under the above mentioned conditions for two photon resonance we can eliminate fast oscillating variables  $c_2, c_3, c_5, c_6$  and effectively reduce the dynamics in terms of slowly oscillating variables  $c_1$  and  $c_4$ . We note that in an adiabatic approximation, where one sets  $\dot{c}_2 = \dot{c}_3 = \dot{c}_5 = \dot{c}_6 = 0$ , does not yield the correct physics of the two atom two photon emission. We relegate the procedure for eliminating fast oscillating variables to the appendix-A. The reduced form of the Eq. (4.8), in terms of slowly oscillating variables, is written as

$$\begin{aligned}
\dot{c}_1 &= -i \left( \frac{2g_1^2\Delta}{\Delta^2 - 2g_1^2} + \frac{2g_2^2\delta}{\delta^2 - 2g_2^2} \right) c_1 + 2ig_1g_2 \left( \frac{\Delta}{\Delta^2 + 2g_1^2} + \frac{\delta}{\delta^2 + 2g_2^2} \right) c_4, \\
\dot{c}_4 &= 2ig_1g_2 \left( \frac{\Delta}{\Delta^2 + 2g_1^2} + \frac{\delta}{\delta^2 + 2g_2^2} \right) c_1 + i \left( \Delta + \delta - \frac{2g_1^2\delta}{\delta^2 - 2g_2^2} - \frac{2g_2^2\Delta}{\Delta^2 - 2g_1^2} \right) c_4. \tag{4.9}
\end{aligned}$$

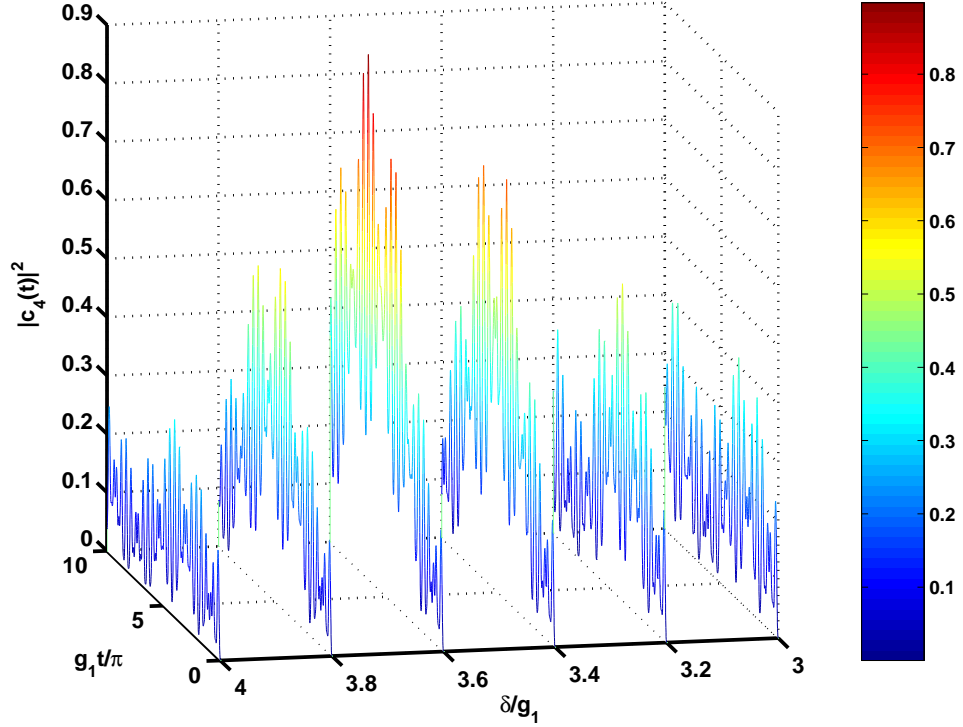


**Figure 4.3:** Two atom two photon emission probability,  $|c_4(t)|^2$  in a system of identical atoms interacting with vacuum in a two mode cavity, for  $g_2/g_1 = 1.5$  and  $\Delta/g_1 = -5.0$ .

The solution of Eq. (4.9) gives

$$|c_4(t)|^2 = \frac{4G^2}{4G^2 + \Omega^2} \sin^2 \frac{\sqrt{4G^2 + \Omega^2}t}{2}, \quad (4.10)$$

$$\text{with } G = 2g_1g_2 \left( \frac{\Delta}{\Delta^2 + 2g_1^2} + \frac{\delta}{\delta^2 + 2g_2^2} \right), \quad (4.11)$$

$$\Omega = \Delta + \delta + 2(g_1^2 - g_2^2) \left( \frac{\Delta}{\Delta^2 - 2g_1^2} - \frac{\delta}{\delta^2 - 2g_2^2} \right). \quad (4.12)$$

Note that in the limit  $g_1 = g_2$  and  $\Delta + \delta = 0$ , the probability amplitude  $c_4$  for two photon emission tends to zero, as both  $\Omega$  and the numerator in Eq. (4.10) become proportional to  $(\Delta + \delta)$ . Thus when couplings to the modes are same, two photon emission probability has no resonance. In this case the transitions from  $|e_1, e_2, 0, 0\rangle$  to  $|g_1, g_2, 1, 1\rangle$  via states  $\frac{1}{\sqrt{2}}(|e_1, g_2\rangle + |g_1, e_2\rangle)|1, 0\rangle$  and  $\frac{1}{\sqrt{2}}(|g_1, e_2\rangle + |e_1, g_2\rangle)|0, 1\rangle$  interfere destructively. We further note that to order  $g_1^2g_2^2$  the two photon resonance does not occur

$$|c_4(t)|^2 = \frac{16g_1^2g_2^2}{\delta^2\Delta^2} \sin^2 \frac{\delta t}{2} \sin^2 \frac{\Delta t}{2}. \quad (4.13)$$

The usual second order perturbation theory cannot lead to inter-atomic two photon resonance. One has to consider higher order terms in  $g_1$  and  $g_2$ . However, then the excitation itself would be negligible. Therefore one needs high quality cavities. The probability of

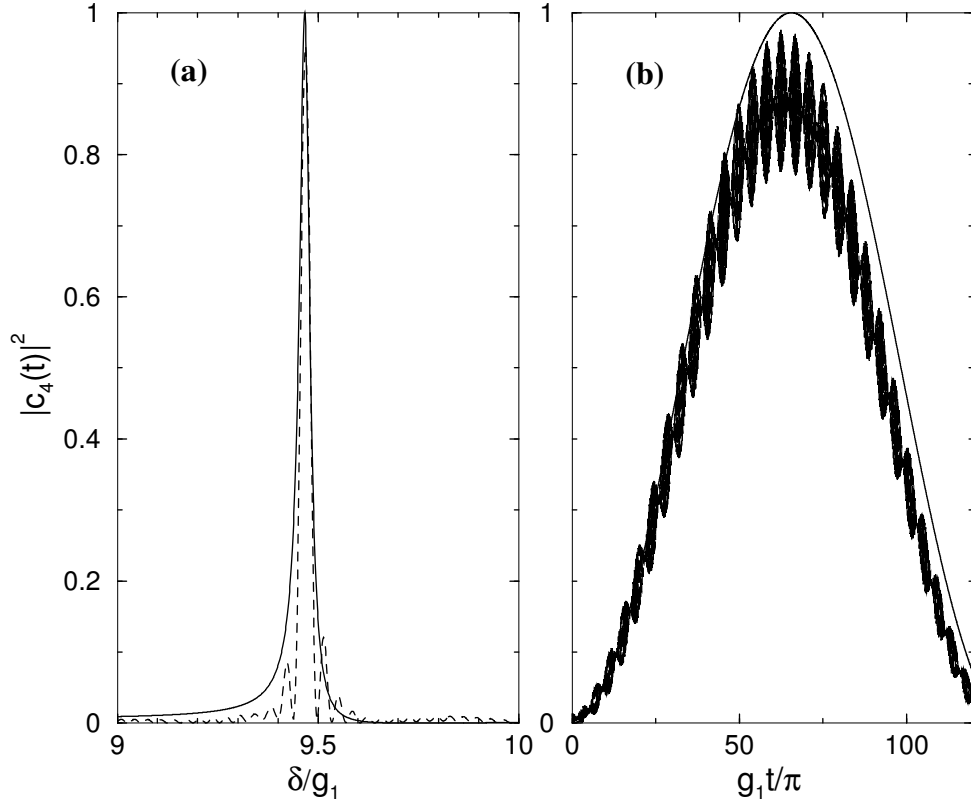


**Figure 4.4:** The maximum value of the two atom two photon emission probability,  $|c_4(t)|^2$  in the system of two identical atoms interacting with vacuum in a two mode cavity, is plotted with respect to (a) detuning  $\delta$  and (b) time, for  $g_2/g_1 = 1.5$  and  $\Delta = -10g_1$ . The solid line is corresponding to approximate result and the dotted line (...) corresponding to exact numerical result.

cooperative emission of two photons in different modes is a periodic function of time. In Fig. 4.4(a), we plot the maximum value of  $|c_4(t)|^2$  as a function of  $\delta$  and in Fig. 4.4(b) as a function of time  $t$ , for fixed values of  $g_1$ ,  $g_2$ , and  $\Delta$ . At two photon resonance the probability corresponding to two photon emission in one of the two modes is much smaller than the probability of two photon emission in different modes. From Eqs. (4.10) and (4.12) it is clear that the two photon resonance occurs at  $\Delta + \delta + 4(g_1^2/\Delta + g_2^2/\delta) \approx 0$ . Thus the interaction with the cavity modifies the condition of two photon resonance. This is seen

quite clearly in Fig. 4.4(a). We note the connection of the resonance frequency  $\Omega$  to the one photon Stark shifts. It is well known that the shift in the frequency of a two level atom in the presence of a field with  $n$  photons is given by  $2g^2(n+1)/\Delta$  which is equal to  $4g^2/\Delta$  for  $n = 1$ . Thus the change  $4(g_1^2/\Delta + g_2^2/\delta)$  is equal to the frequency shift of both the atoms due to the presence of a single photon. However, it should be borne in mind that the exact result is not periodic and exhibits rapid variations though the envelop agrees with the result (4.10). The above mentioned approximate results are valid for larger values of detunings but for larger values of detunings a large interaction time is required to reach the maximum of two atom two photon transition probability. This should be possible with the recently developed method of trapping atoms in a cavity [84]. The other possibility is to work under the conditions of the Fig. 4.3.

### 4.3 Two Photon Emission in two Nonidentical Atoms in a Single Mode Cavity

In this section we analyze a system of two nonidentical atoms interacting with a single mode vacuum field in a cavity (Fig. 4.2). Consider two nonidentical two level atoms having their excited states  $|e_1\rangle$ ,  $|e_2\rangle$  and their ground states  $|g_1\rangle$ ,  $|g_2\rangle$  interacting with a single mode cavity-field of frequency  $\omega$ . The Hamiltonian of this system is

$$H = \hbar \left[ \frac{\omega_1}{2} (|e_1\rangle\langle e_1| - |g_1\rangle\langle g_1|) + \frac{\omega_2}{2} (|e_2\rangle\langle e_2| - |g_2\rangle\langle g_2|) + \omega a^\dagger a \right] + \hbar g_1 (|e_1\rangle\langle g_1| a + a^\dagger |g_1\rangle\langle e_1|) + \hbar g_2 (|e_2\rangle\langle g_2| a + a^\dagger |g_2\rangle\langle e_2|), \quad (4.14)$$

where  $\omega_1$  ( $\omega_2$ ) is transition frequency for first (second) atom,  $a$  and  $a^\dagger$  are annihilation and creation operators for the field, and  $g_1$  ( $g_2$ ) is the coupling constant to the cavity mode with first (second) atom. In a rotating frame the Hamiltonian  $H$  can be written as

$$H = -\hbar\Delta |g_1\rangle\langle g_1| - \hbar\delta |g_2\rangle\langle g_2| + \hbar g_1 (|e_1\rangle\langle g_1| a + a^\dagger |g_1\rangle\langle e_1|) + \hbar g_2 (|e_2\rangle\langle g_2| a + a^\dagger |g_2\rangle\langle e_2|), \quad (4.15)$$

where  $\Delta = \omega_1 - \omega$ ,  $\delta = \omega_2 - \omega$ . Let us consider an initial state  $|\psi(0)\rangle = |e_1, e_2, 0\rangle$  with both atoms in the excited state and cavity in the vacuum state. The state of the system at time  $t$  can be written as

$$|\psi(t)\rangle = c_1(t)|e_1, e_2, 0\rangle + c_2(t)|e_1, g_2, 1\rangle + c_3(t)|g_1, e_2, 1\rangle + c_4(t)|g_1, g_2, 2\rangle, \quad (4.16)$$

where the expansion coefficients  $c_i$  satisfy

$$\begin{aligned}
\dot{c}_1 &= -ig_2c_2 - ig_1c_3, \\
\dot{c}_2 &= i\delta c_2 - ig_1\sqrt{2}c_4 - ig_2c_1, \\
\dot{c}_3 &= i\Delta c_3 - ig_2\sqrt{2}c_4 - ig_1c_1, \\
\dot{c}_4 &= i(\Delta + \delta)c_4 - ig_1\sqrt{2}c_2 - ig_2\sqrt{2}c_3.
\end{aligned} \tag{4.17}$$

The two photon resonance condition for this system would be  $\Delta + \delta = 0$ . For couplings  $g_1, g_2$ , much smaller than  $|\Delta|, |\delta|$ , the solution of Eq. (4.17) gives

$$c_4(t) = -\frac{4g_1g_2\sqrt{2}}{\delta\Delta} \sin\frac{\delta t}{2} \sin\frac{\Delta t}{2} + \text{higher order terms.} \tag{4.18}$$

The first term in Eq. (4.18) represents independent emission by each atom. Clearly, to lowest order in  $g_1g_2$  no two photon resonance occurs. Such a resonance can come from the terms of the higher order. Assuming that  $|\Delta|$  and  $|\delta|$  are large but  $|\Delta + \delta|$  is small, we eliminate fast oscillating variables  $c_2$  and  $c_3$  in a way similar to the previous case and the Eq. (4.17), in terms of slowly oscillating variables reduces, to

$$\begin{aligned}
\dot{c}_1 &= -i\left(\frac{g_1^2}{\Delta} + \frac{g_2^2}{\delta}\right)c_1 + ig_1g_2\sqrt{2}\left(\frac{\Delta}{\Delta + 2g_1^2} + \frac{\delta}{\delta + 2g_2^2}\right)c_4, \\
\dot{c}_4 &= ig_1g_2\sqrt{2}\left(\frac{\Delta}{\Delta + 2g_1^2} + \frac{\delta}{\delta + 2g_2^2}\right)c_1 + i\left(\Delta + \delta + \frac{2g_1^2}{\Delta} + \frac{2g_2^2}{\delta}\right)c_4.
\end{aligned} \tag{4.19}$$

We find the approximate result for the two photon emission probability

$$|c_4(t)|^2 = \frac{4G'^2}{4G'^2 + \Omega'^2} \sin^2 \frac{\sqrt{4G'^2 + \Omega'^2}t}{2}, \tag{4.20}$$

$$\text{with } G' = \sqrt{2}g_1g_2\left(\frac{\Delta}{\Delta^2 + 2g_1^2} + \frac{\delta}{\delta^2 + 2g_2^2}\right), \Omega' = \Delta + \delta + 3\left(\frac{g_1^2}{\Delta} + \frac{g_2^2}{\delta}\right). \tag{4.21}$$

For large  $|\Delta|$  and  $|\delta|$ , the Eq. (4.20) shows two photon resonance at  $\Delta + \delta + 3(g_1^2/\Delta + g_2^2/\delta) \approx 0$ . Further such two atom two photon resonance appears for  $g_1 \neq g_2$ , which disappears when  $g_1 = g_2$ . In the latter case the antisymmetric state  $(|g_1, e_2, 1\rangle - |e_1, g_2, 1\rangle)/\sqrt{2}$  is decoupled from  $|e_1, e_2, 0\rangle$  and  $|g_1, g_2, 2\rangle$ . We present numerical results in Fig. 4.5. The graph shows two photon resonance for  $g_1 \neq g_2$ . It is clear that the position of resonance is shifted from  $\Delta + \delta = 0$ . This shift in the position of resonance is due to larger values of  $g_1$  and  $g_2$ , and depends on the ratio  $g_2/g_1$ . There is a large enhancement in the probability of two photon resonant emission in a high quality cavity. It is expected that such effects can be studied by placing the system used by Hettich *et al.* [76] in a cavity.

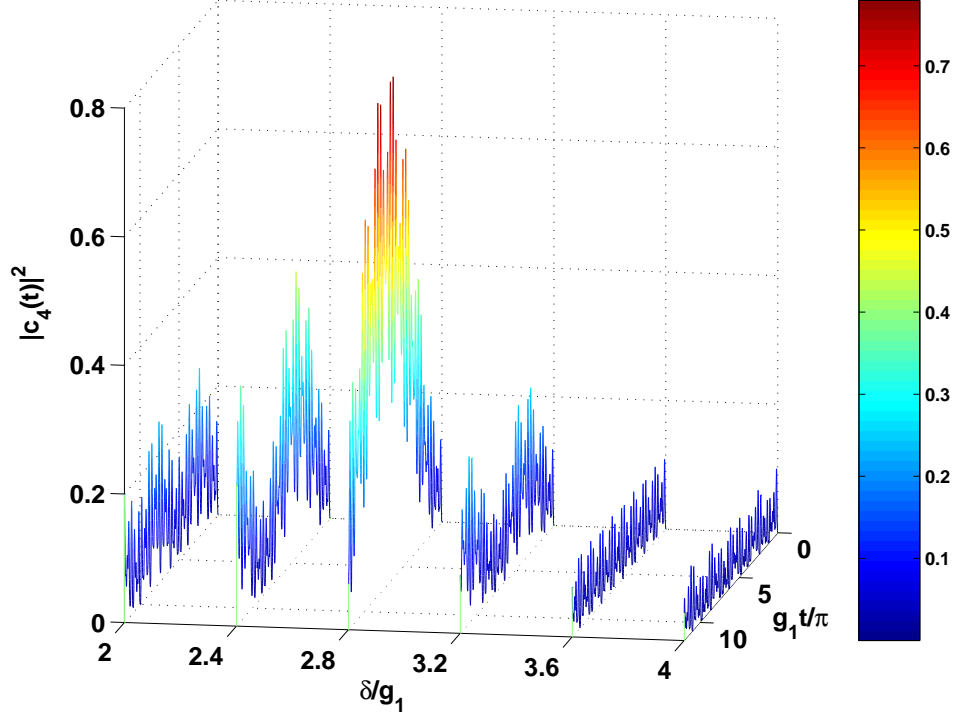


**Figure 4.5:** Two atom two photon emission probability,  $|c_4(t)|^2$  in a system of nonidentical atoms interacting with vacuum in a single mode cavity, for  $\Delta/g_1 = -5.0$  and  $g_2/g_1 = 2.0$ .

#### 4.4 Effects of Cavity Damping

In this section, we examine the effect of cavity decay on two atom two photon vacuum Rabi oscillations. We do a calculation based on master equation. Let  $2\kappa_a$  and  $2\kappa_b$  be the rate of loss of photons from the first mode and the second mode, respectively. The density matrix of the system of two atoms interacting with two mode field in the cavity will evolve according to the master equation

$$\dot{\rho} = -\frac{i}{\hbar}[H, \rho] - \kappa_a (a^\dagger a \rho - 2a \rho a^\dagger + \rho a^\dagger a) - \kappa_b (b^\dagger b \rho - 2b \rho b^\dagger + \rho b^\dagger b). \quad (4.22)$$

The density matrix for this system can be expressed in terms of all the states which are generated by the combined effect of  $H$  and dissipation. Because of the cavity decay, many more states are involved in the dynamics. For example, for identical atoms interacting in a bimodal cavity, the relevant states are  $|e_1, e_2, 0, 0\rangle, |g_1, e_2, 0, 0\rangle, |g_1, e_2, 1, 0\rangle, |g_1, e_2, 0, 1\rangle, |e_1, g_2, 0, 0\rangle, |e_1, g_2, 1, 0\rangle, |e_1, g_2, 0, 1\rangle, |g_1, g_2, 0, 0\rangle, |g_1, g_2, 0, 1\rangle, |g_1, g_2, 1, 0\rangle, |g_1, g_2, 0, 2\rangle, |g_1, g_2, 1, 1\rangle,$

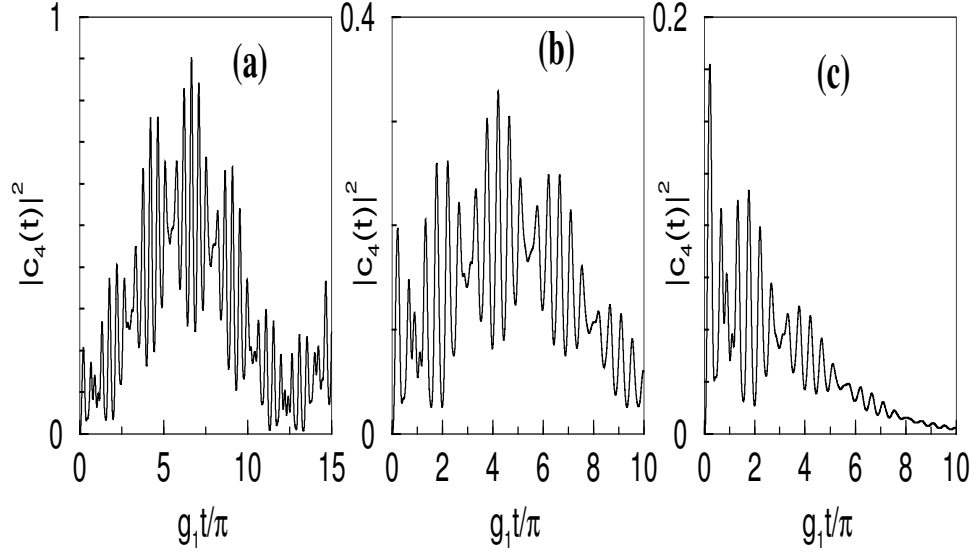


**Figure 4.6:** Periodic behavior of two atom two photon emission probability  $|c_4(t)|^2$ , for identical atoms interacting with vacuum in a bimodal cavity, for  $\delta = 3.5g_1$ ,  $\Delta = -5g_1$ ,  $g_2 = 1.5g_1$  and cavity damping constants, (a)  $\kappa_a = \kappa_b = 0.00$ , (b)  $\kappa_a = \kappa_b = 0.03g_1$ , (c)  $\kappa_a = \kappa_b = 0.1g_1$ .

and  $|g_1, g_2, 2, 0\rangle$ . For this system density matrix is expressed as

$$\rho \equiv \sum_{i', j', i, j=0}^1 \sum_{k'=0}^{i'+j'} \sum_{k=0}^{i+j-k'} \sum_{l'=0}^{i'+j'-k'} \sum_{l=0}^{i+j-k} \rho(i', j', k', l', i, j, k, l) |i', j', k', l'\rangle \langle i, j, k, l|. \quad (4.23)$$

Here  $i, i'$  ( $j, j'$ ) represent states of the first (second) atom with the convention  $|0\rangle$  corresponding to excited state and  $|1\rangle$  corresponding to ground state, the indices  $k, k'$  ( $l, l'$ ) represent the number of photons in the first (second) mode. Thus the dissipation requires considerable numerical work. Results for two identical atoms in a bimodal cavity are shown in Fig. 4.6. We show results for optical cavities with  $g/\kappa \approx 30$  in Fig. 4.6(b) and for currently realizable cavities ( $g/\kappa = 10$ ) in Fig. 4.6(c). The two atom two photon vacuum Rabi oscillations survive in the limit of small damping  $g/\kappa \approx 30$  but for larger damping ( $g/\kappa = 10$ ) die fast. Similar results are found for two nonidentical atoms in a single mode cavity.

## 4.5 Summary

We have reported large two atom two photon vacuum Rabi oscillations in two systems, one having two identical atoms in a two-mode cavity and another having two nonidentical atoms in a single-mode cavity. We have shown that for asymmetric couplings ( $g_1 \neq g_2$ ), the probability of two photon emission is quite large but for symmetric couplings ( $g_1 = g_2$ ), the two photon emission probability is very small. Further, we have shown that the condition of two photon resonance in the case of strong atom-field interaction is modified from its free-space form ( $\Delta + \delta = 0$ ). These two photon transitions involving two atoms can be used for generating and detecting different types of entanglement between two field modes and two atoms [85].

---

## Manipulation of Atomic Lifetime in Cavities Using dc-Fields

---

It is well known that vacuum field drives excited atoms to their ground states in spontaneous emission. The rate of spontaneous decay  $\Gamma$  for a two level atom can be obtained with the help of Fermi golden rule

$$\Gamma = \frac{2\pi}{\hbar^2} |V_{eg}|^2 \rho(\omega_{eg}), \quad (5.1)$$

where  $V_{eg}$  is atomic dipole matrix element corresponding to the transition from the excited state  $|e\rangle$  to the ground state  $|g\rangle$  and  $\rho(\omega_{eg})$  is the vacuum mode density around atomic transition frequency  $\omega_{eg}$ . The mode density  $\rho(\omega_{eg})$  can be changed by putting boundaries around the atom. Cavity structures are most suitable for changing local field density. Inhibition [86, 87, 88, 89] and enhancement [89, 90, 91] of the spontaneous decay in cavities has been studied in detail and realized experimentally. If the cavity is detuned to atomic transition frequency, spontaneous decay is inhibited significantly and enhanced in the case of the resonant cavity.

Typically, there are two regimes according to the atom-field interaction [92, 93, 94], weak coupling regime and strong coupling regime. The weak coupling regime is characterized by the exponential decay and decay rate is enhanced or inhibited from its free space value depending on cavity is resonant or detuned to the transition frequency  $\omega_{eg}$ . On the other hand, strong coupling regime is characterized by reversible Rabi oscillations where spontaneous decay becomes reversible. The basic difference in both the regime is weak coupling regime occurs in low quality cavities while strong coupling regime can occur in high quality cavities, where cavity decay is negligible. A lot of literature is available

on cavity-modified atomic decay [95, 96, 97, 98, 99, 100]. All these theoretical as well as experimental results provide strong base to the cavity quantum electrodynamics.

There are not only static effects for modifying spontaneous emission but few dynamic effects have also been reported to suppress spontaneous emission [101, 102, 103, 104, 105]. A strong resonant driving field can decouple the atom from the vacuum. Lange and Walther [102] in their experiment found that if an external resonant field is injected in to the cavity, spontaneous decay can be almost completely suppressed.

In many experiments of modern quantum optics *viz* quantum computation, lasing without inversion, atom interferometry where long lived excited atomic states and coherence is required, spontaneous emission controls the results and appears as a limiting factor. In such experiments suppression of spontaneous emission is essential. In this chapter, we show how a possible control of spontaneous emission can be obtained by using dc-fields. We find that in the presence of dc-fields in the cavities the spontaneous emission of atoms can be modified significantly as a result of dc-field induced stark shifts which provides an additional control over life time of the atom. Further, the change in spontaneous emission depends on the square of applied dc-field. We find that in the case of cavities resonant to atomic transition, spontaneous emission can be inhibited significantly using dc-fields. In the case of cavities having negligible mode density around atomic frequency the presence of dc field shows significant inhibition or enhancement of spontaneous emission depending on whether the cavity is tuned below the atomic transition frequency or above the transition frequency.

## 5.1 Spontaneous Decay of an Atom inside the Cavity

We consider a two level atom of transition frequency  $\omega_0$  placed in a single mode cavity. The Hamiltonian for the atom-cavity system is

$$H = \hbar\omega a^\dagger a + \hbar\omega_0 S^z + \hbar g(S^+ a + a^\dagger S^-), \quad (5.2)$$

where  $S^z = \frac{1}{2}(|e\rangle\langle e| - |g\rangle\langle g|)$  and  $S^+ = (S^-)^\dagger = |e\rangle\langle g|$  are spin operators associated with the two level atom. We consider that the cavity has finite quality thus there is leakage through the mirrors. The cavity relaxation is described by the master equation for the

density matrix  $\rho$  of the atom-cavity system

$$\frac{d\rho}{dt} = -\frac{i}{\hbar}[H, \rho] + \mathcal{L}\rho, \quad (5.3)$$

$$\mathcal{L}\rho = -\kappa(a^\dagger a \rho - 2a \rho a^\dagger + \rho a^\dagger a), \quad (5.4)$$

where we have assumed that the cavity is nearly at zero temperature so that there are no thermal photons. The constant  $\kappa$  is the damping rate of the photon number in the cavity. It is related to the cavity  $Q$  via  $\kappa = \omega_c/2Q$ . We work in the interaction picture. The density matrix in interaction picture is given by

$$\tilde{\rho} = e^{i(\omega_0 S^z + \omega a^\dagger a)t/\hbar} \rho e^{-i(\omega_0 S^z + \omega a^\dagger a)t/\hbar}. \quad (5.5)$$

The Hamiltonian (5.2) in interaction picture takes the form

$$H_I = \hbar g(S^+ a e^{i\Delta t} + a^\dagger e^{i\Delta t} S^-), \quad (5.6)$$

where  $\Delta = \omega_0 - \omega$ . The master equation (5.3) in this picture becomes

$$\frac{d\tilde{\rho}}{dt} = -\frac{i}{\hbar}[H_I, \tilde{\rho}] + \mathcal{L}\tilde{\rho}. \quad (5.7)$$

We now eliminate the cavity field adiabatically. By adiabatic elimination we obtain the equation of motion for the reduced density matrix  $\tilde{\rho}_a$  of the atom

$$\tilde{\rho}_a = Tr_c \tilde{\rho}, \quad (5.8)$$

where  $Tr_c$  stands for trace over cavity field.

For adiabatic elimination of field variables we proceed as follows. We make transformation to new density matrix  $\rho'$  defined by

$$\rho' = e^{-\mathcal{L}t} \tilde{\rho}. \quad (5.9)$$

On using (5.6) and (5.9), the Eq. (5.7) takes the form

$$\frac{d\rho'}{dt} = -\frac{i}{\hbar}[\bar{H}_I, \rho'], \quad (5.10)$$

where

$$\begin{aligned} \bar{H}_I &= \hbar g(S^+ a(t) e^{i\Delta t} + a(t)^\dagger e^{i\Delta t} S^-), \\ a(t) &= e^{-\mathcal{L}t} a e^{\mathcal{L}t}. \end{aligned} \quad (5.11)$$

Note that Eq. (5.11) involves only the cavity-atom interaction. Now we assume that the cavity is overdamped *i.e.*,  $g \ll \kappa$ . In bad cavity limit, we can do second order perturbation calculation with respect to  $g$ , which is Born approximation. Further, using Markov approximation, Eq. (5.10) leads to

$$\frac{d\tilde{\rho}_a}{dt} = - \int_0^\infty d\tau \text{Tr}_c [\bar{H}_I(t), [\bar{H}_I(t-\tau), \rho_c(0)\tilde{\rho}_a(t)]] , \quad (5.12)$$

where  $\rho_c(0) = \tilde{\rho}_c(0)$  is the density matrix of the cavity in the absence of the atom, and  $\tilde{\rho}_a(t) = \text{Tr}_c \rho'(t) = \text{Tr}_c \tilde{\rho}(t)$ . Now substituting (5.11) in (5.12), we get terms involving correlation functions of the cavity field. These correlations can be derived from the master equation for cavity relaxation [95]. They are

$$\text{Tr}_c a(t)a^\dagger(t-\tau)\rho_c \equiv \langle a(t)a^\dagger(t-\tau) \rangle = (\bar{n}+1)e^{-\kappa\tau} , \quad (5.13)$$

$$\text{Tr}_c a^\dagger(t)a(t-\tau)\rho_c \equiv \langle a^\dagger(t)a(t-\tau) \rangle = \bar{n}e^{-\kappa\tau} , \quad (5.14)$$

where  $\bar{n}$  is the average number of thermal photons inside the cavity. On using correlations (5.13) and (5.14), Eq. (5.12) reduces to

$$\dot{\tilde{\rho}}_a = -i[\delta_0 S^z, \tilde{\rho}_a] - \Gamma_0 (S^+ S^- \tilde{\rho}_a - 2S^- \tilde{\rho}_a S^+ + \tilde{\rho}_a S^+ S^-) , \quad (5.15)$$

where

$$\Gamma_0 = \frac{g^2 \kappa}{\kappa^2 + \Delta^2}, \quad \delta_0 = \frac{g^2 \Delta}{\kappa^2 + \Delta^2}. \quad (5.16)$$

Now transferring result (5.15) to original frame, we get

$$\dot{\rho}_a = -i[(\omega_0 + \delta_0)S^z, \rho_a] - \Gamma_0 (S^+ S^- \rho_a - 2S^- \rho_a S^+ + \rho_a S^+ S^-) . \quad (5.17)$$

For resonant cavity  $\omega_c = \omega_0$ ,  $\delta_0 = 0$  and the decay rate  $\Gamma_0 = g^2/\kappa$ . There is cavity induced enhancement if  $g^2/\kappa$  is greater than the free space decay rate. Note that as the cavity is detuned ( $\Delta \neq 0$ ),  $\Gamma_0$  decreases which is Kleppner's result for a single mode cavity. The first experimental observation of the Purcell effect was made by Goy *et al* [87]. Next we investigate the effect of the applied dc or low frequency field.

## 5.2 Manipulation of Atomic Lifetime Using dc-Fields

We consider a two level atom placed in a cavity, and a dc field (or low frequency field) is injected inside the cavity . The Hamiltonian of the system can be written as

$$H_{\mathcal{E}} = \hbar\omega_0 S^z + \hbar\omega_c a^\dagger a + \hbar g (aS^+ + S^- a^\dagger) + \hbar\mathcal{E} \cos \Omega t (S^+ + S^-) , \quad (5.18)$$

where  $\omega_0$  is atomic transition frequency,  $\omega_c$  is cavity mode frequency, and  $g$  is the atom cavity coupling constant. The term  $\mathcal{E} \cos \Omega t$  corresponds to a low frequency field, if  $\Omega$  is chosen to be very small. Note that  $\mathcal{E}$  has dimensions of frequency. We perform master equation calculation for atom-cavity system. The density matrix of the system  $\rho$  will evolve as

$$\dot{\rho} = -\frac{i}{\hbar}[H_{\mathcal{E}}, \rho] - \kappa \left( a^\dagger a \rho - 2a \rho a^\dagger + \rho a^\dagger a \right). \quad (5.19)$$

We will work in a frame rotating with atomic frequency  $\omega_0$ . The density matrix in this frame is given by

$$\tilde{\rho} = e^{i\omega_0(S^z + a^\dagger a)t/\hbar} \rho e^{-i\omega_0(S^z + a^\dagger a)t/\hbar}. \quad (5.20)$$

Using Eqs. (5.19) and (5.20) we obtain the equation for  $\tilde{\rho}$

$$\dot{\tilde{\rho}} = -\frac{i}{\hbar}[H_a, \tilde{\rho}] - \kappa \left( a^\dagger a \tilde{\rho} - 2a \tilde{\rho} a^\dagger + \tilde{\rho} a^\dagger a \right) - \frac{i}{\hbar}[H_d, \tilde{\rho}], \quad (5.21)$$

where

$$\begin{aligned} H_a &= -\hbar \Delta a^\dagger a + \hbar g \left( a S^+ + S^- a^\dagger \right), \\ H_d &= \hbar \frac{\mathcal{E}}{2} \left\{ S^+ \left( e^{i(\omega_0 + \Omega)t} + e^{i(\omega_0 - \Omega)t} \right) + S^- \left( e^{-i(\omega_0 + \Omega)t} + e^{-i(\omega_0 - \Omega)t} \right) \right\}, \end{aligned} \quad (5.22)$$

and  $\Delta = \omega_0 - \omega_c$  is the detuning. We note that the experiments of Lange and Walther [102] correspond to using a microwave field, and thus  $\Omega \sim \omega_0$ . Note that the last term in the master equation (5.21) is highly oscillating. We do time averaging for this, as such terms oscillating at the cavity frequency would not be normally observed. The time averaging is well justified here, as all other relevant time scales  $g^{-1}, \kappa^{-1}, \Delta^{-1}$  are much larger than  $(\omega_0 \pm \Omega)^{-1}$ . The inequality  $\omega_0 \gg g, \kappa, \Delta$  enables us to do the time averaging in a much simpler fashion, *i.e.*, we can essentially ignore the terms having  $H_a$  and  $\kappa$  in (5.21). We relegate the details of time averaging to the appendix-B. The calculation leads to the following time averaged master equation

$$\dot{\tilde{\rho}} = i \left[ \Delta_e a^\dagger a, \tilde{\rho} \right] - ig \left[ \left( a S^+ + S^- a^\dagger \right), \tilde{\rho} \right] - \kappa \left( a^\dagger a \tilde{\rho} - 2a \tilde{\rho} a^\dagger + \tilde{\rho} a^\dagger a \right), \quad (5.23)$$

where

$$\Delta_e = \Delta + 2\omega_0 \mathcal{E}^2 / (\omega_0^2 - \Omega^2). \quad (5.24)$$

We note that the dc field contributes to the Stark shift of the two levels in question. We further note that these two atomic levels can also be shifted because of the interaction of

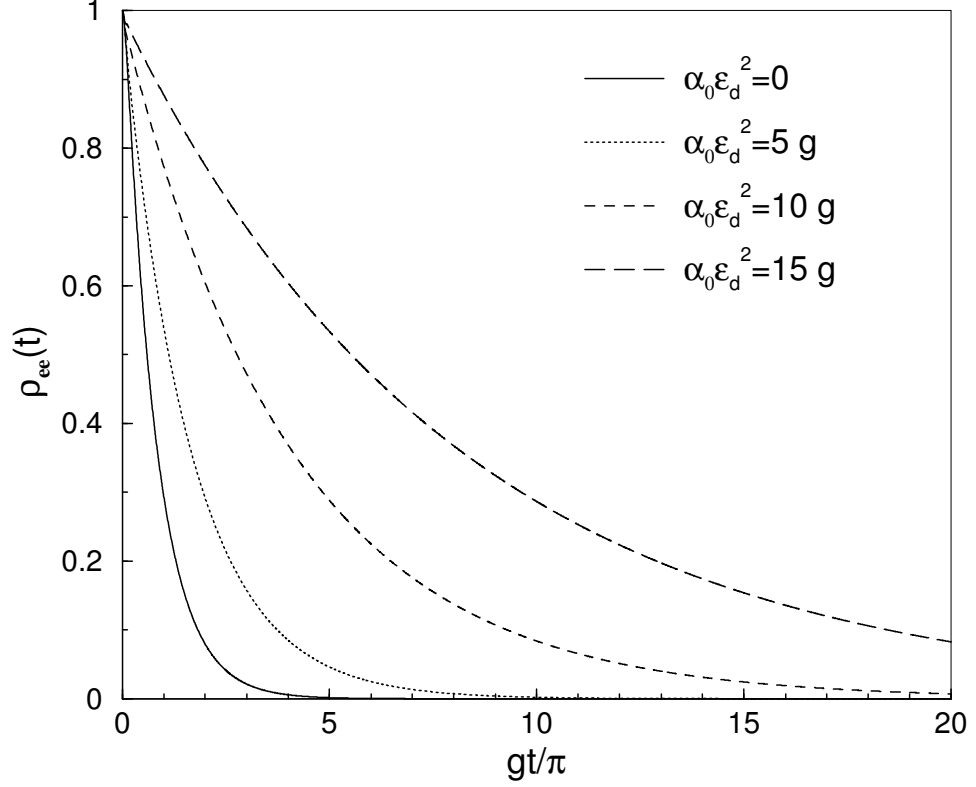


**Figure 5.1:** The probability of the atom remaining in its excited state,  $\rho_{ee} \equiv \langle e, 0 | \rho | e, 0 \rangle$  vs time, for  $\kappa = 5g$ ,  $\Delta = 0$ ,  $\Omega = 0$ , and for the different values of the dc field  $\mathcal{E}_d$ .

the dc field with other levels. These can be accounted for by introducing the polarizabilities  $\alpha_e$  and  $\alpha_g$  of the levels  $|e\rangle$  and  $|g\rangle$  [106, 107]. We can rewrite Eq. (5.24) as

$$\Delta_e = \Delta + \alpha_0 \mathcal{E}_d^2, \quad \alpha_0 = \alpha_e - \alpha_g, \quad (5.25)$$

where  $\mathcal{E}_d$  is now the dc field in esu. The formulation of the appendix-B can also be used to produce the well known expressions for the  $\alpha^s$ . The value of  $\alpha_0$  is known for many low lying as well as Rydberg transitions. The values of  $\alpha_0$  have been calculated in the literature by converting infinite sums into the solution of differential equations.

The Eq. (5.23) can be solved, assuming that the atom is initially excited and the cavity field is in vacuum state. The Eq. (5.23) can be converted into a set of coupled equations in terms of the states  $|e, 0\rangle$ ,  $|g, 1\rangle$ , and  $|g, 0\rangle$ . The results of the numerical integration are shown in the Fig. 5.1 for different values of the parameter  $\Delta_e$ . Clearly there is inhibition

as  $\Delta_e$  increases. The effective detuning  $\Delta_e$  changes due to the applied dc field. For a fixed cavity detuning  $\Delta$  the dc field can make  $\Delta_e$  larger or smaller depending on the sign of  $\Delta$ . The results can be understood by deriving analytical results in the bad cavity limit  $g \ll \kappa$  (and more precisely  $g^2 \ll \kappa^2 + \Delta_e^2$ ). In this limit we can obtain a simpler equation for the atomic density matrix  $\tilde{\rho}_a$  defined by Eq. (5.8). The final result for the atomic system is

$$\dot{\tilde{\rho}}_a = -i[\delta_e S^z, \tilde{\rho}_a] - \Gamma_e (S^+ S^- \tilde{\rho}_a - 2S^- \tilde{\rho}_a S^+ + \tilde{\rho}_a S^+ S^-), \quad (5.26)$$

where

$$\Gamma_e = \frac{g^2 \kappa}{\kappa^2 + \Delta_e^2}, \quad \delta_e = \frac{g^2 \Delta_e}{\kappa^2 + \Delta_e^2}. \quad (5.27)$$

Here,  $\Gamma_e$  is the dc field modified decay parameter and  $\delta_e$  is the net frequency shift. The ratio  $\eta$  of the decays in the presence and absence of dc field is given by

$$\eta = \frac{\Gamma_e}{\Gamma_0} = \frac{\kappa^2 + \Delta^2}{\kappa^2 + \Delta_e^2}. \quad (5.28)$$

Clearly the dc field modifies the decay rate, which depends on the detuning. For the cavity resonant to the atomic transition ( $\Delta = 0$ ), using Eq. (5.24),  $\eta$  reduces to

$$\eta = \frac{\kappa^2}{\kappa^2 + \alpha_0^2 \mathcal{E}_d^4} \approx \left(1 + \frac{4\mathcal{E}^4}{\kappa^2 \omega_0^2}\right)^{-1}, \quad \text{for } \Omega = 0. \quad (5.29)$$

It is clear from the Eq. (5.29) that dc field inhibits the decay rate. Note that the inhibition starts becoming significant for

$$\alpha_0 \mathcal{E}_d^2 \sim \kappa. \quad (5.30)$$

Let us estimate the condition (5.30) for  $Na$  Rydberg transition  $23S_{1/2} \rightarrow 22P_{3/2}$ , whose frequency is  $340GHz$ . For the sake of argument, we also assume  $\alpha_0 \mathcal{E}_d^2 \sim 2\mathcal{E}^2/\omega_0$ . This transition has a dipole moment  $d \sim 10^{-15}esu$ . The atom is placed in the cavity having one mode resonant to the atomic transition. Let us choose the cavity decay rate  $\kappa = 1MHz$ . The condition (5.30) then leads to a Rabi frequency  $\mathcal{E}$  of the order  $400MHz$ , which in turn, requires a dc field of the order of  $10^{-2}esu$ . We note that the required dc field is small enough, so that the perturbative results for the Stark shift hold. We further note that the scalar and tensor polarizabilities are available for some  $S$  and  $P$  levels of  $Na$  [106, 107], though the absolute values for both  $23S_{1/2}$  and  $22P_{3/2}$  level are not available in Fabre *et al.* [106]. However, the reported polarizabilities for say,  $23P$  level, are of the order of

few  $MHz/(Volt/cm)^2$ . Thus the condition (5.30) is realistic, and our finding that the dc field can be used to control spontaneous emission, can be implemented by the appropriate choice of the Rydberg transitions. We emphasize that we are discussing the inhibition or enhancement of spontaneous emission on a given transition which is resonant with the cavity. This, for example, is the transition  $23S \rightarrow 22P$  in the experiments of Goy *et al.* [87]. It must be noted that the field ionization techniques enable one to study transitions selectively [108].

In the case of cavities detuned from the atomic transition, spontaneous decay is smaller and the decay rate is given by  $\Gamma = g^2\kappa/(\kappa^2 + \Delta^2)$ . Further inhibition of decay rate is possible by applying dc field. When cavity is tuned below the atomic transition frequency ( $\Delta$  is positive), then there is significant inhibition of spontaneous decay, which increases further as the applied dc field is increased. On the other hand, when cavity is tuned above the atomic frequency ( $\Delta$  is negative), there is enhancement in the atomic decay, *i.e.*, on increasing the value of applied dc field, the atom decays faster. In Fig5.2 we show the behavior of the factor  $\eta$  as a function of  $\Delta$  for different values of the dc field. The enhancement, as well as inhibition of spontaneous decay, occurs depending on whether the cavity is tuned above or below the atomic frequency. The results shown in the Fig. 5.2 are consistent with the results obtained by direct solution of the Eq. (5.23).

### 5.3 Summary

We find that in presence of dc field, spontaneous emission can be inhibited significantly in the case of cavities resonant to atomic transition. In the case of cavities having negligible mode density around atomic frequency, spontaneous emission itself is smaller, and the presence of dc field shows significant inhibition or enhancement depending on cavity is tuned below the atomic transition frequency or above the transition frequency.

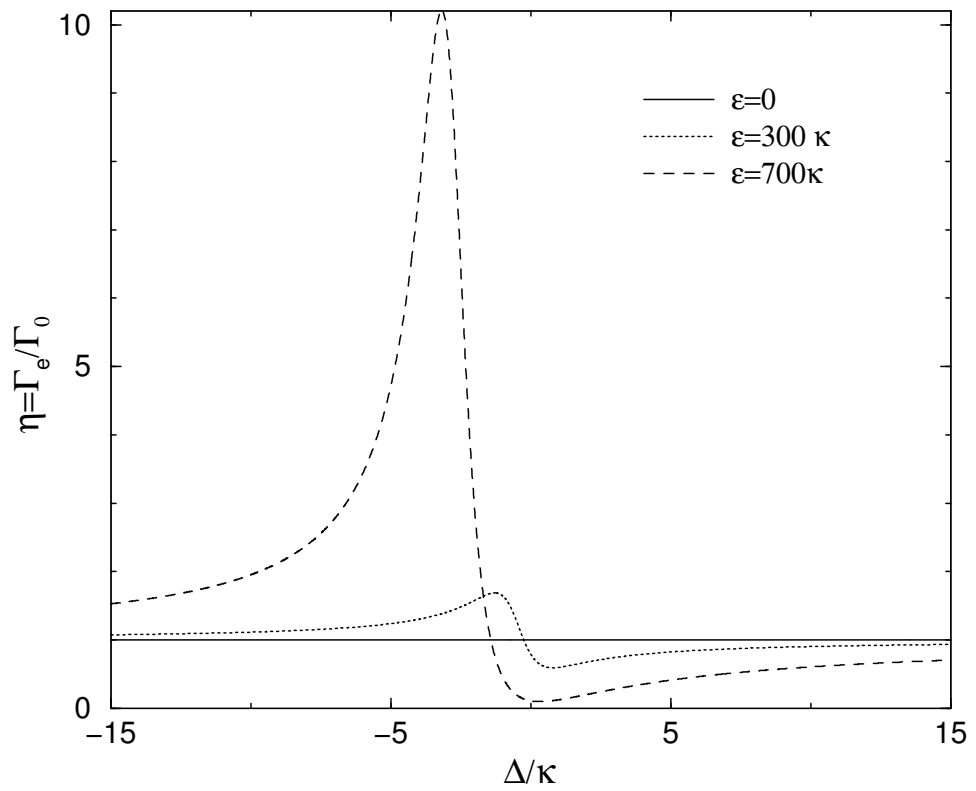


**Figure 5.2:** The ratio ( $\eta$ ) of the decays in the presence and the absence of dc field vs  $\Delta/\kappa$ . The parameters are  $\omega_0 = 3.4 \times 10^5 \kappa$  and  $\Omega = 0$ .

---

## Quantum Random Walk of Photons in High Quality Cavity

---

In classical random walk, a walker flips a coin, and moves one step forward or backward depending on the outcome of the coin [109]. The probability of finding the walker at position  $m$  after  $n$  such steps is given by the binomial distribution

$$P(m) = \frac{n!}{\left(\frac{n+m}{2}\right)! \left(\frac{n-m}{2}\right)!} \left(\frac{1}{2}\right)^n. \quad (6.1)$$

For large values of  $N$ , the probability distribution (6.1) tends to the Gaussian

$$P(m) = \sqrt{\frac{2}{\pi n}} e^{-m^2/2n}. \quad (6.2)$$

Thus, the probability of finding the walker at its initial position is always maximum. In quantum random walk, a system is assigned one additional quantum mechanical degree of freedom, like spin of the particle, and the motion of the system is controlled by this additional degree of freedom. After few steps, the state of the system is exceptionally displaced from the initial position. This exceptional displacement occurs as a result of quantum interference between various states generated in intermediate steps. Quantum random walk is one of the phenomena which are strikingly different from their classical counter parts. In a very interesting paper Aharonov et al. [110] found that the walker's distribution could shift by an amount which could be much larger than the classically possible displacement. Several proposals [110, 111, 112, 113, 114, 115, 116, 117] exist for realizations of the quantum random walk. For example, Aharonov et al gave a cavity QED model where the photon number distribution can get displaced. Sanders et al. [111]

considered a dispersive interaction in the cavity of the form  $S^z(a + a^\dagger)$  and considered the random walk of the field on states on a circle. Other interesting theoretical schemes for implementing quantum walks have been suggested in ion-traps [113] and in optical lattices [114]. Knight et al. [115] further showed that an earlier experiment [116] was a realization of quantum random walk. A scheme using linear optical elements has been recently implemented [117].

In this chapter, we show how quantum random walk can be realized in microcavities. Using resonant interaction between atoms and the field in a high quality cavity, we present a scheme for realizing quantum random walk. The atoms are driven strongly by a classical field. Under conditions of strong driving field, we could realize an effective interaction of the form  $iS^x(a - a^\dagger)$  in terms of the spin operator  $S^x$  associated with the two level atom and the field operators  $a$  and  $a^\dagger$ . This effective interaction generates displacement in the wavefunction of the field depending on the state of the two level atom. Measurements of the state of the two level atom would then generate effective state of the field. Thus in our scheme, measurement of atomic states is corresponding to the flipping of the coin, while the field inside the cavity acts as a walker. Using the homodyne technique, state of the quantum random walker can be monitored. We also discuss the decoherence effects and the time scales at which quantum nature of random walk persists.

## 6.1 Cavity-QED Model for Quantum Random Walk

We consider a two level Rydberg atom having its higher energy state  $|e\rangle$  and lower energy state  $|g\rangle$  interacting with a single mode of the electromagnetic field in a cavity. The atom passes through the cavity and interacts resonantly with the field. Further, the atom is driven by a strong classical field. For simplicity we choose atomic transition frequency, the cavity frequency, and the frequency of the driving field to be same. The schematic arrangement is shown in Fig. 6.1. The Hamiltonian for the system in the interaction picture is written as

$$H = -i\hbar g (S^+ a - a^\dagger S^-) + \hbar (S^+ \mathcal{E} + S^- \mathcal{E}^*), \quad (6.3)$$

where  $g$  and  $\mathcal{E}$  are the coupling constants of the interaction of the atom with the cavity field and with the deriving field. We have chosen  $g$  as real and  $\mathcal{E}$  as complex. The annihilation (creation) operator for the field in the cavity is  $a(a^\dagger)$  and  $S^+$ ,  $S^-$  are atomic spin operators.

The last term in Eq. (6.3) is the interaction with the external field. We further rewrite the above Hamiltonian in a picture in which the interaction with the external field has already been diagonalized :

$$|\bar{\psi}\rangle = e^{iht}|\psi\rangle; h = S^+\mathcal{E} + S^-\mathcal{E}^*, \quad (6.4)$$

where  $|\bar{\psi}\rangle$  is transformed atomic state in new picture from old atomic state  $|\psi\rangle$ . The Hamiltonian in this picture is

$$\bar{H} = -i\hbar g e^{iht}(S^+a - S^-a^\dagger)e^{-iht}, \quad (6.5)$$

$$e^{iht} \equiv \cos(|\mathcal{E}|t) + \frac{i\hbar}{|\mathcal{E}|} \sin(|\mathcal{E}|t). \quad (6.6)$$

The atomic spin operators  $S^\pm$  transform as

$$e^{iht}S^+e^{-iht} \equiv S^+ \cos^2(|\mathcal{E}|t) + \frac{\mathcal{E}^{*2}}{|\mathcal{E}|^2} \sin^2(|\mathcal{E}|t)S^- - \frac{2i\mathcal{E}^*}{|\mathcal{E}|} S^z \sin(|\mathcal{E}|t) \cos(|\mathcal{E}|t), \quad (6.7)$$

$$e^{iht}S^-e^{-iht} \equiv S^- \cos^2(|\mathcal{E}|t) + \frac{\mathcal{E}^2}{|\mathcal{E}|^2} \sin^2(|\mathcal{E}|t)S^+ + \frac{2i\mathcal{E}}{|\mathcal{E}|} S^z \sin(|\mathcal{E}|t) \cos(|\mathcal{E}|t). \quad (6.8)$$

Using Eqs.(6.7) and (6.8), Eq. (6.5) becomes

$$\bar{H} = -i\hbar g \left( S^+ \cos^2(|\mathcal{E}|t) + \frac{\mathcal{E}^{*2}}{|\mathcal{E}|^2} \sin^2(|\mathcal{E}|t)S^- - \frac{2i\mathcal{E}^*}{|\mathcal{E}|} S^z \sin(|\mathcal{E}|t) \cos(|\mathcal{E}|t) \right) a - H.c. \quad (6.9)$$

We note that the Hamiltonian of the above form has been previously used to treat the inhibition of the spontaneous emission [118] and for the production of mesoscopic superposition states [119, 120]. We assume that the atom is driven strongly so that  $|\mathcal{E}|$  is large and hence we drop rapidly oscillating terms from Eq. (6.9) *i.e.*  $e^{\pm 2i|\mathcal{E}|t} \Rightarrow 0$ . Then Eq. (6.9) reduces to

$$\bar{H} = -\frac{i\hbar g}{2} \left( S^+ + \frac{\mathcal{E}^{*2}}{|\mathcal{E}|^2} S^- \right) a - H.c. \quad (6.10)$$

We choose  $\mathcal{E}^{*2}/|\mathcal{E}|^2 = 1$ ; in general, this can also be done by adjusting phases with atomic operators. Then the Eq. (6.10) takes the form

$$\bar{H}_{eff} = \hbar g S^x \left( \frac{a - a^\dagger}{i} \right). \quad (6.11)$$

Note the appearance of the well known displacement  $D(\alpha) = \exp(a^\dagger\alpha - a\alpha^*)$  in the evolution operator  $e^{-iHt/\hbar}$  for Hamiltonian (6.11). Further it should also be noted that  $h$  as defined by Eq. (6.4) commutes with  $\bar{H}_{eff}$ . In the original interaction picture the Hamiltonian for our model will be

$$H_{eff} = \hbar g S^x \left( \frac{a - a^\dagger}{i} \right) + 2\hbar|\mathcal{E}|S^x. \quad (6.12)$$

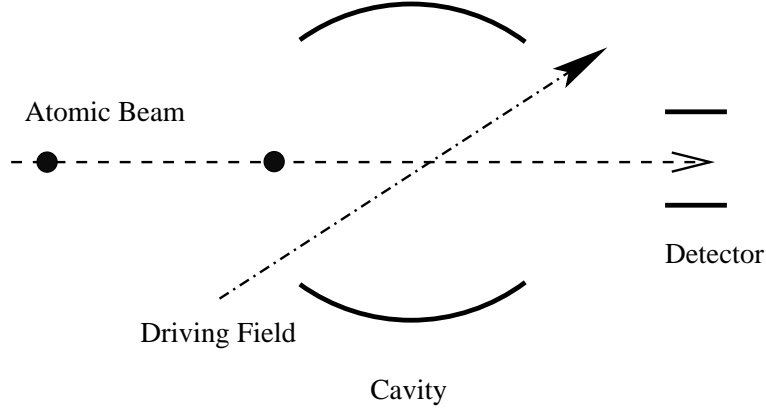


**Figure 6.1:** The schematic arrangements for realizing quantum random walks. A continuous strong driving field inside the cavity can be applied by an external source. The time interval between two atoms in the atomic beam is selected larger than the interaction time in the cavity so that only one atom is presented inside the cavity at a time. The atoms are detected at the exit of the cavity by a state selective detector.

In the effective Hamiltonian (6.12) field displacement operator appears with atomic operator, which can produce a displacement in field state depending on the atomic state.

## 6.2 Quantum Random Walk of Photons

We next discuss the possible realization of quantum random walks in the system of the two level atom and the field inside the cavity. In Fig. 6.1 we show a schematic diagram for realizing quantum random walks. In our scheme atom passes through the cavity and is detected at the exit of the cavity. A continuous strong driving field is applied by using an external source. Let us consider that, initially, the atom is in the superposition state  $|\Phi\rangle = (c_1|e\rangle + c_2|g\rangle)$  and the field inside the cavity is in a coherent state  $|\alpha\rangle$ . Using Eq. (6.12) the combined state of the atom-cavity system after time  $t$  is given by

$$|\psi(t)\rangle = \exp \left[ gtS^x (a^\dagger - a) - 2i|\mathcal{E}|tS^x \right] |\Phi\rangle |\alpha\rangle, \quad (6.13)$$

$$= \frac{c_+ e^{-i\phi}}{2} (|g\rangle + |e\rangle) |\alpha + gt/2\rangle + \frac{c_- e^{i\phi}}{2} (|g\rangle - |e\rangle) |\alpha - gt/2\rangle, \quad (6.14)$$

$$= |g\rangle \left[ \frac{c_+ e^{-i\phi}}{2} |\alpha + gt/2\rangle + \frac{c_- e^{i\phi}}{2} |\alpha - gt/2\rangle \right] \\ + |e\rangle \left[ \frac{c_+ e^{-i\phi}}{2} |\alpha + gt/2\rangle - \frac{c_- e^{i\phi}}{2} |\alpha - gt/2\rangle \right]; \quad (6.15)$$

$$\phi = \left( |\mathcal{E}| + \frac{g}{2} \text{Im}(\alpha) \right) t; \quad (6.16)$$

where  $c_+ = c_1 + c_2$  and  $c_- = c_1 - c_2$ . Using normalization of atomic states we can select  $c_-/c_+ = \tan \theta$ . Thus the detection of the atom in state  $|e\rangle$  or  $|g\rangle$  leaves the cavity field in a superposition of states  $|\alpha + gt/2\rangle$  and  $|\alpha - gt/2\rangle$ . For small values of  $gt$  the states  $|\alpha + gt/2\rangle$  and  $|\alpha - gt/2\rangle$  overlap completely and thus quantum interference effects between  $|\alpha + gt/2\rangle$  and  $|\alpha - gt/2\rangle$  becomes significant. If we assume that the atom is detected in its ground state  $|g\rangle$ , then the state of the field inside the cavity can be written as

$$|\psi_f\rangle \propto \left[ e^{-i|\mathcal{E}|t} D(gt/2) + e^{i|\mathcal{E}|t} \tan(\theta) D(-gt/2) \right] |\alpha\rangle, \quad (6.17)$$

Clearly after passing one atom through the cavity the field inside the cavity is displaced backward or forward along the line in a random way by the step of  $gt/2$ . We can now iterate the above step to obtain the state of the field after the passage of  $N$  atoms. We assume that atoms enter in the cavity in the state  $|\Phi\rangle$  and after interaction with the field inside the cavity detected in their ground state  $|g\rangle$ . Note that the displacement operators appearing in the above state commute with each other  $[D(gt/2), D(-gt/2)] = 0$  for real  $gt$ . Thus the field state after the passage of  $N$  atoms is given by

$$|\psi_f(N)\rangle = C \left[ e^{-i|\mathcal{E}|t} D(gt/2) + e^{i|\mathcal{E}|t} \tan(\theta) D(-gt/2) \right]^N |\alpha\rangle, \quad (6.18)$$

$$\begin{aligned} &= C \sum_{m=0}^N \binom{N}{m} \left[ e^{-im|\mathcal{E}|t} D^m \left( \frac{gt}{2} \right) e^{i(N-m)|\mathcal{E}|t} (\tan \theta)^{N-m} D^{N-m} \left( -\frac{gt}{2} \right) \right] |\alpha\rangle, \\ &= C \sum_{m=0}^N \binom{N}{m} e^{i(N-2m)|\mathcal{E}|t} (\tan \theta)^{N-m} D^{N-2m}(-gt/2) |\alpha\rangle, \end{aligned} \quad (6.19)$$

$$= C \sum_{m=0}^N \binom{N}{m} e^{i(N-2m)\phi} (\tan \theta)^{N-m} |\alpha - (N-2m)gt/2\rangle, \quad (6.20)$$

where  $C$  is normalization constant and we have used the property of the displacement operator  $D^{-1}(\alpha) = D(-\alpha)$ . On writing the above result in coordinate space representation, we get the wavefunction  $\psi_N(x, \alpha) = \langle x | \psi_f(N) \rangle$

$$\psi_N(x, \alpha) = C \sum_{m=0}^N \binom{N}{m} e^{i(N-2m)\phi} (\tan \theta)^{N-m} \psi_\alpha(x + [N-2m]l), \quad (6.21)$$

where  $\psi_\alpha(x) \equiv \langle x | \alpha \rangle$  is the wavefunction corresponding to the initial cavity field state  $|\alpha\rangle$  which is centered at  $x = \alpha$  and the step size of the random walker is  $l = gt/2$ .

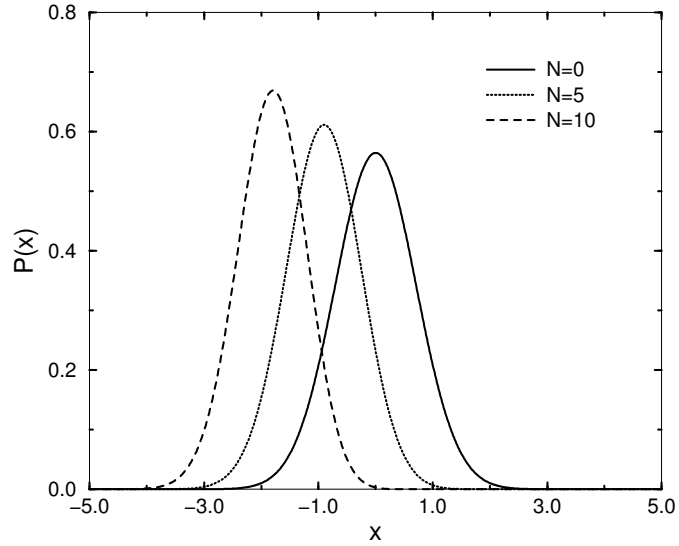


**Figure 6.2:** The probability distribution  $P(x)$  for the position of the quantum random walker, assuming initial wave packet as Gaussian  $\exp[-(x - \alpha)^2/2]$  for  $\alpha = 0$ , step size  $l = 0.05$ ,  $\phi = 2\pi$  and  $\theta = 2\pi/3$ .

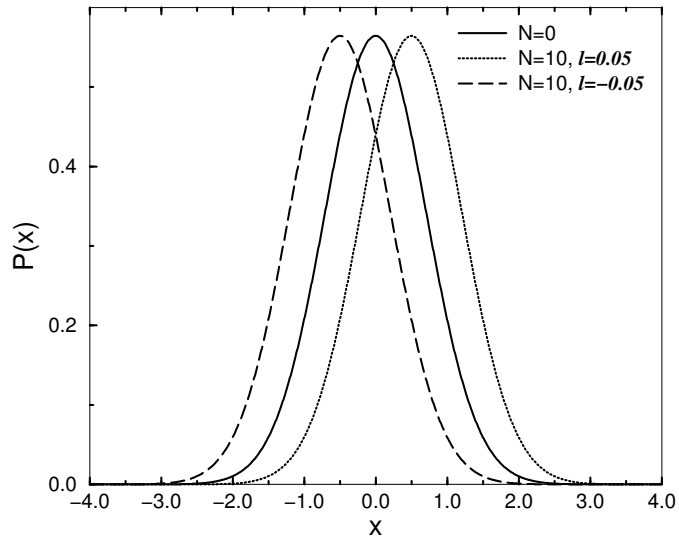


**Figure 6.3:** The probability distribution  $P(x)$  for the position of the quantum random walker, after dropping off-diagonal terms. Parameters used are same parameters as in FIG. 6.2.

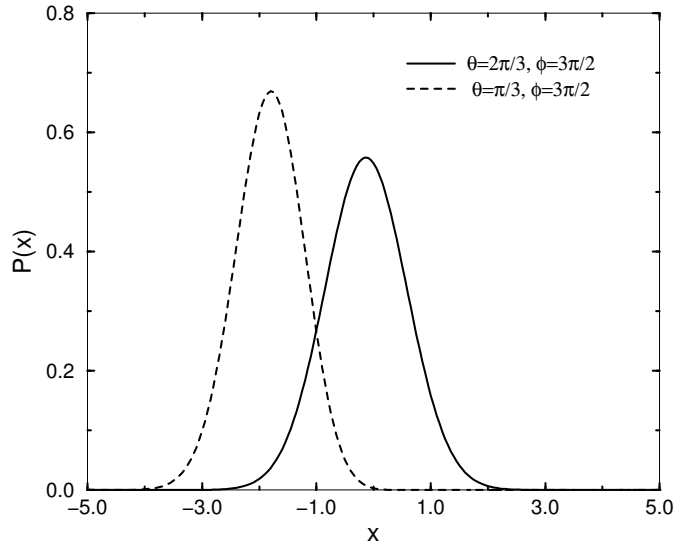


**Figure 6.4:** The probability distribution  $P(x)$  for the position of the quantum random walker after 10 steps, using different set of values of  $\theta$  and  $\phi$  and for  $\alpha = 0$ , step size  $l = 0.05$ .

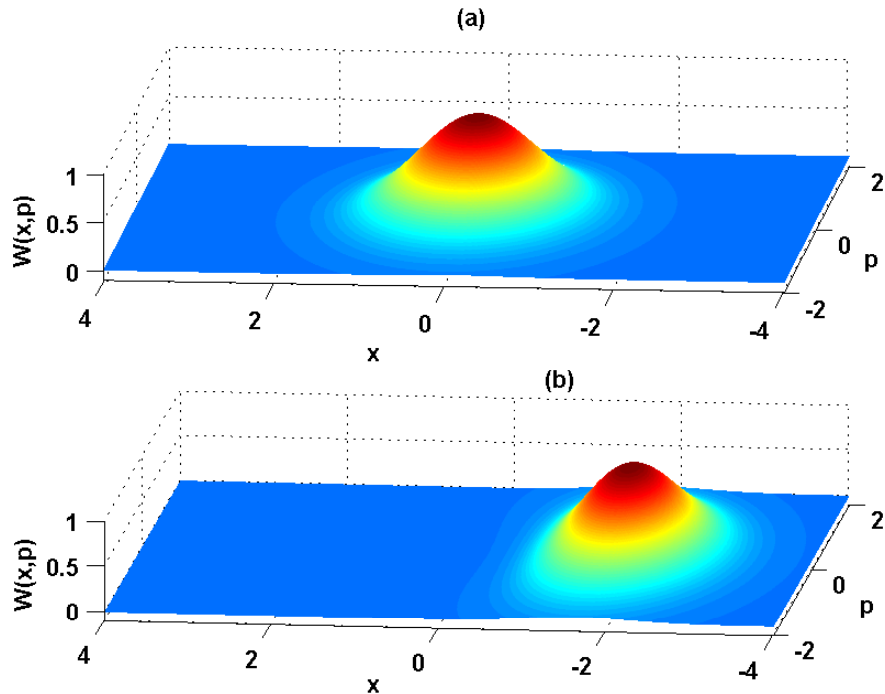


**Figure 6.5:** The Wigner function  $W(x, p)$  of the state of the random walker, after number of steps (a)  $N = 0$  (b)  $N = 10$ , using same parameters as in FIG. 6.2.

We note that we have recovered the result of Aharonov et al [110]. In Fig. 6.2 we have plotted the probability amplitude distribution for initial wave function  $\psi_\alpha(x) \sim \exp[-(x - \alpha)^2/2]$  for real values of  $x$  and  $\alpha = 0$ . The displacement depends on  $\theta$ ,  $\phi$ , and, the number of steps,  $N$ . The unexpected displacement in the state of the random walker is the result of constructive quantum interference between the states generated in various steps which comes from the off diagonal terms in  $P(x) = |\psi_N(\alpha, x)|^2$ . The displacement of the random walker is not bounded by the classically possible maximum and minimum displacements  $\pm Nl$ . The quantum interference leads to an arbitrary displacement in the random walker's position and can be much larger than  $\pm Nl$ . We have checked this by dropping the off diagonal terms in  $P(x)$ . In Fig. 6.3, we show the results after dropping the off diagonal terms in  $|\psi_N(\alpha, x)|^2$  in this case  $P(x)$  remains same in shape as for the initial wave packet but shifts by an amount  $Nl$ .

A small squeezing in the wavepacket is also generated from these interference effects. The selection of phases  $\phi$  and  $\theta$  is also critical for displacement in the position of quantum walker. This can be understood from Eq. (6.21), each term in Eq. (6.21) corresponding to a particular value of  $m$  represents a possible state of the quantum walker. The final displacement of walker after  $N$  steps comes as a result of quantum interference among all such possible states. Thus the final displacement depends on the relative weights and the relative phases of these states. The relative weights of the states in Eq. (6.21) are proportional to  $(\tan \theta)^{N-m}$  while the relative phases are given by  $\phi$ . Depending on the the values of  $\theta$  and  $\phi$ , final displacement in the position of quantum walker can take any value from the possible maximum to the minimum. For example, for the parameters used in Fig. 6.2 we plot  $P(x)$  using different values of  $\theta$  and  $\phi$  in Fig. 6.4. The displacement in the position of quantum walker is minimum when  $\theta = 2\pi/3$  and  $\phi$  is half integer multiple of  $\pi$ . Further for  $\theta = \pi/3$  and  $\phi = 3\pi/2$  the displacement is maximum again.

For visualizing quantum interferences, we plot the Wigner function of the random walker in Fig. 6.5. The Wigner distribution for any state  $\psi(x)$  can be obtained by using the definition [21],

$$W(x, p) = \frac{1}{\pi\hbar} \int e^{2ipy/\hbar} \psi(x-y) \psi^*(x+y) dy. \quad (6.22)$$

In the Fig. 6.5(a) the field is in its initial coherent state and the Wigner function is perfect Gaussian. As the field is displaced by random steps, by passing atoms through the cavity,

quantum interference effects start deforming the shape of the Wigner function from the Gaussian. After few steps the Wigner function is squeezed in  $x$  quadrature and gets displaced by an arbitrary distance in  $x$ . In Fig. 6.5(b) (see also Fig. 6.7(a)), we have shown the Wigner function after 10 random steps for initial Gaussian wave packet. The squeezing is also clear from the Fig. 6.2 which shows the narrowing of the distribution  $P(x)$ . It is clear that the displacement in the position of random walker comes as a result of quantum interference which is consequence of quantum coherence between the states generated in random steps.

Here it should be noted that the quantum walks appear as a consequence of quantum interference. Thus maintaining coherence of the system through out the experiment is an essential requirement. In the context of currently available technologies these requirements can be fulfilled by using Rydberg atoms in a very-high-quality cavity. We also note the recent success in trapping atoms in high-quality cavities [121, 122]. The question is if one can use trapped atoms to realize the quantum random walk instead of flying atoms. We believe that this should be possible by using (i) a trigger pulse, the duration of which would set the interaction time (ii) the detection of atomic state possibly by using a very short pulse, and (iii) resetting of the atomic state. In this arrangement the same atom is used repeatedly rather than sending atoms one by one. As a matter of fact some of these ideas are in vogue [123].

### 6.3 Measurement of the State of the Random Walker

We next discuss how we can probe the quantum state of the random walker. We propose homodyne techniques [30] for measuring the state of the random walker. Such homodyne measurement can be performed by mixing an external resonant coherent field to the cavity and then probing the resultant cavity field by passing a test atom through the cavity. In the previous section, we have shown how the cavity field is displaced backward or forward in a random step by passing single atom through the cavity. The state of the field in the cavity after such  $N$  steps can be monitored by homodyne measurements which can be implemented in the same experimental set up. After displacing the field inside the cavity by  $N$  random steps, by passing  $N$  atoms, a resonant external coherent field  $|\beta\rangle$  is injected into the cavity. After adding the external field, the state of the resultant field in the cavity

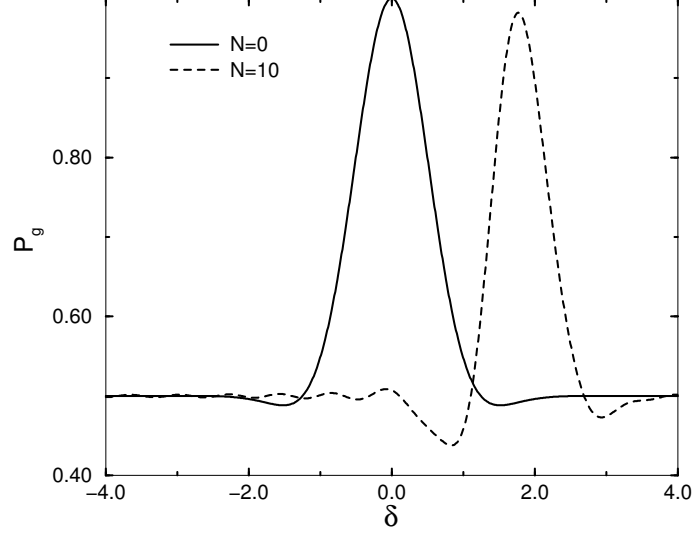


**Figure 6.6:** The probability of detecting probe atom in its ground state as a function of  $\delta$  for the state of the quantum random walker after number of steps  $N = 0$  (solid line) and  $N = 10$  (dashed line). The parameters used are same as in Fig. 6.2 and the interaction time for the probe atom is selected such that  $gt_p = 1.5\pi$ .

is

$$\begin{aligned}
 |\psi_H\rangle &= C \sum_{m=0}^N \binom{N}{m} e^{i(N-2m)\phi} (\tan\theta)^{N-m} D(\beta) |\alpha - (N-2m)gt/2\rangle, \\
 &= C \sum_n \sum_{m=0}^N \binom{N}{m} e^{i(N-2m)\phi} (\tan\theta)^{N-m} \langle n | D(\beta) |\alpha - (N-2m)gt/2\rangle |n\rangle, \\
 &= \sum_n F_n |n\rangle
 \end{aligned} \tag{6.23}$$

$$F_n = C \sum_{m=0}^N \binom{N}{m} e^{i(N-2m)\phi} (\tan\theta)^{N-m} \langle n | D(\beta) |\alpha - (N-2m)gt/2\rangle. \tag{6.24}$$

Now we bring a similar atom in its lower energy state  $|g\rangle$  to probe the cavity field. The probability of detecting the probe atom in its lower state  $|g\rangle$  after crossing the cavity in time  $t_p$  is

$$P_g = \sum_n |F_n|^2 \cos^2(gt_p \sqrt{n}). \tag{6.25}$$

The interaction time  $t_p$  for the probe atom is selected such that if there are photons in the cavity, it leaves the cavity in its higher energy state  $|e\rangle$  with larger probability. If we choose

the external field  $|\beta\rangle$  such that  $\beta = -\alpha + \delta$ , the probe atom will leave the cavity in its ground state with larger probability when the value of  $\delta$  will be opposite and equal to the displacement of the random walker from the initial position  $\alpha$ . Thus the probability of the probe atom leaving the cavity in its lower state  $|g\rangle$  would, as a function of  $\delta$ , have peak corresponding to the positions of the random walker after  $N$  steps. In Fig. 6.6, we plot the probability of detecting the probe atom in its lower state with  $\delta$ . The solid line curve is result of homodyne measurement of the position of the random walker corresponding to its initial state. The dashed line curve corresponds to the homodyne measurement after 10 steps using the same parameter as in Fig. 6.2. Clearly the homodyne measurement yields the state of the quantum walker (Fig. 6.2). Thus the homodyne measurement can be an elegant way for monitoring the position of the random walker in our model of realizing quantum random walks.

## 6.4 Decoherence in Quantum Random Walk

Quantum random walks are different from the classical random walks in the sense of quantum interferences which may lead to much larger displacements in the position of quantum random walker than the classically possible maximum displacements. These quantum interferences are the consequences of coherence in the system. Clearly we need the coherence to live for a long time, and thus it is important to study the effects of the decoherence of the system. In this section we study the decoherence of the state of the random walker due to damping in the cavity. This can be done using the master equation

$$\dot{\rho} = -\frac{\kappa}{2}(a^\dagger a \rho - 2a \rho a^\dagger + \rho a^\dagger a), \quad (6.26)$$

where  $\kappa$  is cavity field decay parameter and we carry the analysis in the absence of thermal photons. For the initial state (6.20) we find the density matrix after time  $t$  :

$$\begin{aligned} \rho(t) &= |C|^2 \sum_{m=0}^N \sum_{n=0}^N \binom{N}{m} \binom{N}{n} e^{2i(n-m)\phi} (\tan \theta)^{2N-m-n} \\ &\quad \langle \alpha - (N-2m)l | \alpha - (N-2n)l \rangle^{(1-e^{-\kappa t})} \\ &\quad | \alpha - (N-2m)l \rangle_t \langle \alpha - (N-2n)l |_t, \end{aligned} \quad (6.27)$$

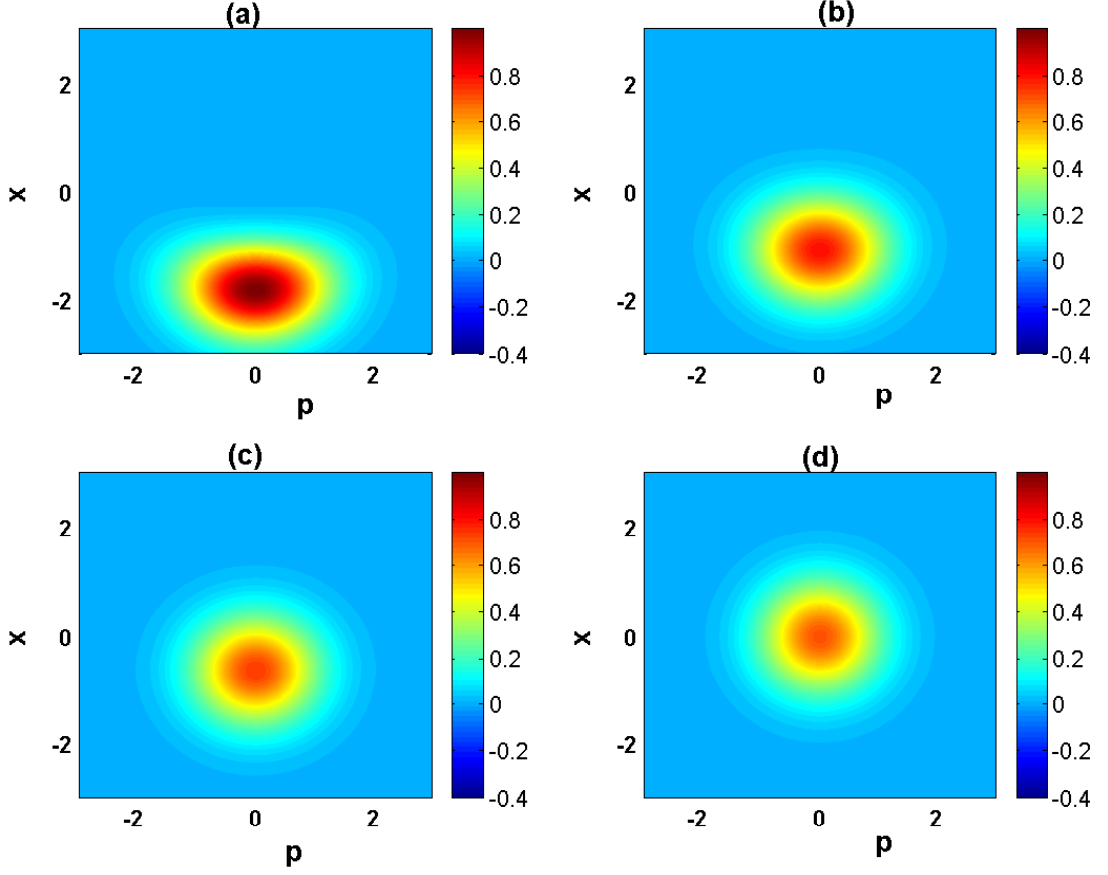


**Figure 6.7:** The decoherence of the state of the random walker in terms of Wigner function at different times, for  $N = 10$ ,  $l = 0.05$ ,  $\theta = 2\pi/3$ ,  $\phi = 2\pi$ , and (a)  $\kappa t = 0$ , (b)  $\kappa t = 1/4N^2l^2$ , (c)  $\kappa t = 1/2N^2l^2$ , (d)  $\kappa t = 2/N^2l^2$ .

where  $|\zeta\rangle_t \equiv |\zeta e^{-\kappa t/2}\rangle$ . In the limit  $\kappa t \ll 1$ , Eq. (6.27) simplifies to

$$\rho(t) = |C|^2 \sum_{m=0}^N \sum_{n=0}^N \binom{N}{m} \binom{N}{n} e^{2i(n-m)\phi} (\tan \theta)^{2N-m-n} e^{-2\kappa t l^2 (n-m)^2} |\alpha - (N-2m)l\rangle \langle \alpha - (N-2n)l|. \quad (6.28)$$

Thus the coherence of the state decays on the time scales  $1/2N^2l^2$ . In Fig. 6.7 we show the decoherence effects due to the cavity damping in the state of the quantum random walker in terms of the Wigner function. As the time progresses from (a) to (d) the decoherence reduces the quantum interference effects and the state of the random walker decays to its initial state. In Fig. 6.7(a) the Wigner function for the state of the random walker after 10 steps using the parameters of Fig. 6.5(b) is plotted which is squeezed in  $x$  quadrature and

centered at  $x \approx -2$ . As a result of decoherence due to cavity damping the quantum interferences start decaying and the Wigner function changes to the perfect Gaussian shape, Fig. 6.7(c) centered at  $x = Nl$ . Now the field inside the cavity is almost in a coherent state and decays with the cavity damping rate. Further the lifetime for the state of the quantum random walker is given by  $T_N = T_c/2N^2l^2$  where  $T_c = 1/\kappa$  is the lifetime for field in the cavity.

## 6.5 Summary

We have presented a simple possible realization of quantum random walks using cavity QED. We have proposed homodyne detection for monitoring the position of the random walker. We have also discussed the decoherence effects and the time scales at which quantum nature of random walks survives. As a result of new emerging technologies various improved cavities are feasible these days which makes our proposal much interesting and realistic. Such a realization of quantum random walks may be useful for implementing various algorithms [124] based on quantum random walks.

---

## Conclusions and Future Outlook

---

In conclusion, this thesis reports various interesting phenomenons occurring in cavity quantum electrodynamics as a result of quantum entanglement and quantum interference.

In chapter 2, we have proposed cavity quantum electrodynamics schemes to generate superposition of four coherent states,  $|\psi\rangle \sim |\alpha\rangle + |i\alpha\rangle + |-\alpha\rangle + |-i\alpha\rangle$  using resonant as well as dispersive interaction between atoms and the field inside the cavity. We have discussed the nonclassical character of these states in terms of negativity of the Wigner function as well as zeros of Q-distribution. We have also shown that these superposition states can exhibit regions in phase space with sub-Planck structures, i. e., the area of the variations of the two quadratures can be much smaller than  $\hbar$ . These structures are direct signatures of quantum coherence and are formed as a result of interference between two superposed cat states. We have discussed decoherence of such superposition due to the leakage of photons from the cavity. We have also discussed methods for monitoring these superposition states in the cavity. These studies need further exploration for efficient methods of tomography of such states. The central pattern in the Wigner function of such superposition states depends on the phases of coherent states in the superposition, thus there is possibility of investing new methods of quantum metrology [V. Giovannetti et al., Phys. Rev. Lett. **96**, 010401 (2006)], using superposition of multiple coherent states.

In chapter 3, we have studied Ramsey interferometer with quantized fields and discussed the effects of field statistics on the visibility of interference fringes. We found that interferences do not occur if the fields in two Ramsey zones have precise number of photons i.e. in Fock states, however, by passing two atoms one by one it has been shown how atom-atom correlation interferometry can be used to restore interferences. We have

also discussed interferences at a single photon level. Though interferences are absent with precise number of photons in Ramsey zones but for states like  $|0\rangle + |1\rangle$  interferences are restored. This occurs because of lack of information about the cavity in which atom makes transition. We also discussed generation of various maximally entangled states, as well as, the transfer of entanglement from atoms to photons and vice versa using Ramsey interferometer. Transfer of entanglement can have very useful applications in quantum computation. Further, these studies can be explored for realizing various quantum logics, as well as, for teleporting quantum states from one cavity to another cavity.

In chapter 4, we have reported an unusual cooperative effect involving two atoms in a non-resonant cavity. This cooperative effect arises when the atoms interact with a common field in the cavity and can lead to a two-photon two-atom resonant absorption phenomenon. Earlier studies of dipole-dipole induced two photon processes involving two atoms in free space require very high resolution because of very small interatomic separation. In high quality cavities inter-atomic interactions can arise when different atoms interact with a common quantized field. The cavity induced interatomic interactions do not need small interatomic separation and atom can be placed anywhere inside the cavity. We have demonstrated that in a high quality cavity the two-atom two-photon resonant effect could be very large thus opening up the possibility of a variety of multi-photon cooperative phenomena in non-resonant cavities. We have derived two-photon two-atom resonance condition. We have studied such two-photon resonant processes in two different systems: (1) two identical atoms interacting with field in a two mode cavity, (2) two nonidentical atoms in a single mode cavity.

In chapter 5, we have discussed a new method of controlling spontaneous emission by using dc-fields. We have shown that in the presence of dc-fields in the cavities the spontaneous emission of atoms can be modified significantly as a result of dc-field induced stark shifts. Further, the change in spontaneous emission depends on the square of applied dc-field. We have found that in the case of cavities resonant to atomic transition spontaneous emission can be inhibited significantly using dc-fields. In the case of cavities having negligible mode density around atomic frequency the presence of dc-field shows significant inhibition or enhancement of spontaneous emission depending on whether the cavity is tuned below the atomic transition frequency or above the transition frequency. These studied need further exploration in the case of high quality cavities where we can

not neglect the back action of the field.

Random walk is a very useful tool in various computational algorithms, in a similar fashion, quantum version of random walk, i.e., quantum random walk can also be used more efficiently in quantum computation. In chapter 6, we have shown how quantum random walk can be realized in microcavities as a consequence of quantum interference. Using a homodyne technique, the state of the quantum random walker can be monitored. We have also discussed the decoherence effects and the time scales at which quantum nature of random walks survives. So far most of the models for realizing quantum random walk are proposed using classical states of walker. Thus, these studies need further exploration about the question, what could be the actual quantum random walk which depends on the quantum nature of the state of the walker.

## A. Averaging over Fast Oscillating Variables

Our procedure for eliminating fast oscillating variables is extended form of the procedure discussed in Ref.[125]. The Hamiltonian (4.5) can be written as

$$H = H_0 + \epsilon V,$$

where

$$H_0 = -\Delta a^\dagger a - \delta b^\dagger b, \quad \epsilon V = \sum_{i=1,2} \hbar \left[ |e_i\rangle \langle g_i| (g_1 a + g_2 b) + |g_i\rangle \langle e_i| (g_1 a^\dagger + g_2 b^\dagger) \right]. \quad (\text{A.1})$$

The eigenstates and corresponding eigenvalues of  $H_0$  are

$$\begin{aligned} |1\rangle &\equiv |e_1, e_2, 0, 0\rangle & E_1 &\equiv 0, \\ |2\rangle &\equiv 2^{-1/2}(|e_1, g_2\rangle + |g_1, e_2\rangle)|1, 0\rangle & E_2 &\equiv -\Delta, \\ |3\rangle &\equiv 2^{-1/2}(|e_1, g_2\rangle + |g_1, e_2\rangle)|0, 1\rangle & E_3 &\equiv -\delta, \\ |4\rangle &\equiv |g_1, g_2, 1, 1\rangle & E_4 &\equiv -(\Delta + \delta), \\ |5\rangle &\equiv |g_1, g_2, 2, 0\rangle & E_5 &\equiv -2\Delta, \\ |6\rangle &\equiv |g_1, g_2, 0, 2\rangle & E_6 &\equiv -2\delta. \end{aligned}$$

The resolvent for  $H_0$  is the function

$$G_0(z) = \frac{1}{z - H_0}, \quad (\text{A.2})$$

where  $z$  is complex. If  $P_i$  is projection operator for the eigenstates of  $H_0$

$$P_i = |i\rangle \langle i|; \quad i = 1, 2 \dots 6. \quad (\text{A.3})$$

The resolvent  $G_0$  can be expressed as

$$G_0(z) = \sum_i \frac{P_i}{z - E_i}. \quad (\text{A.4})$$

The resolvent for the full Hamiltonian  $H$  is

$$\begin{aligned} G(z) &= \frac{1}{z - H_0 - \epsilon V}, \\ &= \frac{1}{z - H_0} \left( 1 + \epsilon V \frac{1}{z - H} \right), \\ &= G_0(1 + \epsilon V G). \end{aligned} \quad (\text{A.5})$$

From Eq. (A.5) the resolvent for the full Hamiltonian  $H$  can be expressed in the power series of  $\epsilon$  as

$$G = \sum_n \epsilon^n G_0 (V G_0)^n. \quad (\text{A.6})$$

For small values of  $\epsilon$ ,  $G(z)$  has singularities in the complex  $z$ -plane in the neighborhood of

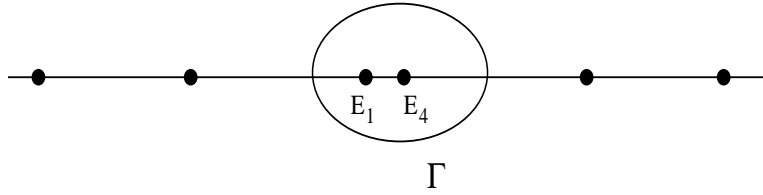


**Figure A.1:** The contour in complex plane shielding two eigenvalues  $E_1$  and  $E_4$  and leaving others outside.

poles of function  $G_0$ , i.e., eigenvalues of  $H_0$ . Further eigenvalues  $E_1$  and  $E_4$  are very close to each other under the condition  $\Delta + \delta \approx 0$  and other eigenvalues are largely separated. We consider a contour,  $\Gamma$  in the  $z$ -plane that encloses eigenvalues  $E_1$  and  $E_4$  only and leaves others outside as shown in the Fig.A.1. We define a new projection operator  $P_\Gamma$  as

$$\begin{aligned} P_\Gamma &= \bar{P}_1 + \bar{P}_4, \\ &= \frac{1}{2i\pi} \oint_\Gamma G(z) dz. \end{aligned} \quad (\text{A.7})$$

Here  $\bar{P}_1$  and  $\bar{P}_4$  are the projection operators for eigenstates of full Hamiltonian  $H$  corresponding to the eigenvalues inside the contour. The effective Hamiltonian will have the form

$$H_{eff} \equiv (P_1 + P_4) H P_\Gamma (P_1 + P_4). \quad (\text{A.8})$$

From the definition of the resolvent we have

$$(z - H)G \equiv G(z - H) \equiv 1. \\ HP_\Gamma = \frac{1}{2i\pi} \oint_\Gamma zG(z)dz. \quad (\text{A.9})$$

Substituting value of  $G(z)$  from Eq. (A.6) in Eq. (A.9) and interchanging summation to the integration we have

$$HP_\Gamma = \sum_n \frac{1}{2i\pi} \oint_\Gamma zG_0(VG_0)^n dz. \quad (\text{A.10})$$

The effective Hamiltonian can be expressed as

$$H_{eff} = E_1P_1 + E_4P_4 + \sum_{n=1}^{\infty} \epsilon^n A^{(n)}; \\ A^{(n)} = (P_1 + P_4) \sum_{n=1}^{\infty} \frac{1}{2i\pi} \oint_\Gamma zG_0(VG_0)^n dz (P_1 + P_4). \quad (\text{A.11})$$

Inside the contour  $\Gamma$ ,  $G_0$  has singularities at  $E_1$  and  $E_4$  only so the integral in the Eq. (A.11) is nothing but the sum of the residues at  $z = E_1$  and  $z = E_4$ . Further as in our case  $\epsilon P_1VP_1$ ,  $\epsilon P_4VP_4$  and  $\epsilon P_1VP_4$  equal to zero, there is no first order and third order terms. The second order term is

$$A^{(2)} = P_1VQ_1VP_1 + P_4VQ_4VP_4 + P_1VQ_4VP_4 + P_4VQ_4VP_1, \quad (\text{A.12}) \\ Q_j = \sum_{i \neq 1,4} \frac{P_i}{E_j - E_i}.$$

The forth order term is

$$A^{(4)} = \frac{1}{2i\pi} \oint_\Gamma z \left( \frac{P_1}{z - E_1} + \frac{P_4}{z - E_4} \right) V \sum_{i \neq 1,4} \frac{P_i}{z - E_i} V \otimes \\ \left( \frac{P_1}{z - E_1} + \frac{P_4}{z - E_4} + \sum_{j \neq 1,4} \frac{P_j}{z - E_j} \right) V \sum_{k \neq 1,4} \frac{P_k}{z - E_k} V \left( \frac{P_1}{z - E_1} + \frac{P_4}{z - E_4} \right) dz \quad (\text{A.13})$$

For simplification we use the condition for resonance  $\Delta + \delta = 0$ , i.e.,  $E_1 = E_4$ . Thus the forth order term is

$$A^{(4)} = \frac{1}{2i\pi} \oint_\Gamma z \left( \frac{P_1}{z - E_1} + \frac{P_4}{z - E_1} \right) V \sum_{i \neq 1,4} \frac{P_i}{z - E_i} V \otimes \\ \sum_{j \neq 1,4} \frac{P_j}{z - E_j} V \sum_{k \neq 1,4} \frac{P_k}{z - E_k} V \left( \frac{P_1}{z - E_1} + \frac{P_4}{z - E_1} \right) dz. \quad (\text{A.14})$$

Integrating Eq. (A.14) we have the forth order term

$$A^{(4)} = (P_1 + P_4) V Q_1 V Q_1 V Q_1 V (P_1 + P_4). \quad (\text{A.15})$$

Using the values of  $E_1, E_2, E_3, E_4, E_5, E_6$ , and  $V$  the effective Hamiltonian expressed in basis  $|e_1, e_2, 0, 0\rangle$  and  $|g_1, g_2, 1, 1\rangle$  is

$$H_{eff} = \begin{bmatrix} \frac{2g_1^2}{\Delta} + \frac{2g_2^2}{\delta} + \frac{4g_1^4}{\Delta^3} + \frac{4g_2^4}{\delta^3} & -\frac{2g_1g_2}{\Delta} - \frac{2g_1g_2}{\delta} + \frac{4g_1^3g_2}{\Delta^3} + \frac{4g_1g_2^3}{\delta^3} \\ -\frac{2g_1g_2}{\Delta} - \frac{2g_1g_2}{\delta} + \frac{4g_1^3g_2}{\Delta^3} + \frac{4g_1g_2^3}{\delta^3} & -(\Delta + \delta) - \frac{2g_2^2}{\delta} - \frac{2g_1^2}{\Delta} + \frac{4g_1^2g_2^2}{\Delta^3} + \frac{4g_1^2g_2^2}{\delta^3} \end{bmatrix}. \quad (\text{A.16})$$

With some algebraic manipulation and considering  $g_1$  and  $g_2$  up to forth order effectively the Hamiltonian (4.5) reduces to

$$H_{eff} = \begin{bmatrix} \frac{2g_1^2\Delta}{\Delta^2-2g_1^2} + \frac{2g_2^2\delta}{\delta^2-2g_2^2} & -2g_1g_2 \left( \frac{\Delta}{\Delta^2+2g_1^2} + \frac{\delta}{\delta^2+2g_2^2} \right) \\ -2g_1g_2 \left( \frac{\Delta}{\Delta^2+2g_1^2} + \frac{\delta}{\delta^2+2g_2^2} \right) & - \left( \Delta + \delta - \frac{2g_2^2\Delta}{\Delta^2-2g_1^2} - \frac{2g_1^2\delta}{\delta^2-2g_2^2} \right) \end{bmatrix}. \quad (\text{A.17})$$

It should be noted here as two-atom two-photon resonance appears at large interaction time in dispersive limit, the terms in the effective Hamiltonian up to forth order are important to predict correct evolution. Using the effective Hamiltonian (A.17) the Eq. (4.8) reduces to Eq. (4.9).

## B. Time Averaging

We outline how the time averaging is to be done. Let us consider schrodinger equation

$$\frac{\partial}{\partial t}|\psi(t)\rangle = -\frac{i}{\hbar}V(t)|\psi(t)\rangle, \quad (\text{B.1})$$

where  $V(t)$  consists of rapidly oscillating terms only, so that the time average of  $V(t)$  is zero. Let  $|\psi\rangle$  be written as

$$|\psi\rangle = |\bar{\psi}\rangle + |\phi\rangle, \quad (\text{B.2})$$

where  $|\bar{\psi}\rangle$  is time averaged part and  $|\phi\rangle$  is the rapidly oscillating part. On substituting (B.2) in Eq (B.1) we find that to the lowest order in  $V(t)$ ,

$$|\phi\rangle = -\frac{i}{\hbar} \int_0^t V(\tau) d\tau |\bar{\psi}\rangle, \quad (\text{B.3})$$

and

$$\frac{\partial}{\partial t}|\bar{\psi}(t)\rangle = -\frac{i}{\hbar}\bar{V}(t)|\bar{\psi}\rangle, \quad (\text{B.4})$$

where

$$\bar{V}(t) = -\frac{i}{\hbar} \overline{V(t) \int_0^t V(\tau) d\tau}. \quad (\text{B.5})$$

The field induced shift term in (5.23) is obtained by using Eq. (B.5).

---

## References

---

- [1] *Cavity Quantum Electrodynamics* ed. P. R. Berman (Academic, New York, 1994).
- [2] J. D. Jackson, *Classical Electrodynamics*, (Wiley, New York, 1962).
- [3] M. O. Scully and M.S. Zubairy, *Quantum Optics*, (Cambridge University Press, Cambridge, 1997).
- [4] L. I. Schiff, *Quantum Mechanics*, ( McGraw-Hill Companies, 1968).
- [5] A. Einstein, Phys. Z. **18**, 121(1917).
- [6] R.Loudon, *The quantum theory of light*, (Oxford, 1973).
- [7] J. M. Raimond, M. Brune, and S. Haroche, Rev. Mod. Phys. **73**, 565 (2001).
- [8] E. T. Jaynes and F. W. Cummings, Proc. IEEE **51**, 89 (1963).
- [9] H. -I. Yoo and J. H. Eberly, Phys. Rep. **118**, 239 (1985).
- [10] H. Walther, Adv. At. Mol. Opt. Phys. **32**, 379 (1994).
- [11] A. Einstein, B. Podolsky, and N. Rosen, Phys. Rev. **47**, 777 (1935).
- [12] A. Ekert, Phys. Rev. Lett. **67**, 661 (1991).
- [13] C.H. Bennett, G. Brassard, C. Crepeau, R. Jozsa, A. Peres, and W. K. Wootters, Phys. Rev. Lett. **70**, 1895 (1993).
- [14] E. Wigner, Phys. Rev. **40**, 749 (1932).

- [15] K. Vogel and H. Risken, *Phys. Rev. A* **40**, 2847 (1989).
- [16] D. T. Smithey, M. Beck, and M. G. Raymer, *Phys. Rev. Lett.* **70**, 1244 (1993).
- [17] K. Banaszek and K. Wódkiewicz, *Phys. Rev. Lett.* **76**, 4344 (1996); K. Banaszek, C. Radzewicz, and K. Wódkiewicz, *Phys. Rev. A* **60**, 674 (1999).
- [18] U. Leonhardt, in *Measuring the Quantum State of Light*, (Cambridge University Press, Cambridge, 1997).
- [19] L. G. Lutterbach, and L. Davidovich, *Phys. Rev. Lett.* **78**, 2547 (1997).
- [20] P. Bertet, A. Auffeves, P. Mailoni, S. Osnaghi, T. Meunier, M. Brune, J. M. Raimond, and S. Haroche, *Phys. Rev. Lett.* **89**, 200402 (2002).
- [21] G. S. Agarwal and E. Wolf, *Phys. Rev. D* **2**, 2161 (1970); M. Hillery, R. F. O'Connell, M. O. Scully, and E. P. Wigner, *Phys. Rep.* **106**, 121(1984).
- [22] D. Leibfried, D. M. Meekhof, B. E. King, C. Monroe, W. M. Itano, and D. J. Wineland, *Phys. Rev. Lett.* **77**, 4281 (1996).
- [23] E. C. G. Sudarshan, *Phys. Rev. Lett.* **10**, 277 (1963).
- [24] R. J. Glauber, *Phys. Rev.* **131**, 2766 (1963).
- [25] U. Leonhardt and H. Paul, *Phys. Rev. A* **47**, R2460 (1993).
- [26] E. Schrödinger, *Naturwissenschaften* **23**, 807 (1935).
- [27] Wolfgang P. Schleich in *Quantum Optics in Phase Space* (John Wiley & Sons, 2001).
- [28] V. Buzek and P. L. Knight, in *Progress in Optics* Vol. XXXIV, Ed. by E. Wolf (North Holland, Amsterdam, 1995).
- [29] L. Davidovich, M. Brune, J. M. Raimond, and S. Haroche, *Phys. Rev. A* **53**, 1295 (1996).
- [30] A. Auffeves, P. Maioli, T. Meunier, S. Gleyzes, G. Nogues, M. Brune, J. M. Raimond, and S. Haroche, *Phys. Rev. Lett.* **91**, 230405 (2003).

- [31] M. Brune, E. Hagley, J. Dreyer, X. Maitre, A. Maali, C. Wunderlich, J. M. Raimond, and S. Haroche, *Phys. Rev. Lett.* **77**, 4887 (1996).
- [32] J. M. Raimond, M. Brune, and S. Haroche, *Phys. Rev. Lett.* **79**, 1964 (1997).
- [33] C. Monroe, D. M. Meekhof, B. E. King, and D. J. Wineland, *Science* **272**, 1131 (1996).
- [34] M. W. Noel and C. R. Stroud, Jr., *Phys. Rev. Lett.* **77**, 1913 (1996).
- [35] K. Tara, G. S. Agarwal, and S. Chaturvedi, *Phys. Rev. A* **47**, 5024 (1993).
- [36] C. Ottaviani, D. Vitali, M. Artoni, F. Cataliotti, and P. Tombesi, *Phys. Rev. Lett.* **90**, 197902 (2003).
- [37] S. J. van Enk, *Phys. Rev. Lett.* **91**, 017902 (2003).
- [38] A. Imamoglu, H. Schmidt, G. Woods, and M. Deutsch, *Phys. Rev. Lett.* **79**, 1467 (1997).
- [39] G. S. Agarwal and J. Banerji, *Phys. Rev. A* **64**, 023815 (2001).
- [40] J. Banerji and G. S. Agarwal, *Phys. Rev. A* **59**, 4777 (1999), G. S. Agarwal and J. Banerji, *ibid.* **57**, 3880 (1998).
- [41] J. A. Yeazell and C. R. Stroud, Jr., *Phys. Rev. A* **43**, 5153 (1991).
- [42] C. C. Gerry, *Phys. Rev. A* **53**, 3818 (1996).
- [43] M. Brune, S. Haroche, V. Lefevre, J. M. Raimond, and N. Zagury, *Phys. Rev. Lett.* **65**, 976 (1990); P. Maioli, T. Meunier, S. Gleyzes, A. Auffeves, G. Nogues, M. Brune, J. M. Raimond, and S. Haroche, *ibid.* **94**, 113601 (2005).
- [44] J. Eiselt, and H. Risken, *Opt. Commun.* **72**, 351 (1989).
- [45] J. Gea-Banacloche, *Phys. Rev. A* **44**, 5913 (1991); I. Sh. Averbukh, *ibid.* **46**, R2205 (1992); V. Buzek, H. Moya-Cessa, P. L. Knight, and S. J. D. Phoenix, *ibid.* **45**, 8190 (1992); M. S. Kim and G. S. Agarwal, *J. Mod. Opt.* **46**, 2111 (1999).
- [46] W. H. Zurek, *Nature (London)* **412**, 712 (2001).

- [47] J. R. Kuklinski and J. L. Madajczyk, *Phys. Rev. A* **37**, R3175 (1988); R. R. Puri and G. S. Agarwal, *Phys. Rev. A* **33**, R3610 (1986).
- [48] M. S. Kim, G. Antesberger, C. T. Bodendorf, and H. Walther, *Phys. Rev. A* **58**, R65 (1998).
- [49] D. M. Greenberger, M.A. Horne, and A. Zeilinger, *Am. J. Phys.* **58**, 1131 (1990).
- [50] Entanglement resulting from the process of detection is being discussed extensively, J. M. Raimond, M. Brune and S. Haroche, *Rev. Mod. Phys.* **73**, 565 (2001); L. M. Duan, M. D. Lukin, J. I. Cirac and P. Zoller, *Nature(London)* **414**, 413 (2001); G. S. Agarwal, J. von Zanthier, C. Skornia and H. Walther, *Phys. Rev.A*, **65**, 053826 (2002).
- [51] A. Rauschenbeutel, G. Nogues, S. Osnaghi, P. Bertet, M. Brune, J. M. Raimond, and S. Haroche, *Phys. Rev. Lett.* **83**, 5166 (1999); T. Sleator and H. Weinfurter, *ibid.* **74**, 4087 (1995).
- [52] A. Steane, *Phys. Rev. Lett.* **77**, 793 (1996); S. J. Van Enk, J. I. Cirac, and P. Zoller, *ibid.* **78**, 4293 (1997).
- [53] J. W. Pan, D. Bouwmeester, M. Daniell, H. Weinfurter, and A. Zeilinger, *Nature (London)* **403**, 515 (2000).
- [54] A. Rauschenbeutel, P. Bertet, S. Osnaghi, G. Nogues, M. Brune, J. M. Raimond, S. Haroche, *Phys. Rev. A* **64**, 050301 (2001).
- [55] B. Julsgaard, A. Kozhekin and E. S. Polzik, *Nature(London)* **413**, 400 (2001).
- [56] N. F. Ramsey, *Phys. Rev.* **78**, 695, (1950).
- [57] M. O. Scully and M. S. Zubairy, **Quantum Optics**, (Cambridge University Press, Cambridge 1997), Sec 20.4.
- [58] Conditional measurements on successive atoms passing through a single high quality cavity have led to the successful generation of trapped and Fock states of radiation field, M. Weidinger, B. T. H. Varcoe, R. Heerlein and H. Walther, *Phys. Rev. Lett.* **82**, 3795 (1999); B. T. H. Varcoe, S. Brattke, M. Weidinger and H. Walther, *Nature(London)* **403**, 743 (2000); S. Brattke, B. T. H. Varcoe and H. Walther, *Phys. Rev. Lett.* **86**, 3534 (2001).

- [59] M. M. Salour and C. Cohen-Tannoudji, *Phys. Rev. Lett.* **38**, 757 (1977); J. C. Bergquist, S. A. Lee, and J. L. Hall, *ibid.* **38**, 159 (1977); M. M. Salour, *Rev. Mod. Phys.* **50**, 667 (1978).
- [60] G. Nogues, A. Rauschenbeutel, S. Osnaghi, M. Brune, J. M. Raimond and S. Haroche, *Nature(London)* **400**, 239 (1999).
- [61] P. Bertet, S. Osnaghi, A. Rauschenbeutel, G. Nogues, A. Auffeves, M. Brune, J. M. Raimond and S. Haroche, *Nature(London)* **411**, 166 (2001), for the theoretical proposal see S. B. Zheng, *Opt. Commun.* **173**, 265 (2000). Note that quantum eraser concept was proposed by M. O. Scully and K. Drühl, *Phys. Rev. A* **25**, 2208 (1982).
- [62] For extensive reviews on cavity quantum electrodynamics, see G. Raithel, C. Wagner, H. Walther, L.M. Narducci and M.O. Scully, in **Cavity Quantum Electrodynamics**, edited by P. R. Berman (Academic, Boston, 1994), p. 57; S. Haroche and J. M. Raimond, *ibid.* p. 123; H. J. Kimble, *ibid.* p. 203 ; P. Meystre in **Progress in Optics**, edited by E. Wolf (Elsevier, Amsterdam, 1992) Vol.**30**, 261; B. G. Englert et al, *Fortschr. Phys.***46**, 900 (1998).
- [63] M. O. Scully, H. Walther, G. S. Agarwal, Tran Quang and W. Schleich, *Phys. Rev. A* **44**, 5992 (1991); R. J. Brecha, A. Peters, C. Wagner and H. Walther, *ibid.* **46**, 567 (1992).
- [64] M. O. Scully, B. G. Englert and H. Walther, *Nature(London)* **351**, 111 (1991); B. G. Englert, M. O. Scully and H. Walther, *ibid.* **375**, 367 (1995).
- [65] A number of very interesting optical interference experiments have been reported with fields at single photon level, P. Hariharan and B. C. Sanders in **Progress in Optics** (North-Holland, Amsterdam, 1996) Vol.**36**, p.49.
- [66] A. I. Lvovsky and J. Mlynek, *Phys. Rev. Lett.* **88**, 250401 (2002).
- [67] K. J. Resch, J. S. Lundeen and A. M. Steinberg, *Phys. Rev. Lett.* **88**,113601 (2002).
- [68] For a preliminary discussion see, G. S. Agarwal and M. O. Scully, *Phys. Rev. A* **53**, 467 (1996).
- [69] X. Maître, E. Hagley, G. Nogues, C. Wunderlich, P. Goy, M. Brune, J. M. Raimond, S. Haroche, *Phys. Rev. Lett.* **79**, 769 (1997).

- [70] P. Meystre, in *Progress in Optics XXX*, edited by E. Wolf (Elsevier Science, New York, 1992), p.338.
- [71] R. Ghosh and L. Mandel, *Phys. Rev. Lett.* **59**, 1903 (1987); Z. Y. Ou and L. Mandel, *ibid.* **62**, 2941 (1989); Z. Y. Ou, X. Y. Zou, L. J. Wang and L. Mandel, *ibid.* **65**, 321 (1990).
- [72] J. H. Eberly, N. B. Narozhny, and J. J. Sanchez-Mondragon, *Phys. Rev. Lett.***44**, 1323 (1980).
- [73] G. Raithel, C. Wagner, H. Walther, L. M. Narducci, and M. O. Scully, in *Advances in Atomic, Molecular and optical Physics* (Supplement 2, 1994), p.57.
- [74] L. A. Lugiato, in *Progress in Optics Vol.XXI*, edited by E. Wolf (North-Holland, Amsterdam, 1984), p.69.
- [75] G. V. Varada, and G. S. Agarwal, *Phys. Rev. A* **45**, 6721 (1992); A. Beige, and G. C. Hegerfeldt, *ibid.* **58**, 4133 (1998).
- [76] C. Hettich, C. Schmitt, J. Zitzmann, S. Kuhn, I. Gerhardt, and V. Sandoghdar, *Science* **298**, 385 (2002).
- [77] E. V. Goldstein, and P. Meystre, *Phys. Rev. A* **56**, 5135 (1997).
- [78] M. S. Kim and G. S. Agarwal, *Phys. Rev. A* **57**, 3059-3064 (1998).
- [79] L. Davidovich, J. M. Raimond, M. Brune, and S. Haroche, *Phys. Rev. A* **36**, 3771 (1987); M. Brune, J. M. Raimond, and S. Haroche, *Phys. Rev. A* **35**, 154 (1987); M. Brune, J. M. Raimond, P. Goy, L. Davidovich, and S. Haroche, *Phys. Rev. Lett.* **59**, 1899 (1987).
- [80] J. J. Sanchez-Mondragon, N. B. Narozhny, and J. H. Eberly, *Phys. Rev. Lett.* **51**, 550 (1983).
- [81] G. S. Agarwal, *J. Opt. Soc. Am. B* **2**, 480 (1985); G. S. Agarwal, *Phys. Rev. Lett.* **53**, 1732 (1984).
- [82] H. J. Kimble, in *Cavity Quantum Electrodynamics*, edited by P. Berman (Academic Press, London, 1994), p.203.

- [83] T. W. Mossberg and M. Lewenstein, in *Cavity Quantum Electrodynamics*, edited by P. Berman (Academic Press, London, 1994), p.171.
- [84] J. McKeever, J. R. Buck, A. D. Boozer, A. Kuzmich, H.-C. Nägerl, D. M. Stamper-Kurn, and H. J. Kimble, *Phys. Rev. Lett.* **90**, 133602, (2003).
- [85] J. D. Franson, and T. B. Pittman, *Phys. Rev. A* **60**, 917 (1999).
- [86] E. M. Purcell, *Phys. Rev.* **69**, 681 (1946).
- [87] P. Goy, J. M. Raimond, M. Gross, and S. Haroche, *Phys. Rev. Lett.* **50**, 1903 (1983).
- [88] A. Rahmani, and G. W. Bryant, *Phys. Rev. A* **65**, 023803 (2002).
- [89] D. J. Heinzen, J. J. Childs, J. E. Thomas, and M. S. Feld, *Phys. Rev. Lett.* **58**, 1320 (1987); D. J. Heinzen, and M. S. Feld, *ibid* **59**, 2623 (1987).
- [90] D. Kleppner *Phys. Rev. Lett.* **47**, 233 (1981); R. G. Hulet, E. S. Hilfer, and D. Kleppner, *ibid* **55**, 2137 (1985); W. Jhe, A. Anderson, E. A. Hinds, D. Meschede, L. Moi, and S. Haroche *ibid* **58**, 666 (1987).
- [91] H. Schniepp, and V. Sandoghdar, *Phys. Rev. Lett.* **89**, 257403 (2002).
- [92] R. J. Thompson, G. Rempe, and H. J. Kimble, *Phys. Rev. Lett.* **68**, 1132 (1992); C. Weisbuch, M. Nishioka, A. Ishikawa, and Y. Arakawa, *ibid* **69**, 3314 (1992).
- [93] H. Giesen, J. D. Berger, G. Mohs, P. Meystre, and S. F. Yelin, *Phys. Rev. A* **53**, 2816 (1996).
- [94] H. T. Dung, L. Knoll, and D. G. Welsch, *Phys. Rev. A* **62**, 053804 (2000).
- [95] G. S. Agarwal, in *Springer Tracts in Modern Physics*, edited by G. Hohler *et al* (Springer, New York, 1974), Vol **70**.
- [96] K. Tanaka, T. Nakamura, W. Takamatsu, M. Yamanishi, Y. Lee, and T. Ishihara, *Phys. Rev. Lett.* **74**, 3380 (1995); F. De Martini, G. Innocenti, G. R. Jacobovitz, and P. Mataloni, *ibid* **59**, 2955 (1987); S. T. Ho, S. L. McCall, and R. E. Slusher, *Opt. Lett.* **18**, 909 (1993).
- [97] Y. Xu, R. K. Lee, and A. Yariv, *Phys. Rev. A* **61**, 033807 (2000).

- [98] O. Jedrkiewicz, and R. Loudon, *Phys. Rev. A* **60**, 4951 (1999).
- [99] I. Takahashi, and K. Ujihara, *Phys. Rev. A* **56**, 2299 (1997).
- [100] R. W. F. vander Plank, and L. G. Suttorp, *Phys. Rev. A* **54**, 2464 (1996).
- [101] M. Lewenstein, T. W. Mossberg, and R. J. Glauber, *Phys. Rev. Lett.* **59**, 775 (1987); H. Friedhoff, and T. Quang, *ibid.* **72**, 474 (1994).
- [102] W. Lange, and H. Walther, *Phys. Rev. A* **48**, 4551 (1993); G. S. Agarwal, W. Lange, and H. Walther, *ibid.* **48**, 4555 (1993); C. H. Keitel, *Phys. Rev. Lett.* **83**, 1307 (1999); P. Zhou, and S. Swain, *Phys. Rev. A* **58**, 1515 (1998).
- [103] W. Lange, H. Walther, and G. S. Agarwal, *Phys. Rev. A* **50**, R3596 (1994).
- [104] M. Elk, and P. Lambropoulos, *Phys. Rev. A* **50**, 1490, (1994).
- [105] E. Paspalakis, C. H. Keitel, and P. L. Knight, *Phys. Rev. A* **58**, 4868 (1998).
- [106] C. Fabre, S. Haroche, and P. Goy, *Phys. Rev. A* **18**, 229 (1978).
- [107] T. F. Gallagher, *Rep. Prog. Phys.* **51**, 143, (1988).
- [108] W. P. Spencer, A. G. Vaidyanathan, D. Kleppner, and T. W. Ducas, *Phys. Rev. A* **24**, 2513 (1981); present measurements of the lifetimes of sodium Rydberg states.
- [109] S. Chandrasekhar, *Rev. Mod. Phys.* **15**, 1 (1943).
- [110] Y. Aharonov, L. Davidovich, and N. Zagury, *Phys. Rev. A* **48**, 1687 (1993).
- [111] B. C. Sanders, S. D. Bartlett, B. Tregenna, and P. L. Knight, *Phys. Rev. A* **67**, 042305 (2003).
- [112] T. Di, M. Hillery, and M. S. Zubairy, *Phys. Rev. A* **70**, 032304 (2004).
- [113] B. C. Travaglione and G. J. Milburn, *Phys. Rev. A* **65**, 032310 (2002).
- [114] W. Dür, R. Raussendorf, V. M. Kendon, and H. -J. Briegel, *Phys. Rev. A* **66**, 052319 (2002); K. Eckert, J. Mompart, G. Birkel, M. Lewenstein, e-print quant-ph/0503084.
- [115] P. L. Knight, E. Roldan, and J. E. Sipe, *Phys. Rev. A* **68**, R020301 (2003); *Opt. Commun.* **227**, 147 (2003).

- [116] D. Bouwmeester, I. Marzoli, G. P. Karman, W. Schleich, and J. P. Woerdman, *Phys. Rev. A* **61**, 013410 (2000).
- [117] B. Do, M. L. Stohler, S. Balasubramanian, D. S. Elliott, C. Eash, E. Fischbach, M. A. Fischbach, A. Mills, B. Zwickl, *J. Opt. Soc. Am. B*, **22**, 499 (2005); H. Jeong, M. Paternostro, and M. S. Kim, *Phys. Rev. A* **69**, 012310 (2004).
- [118] G. S. Agarwal, W. Lange, and H. Walther, *Phys. Rev. A* **48**, 4555 (1993); W. Lange and H. Walther, *ibid.* **48**, 4551 (1993).
- [119] E. Solano, G. S. Agarwal, and H. Walther, *Phys. Rev. Lett.* **90**, 027903 (2003).
- [120] P. Lougovski, F. Casagrande, A. Lulli, B.-G. Englert, E. Solano, and H. Walther, *Phys. Rev. A* **69**, 023812 (2004).
- [121] A. Boca, R. Miller, K. M. Birnbaum, A. D. Boozer, J. McKeever, and H. J. Kimble, *Phys. Rev. Lett.* **93**, 233603 (2004).
- [122] P. Maunz, T. Puppe, I. Schuster, N. Syassen, P. W. H. Pinkse, G. Rempe, *Nature* **428**, 50 (2004).
- [123] T. Legero, T. Wilk, M. Hennrich, G. Rempe, and A. Kuhn, *Phys. Rev. Lett.* **93**, 070503 (2004).
- [124] N. Shenvi, J. Kempe, and K. BirgittaWhaley, *Phys. Rev. A* **67**, 052307 (2003).
- [125] A. Messiah, *Quantum Mechanics*, (Dover Publications, 1999), p.685.

---

## List of Publications

---

### I. Papers in Journals:

1. *Single-atom and two-atom Ramsey interferometry with quantized fields*,  
G. S. Agarwal, P. K. Pathak, and M. O. Scully, Phys. Rev. A **67**, 043807 (2003).
2. *Large two-atom two-photon vacuum Rabi oscillations in a high-quality cavity*,  
P. K. Pathak and G. S. Agarwal, Phys. Rev. A **70**, 043807 (2004).
3. *dc-field-induced enhancement and inhibition of spontaneous emission in a cavity*,  
G. S. Agarwal and P. K. Pathak, Phys. Rev. A **70**, 025802 (2004).
4. *Mesoscopic superposition of states with sub-Planck structures in phase space*,  
G. S. Agarwal and P. K. Pathak, Phys. Rev. A **70**, 053813 (2004).
5. *Generation of a superposition of multiple mesoscopic states of radiation in a resonant cavity*,  
P. K. Pathak and G. S. Agarwal, Phys. Rev. A **71**, 043823 (2005).
6. *Quantum random walk of the field in an externally driven cavity*,  
G. S. Agarwal and P. K. Pathak, Phys. Rev. A **72**, 033815 (2005).
7. *Quantum random walk of two entangled qubits*,  
P. K. Pathak and G. S. Agarwal, submitted to Phys. Rev. A (not included in thesis).

### II. Abstracts of International and National Conferences:

1. *Two photon absorption from cooperative effects*, P. K. Pathak and G. S. Agarwal, "Indian Society of Atomic & Molecular Physics (ISAMP)", held at Physical Research Laboratory, Ahmedabad, India, Dec, 2004.

2. *Mesoscopic Superposition of States with Sub-Planck Structures in Phase Space*, G. S. Agarwal and P. K. Pathak, "Frontiers in Optics", sponsored by Optical Society of America, Oct. 2005.
3. *Quantum random walk of the field in an externally driven cavity*, G. S. Agarwal and P. K. Pathak, "Frontiers in Optics", sponsored by Optical Society of America, Oct. 2005.